Technical University Graz
Faculty of Civil Engineering
Hydraulic Engineering and Water Resources Management

Development of a Micro Electromechanical System Accelerometer for Measurements of Sediment Transport in Mountain Torrents

Master Thesis

submitted by

Carina Tamara Bernecker

First Reviewer: Assoc.Prof. Dipl.-Ing. Dr.nat.techn. Josef Schneider

Second Reviewer: Dipl.-Ing. Sebastian Gegenleithner

Graz, October 31, 2018

Abstract

Heavy rainfall often leads to flood events, which can cause severe transport of debris and sediment load in rivers. Especially in mountain torrents and rivers, this causes for jamming of the bridges due to driftwood but also to an immense amount of destruction of not only the riverbed itself but bridges, roads and cities because the water level in mountain torrents can rise rapidly in a short period of time. After a destructive flood event in Oberwölz in 2011 research programs were started for the Schöttlbach catchment, to gain more information about sediment and bedload transport in alpine mountain torrents and rivers, to develop warning systems, to reduce the risk of destructive events like this and to generally gain more information about this matter.
This thesis includes theoretical background on mountain torrents and rivers and how they can be categorized, theoretical information about the project area and its characteristics in respect to its hydrology as well as geology and geomorphology. Measuring techniques that are useful for sediment and bed load transport are described and appropriate methods for alpine mountain torrents and rivers are applied in the project area, evaluated and validated. Flow, respectively discharge, as well as turbidity measurements and the development and trial tests of a new sensor for bed load measurements (Micro Electromechanical System Accelerometer) are described in this thesis.

Kurzbeschreibung

Starke Regenfälle führen oft zu Hochwasserereignissen, die zu hohen Sedimenttransportarten in Flüssen führen können. Vor allem in Gebirgsbächen und -flüssen kann dies zu einer immensen Zerstörung im Flussbett selbst, aber auch an Brücken, Straßen und Städten führen, da ein starker Anstieg des Wasserspiegels innerhalb weniger Minuten möglich ist. Die Verklausung von Brücken stellt weiters ein erhebliches Risiko dar.
Nach einem verheerenden Hochwasserereignis in Oberwölz im Jahr 2011 wurden mehrere Forschungsprogramme für das Einzugsgebiet des Schöttlbaches gestartet, um zusätzliche Informationen über Sediment- und Geschiebetransport in Wildbächen zu erhalten, Warnsysteme entwickeln zu können, das Risiko von zerstörerischen Ereignissen einschätzen zu können und um allgemein mehr Informationen über den Geschiebe- und Sedimenttransport zu bekommen.
Diese Arbeit beinhaltet theoretische Hintergründe zu Wildbächen und Flüssen und wie diese zu kategorisieren sind. Theoretische Informationen über das Projektgebiet und seine Eigenschaften in Bezug auf die Hydrologie sowie Geologie und Geomorphologie werden erläutert. Beschreibungen über Messtechniken, die für den Sediment- und Geschiebetransport anwendbar sind und geeignete Methoden für Gebirgsbäche und -flüsse werden im Projektgebiet angewendet, bewertet und validiert. Im Zuge dieser Masterarbeit sind Geschwindigkeits-, Durchfluss- und Trübemessungen durchgeführt worden. Desweiteren wird die Entwicklung und Erprobung eines neuen Sensors für die Messung von Sediment- und Geschiebetransport (Micro Electromechanical System Accelerometer) beschrieben.

Acknowledgement

My love and gratitude goes out to:

Those who love sediments.
Those who don‘t.

But especially to my supervisor Josef Schneider and co-supervisor Sebastian Gegenleithner. Without them, this master thesis would not exist. Thank you Joe, for organizing trips to Oberwölz, providing me with useful information and guiding me through this time. Sebastian, thank you for your mad Python skills, for providing informative literature and for convincing me to write my thesis in LaTeX. It really did make a difference.
Didi Schäfauer, thank you for all your hard work, your inventive spirit when constructing release mechanisms (and so many other things) and all the on-call support you provided.

Lastly, I want to say thank you to Michael, who accompanied me on this emotional ride and made sure I stayed on track.

Statutory declaration

I declare that I have authored this thesis independently, that I have not used other than the declared sources / resources, and that I have explicitly marked all material which has been quoted either literally or by content from the used sources.

October 31, 2018

. . . . . .

Date

. . . . . .

Signature

Contents

1 Introduction

1.1 Motivation

Sediment and bedload transport in alpine mountain rivers and torrents are amongst the biggest reasons as to why cities, rivers, roads and heritage are destructed after a strong rain or flood event. The Austrian Wölzertal, especially the city of Oberwölz, has been subject to catastrophic flood events over the last decades, that caused severe damages to infrastructure but also to human life.

To reduce the risk of destruction and to learn from past events, research programs in the alpine region of Oberwölz were started. After a severe flood event in 2011, that caused immense destruction along the catchment area of the river Schöttlbach and in the city of Oberwölz, the project ClimCatch was introduced. For the period of roughly three years, sediment and bed load transport were researched with the aid of numerous measuring systems and techniques (Sass et al. (2015)). In 2016 the project RunSed-CC was started, which continues the research of the ClimCatch project. The aim of the project is to establish a coherent model chain consisting of field investigations, hydrological and hydrometric modeling (Universität Graz (2018)).

Both of these projects were initiated by the Department of Geography and Regional Science at the University of Graz in cooperation with the Institute for Hydraulic Engineering and Water Resources Management at the Graz University of Technology.

1.2 Goal of this Thesis

Goal of this thesis is to comprise theoretical aspects on mountain torrents and rivers, to summarize theoretical background of measuring systems and techniques that can be applied for measuring sediment and bed load transport in rivers and to research methods that were used during the ClimCatch project. Additionally, measuring methods that were revised and redesigned within the framework of this thesis are described.

1.3 Overview

In Chapter 2, a general overview of the project area is given with a summary of the measuring stations and installed methods as well as a short description of the two research projects in this area. Additionally, it includes hydrological characteristics for the catchment area, geological and geomorphological information and a historical time-line of flood events for the area of Oberwölz. Chapter 3 describes theoretical background and literature study on river characteristics, suspended sediment, discharge measuring as well as bed load measuring systems. Some of these techniques and systems are applied in Oberwölz and are described more detailed for the project area specifically. The main aim of Chapter 4 is to describe the methodology used during this thesis. A bed load measuring sensor was developed that shall measure the transport of sediment in the river Schöttlbach. Laboratory tests as well as construction manuals are shown here. In Chapter 5, the data that was collected during this thesis is evaluated and validated. The final Chapter 6 includes general conclusions and recommendations for future measurements in the project area, but also specific recommendations for the on-going development of the newly designed bed load measuring system (MEMS).

2 Project Area

The project area includes the city of Oberwölz and the Schöttlbach with its origin in the northern part of the valley. The boundaries of the project area are defined by the catchment area of the Schöttlbach from its spring and reaching until the Hintereggertor cross section in the city center.

2.1 Oberwölz

The project area (see Figure 2.1) is situated in the Wölzertal in the northern part of Styria, in the district of Murau. It consists of four municipalities, which inhabit roughly 3500 people in total and is spread over more than 200 km^2. Oberwölz, being one of these municipalities, is also one of the smallest cities in Austria and the smallest city in Styria. It inhabits approximately 1000 people and lies at an elevation of 832 m a.s.l. (Stadtgemeinde Oberwölz (2018)).

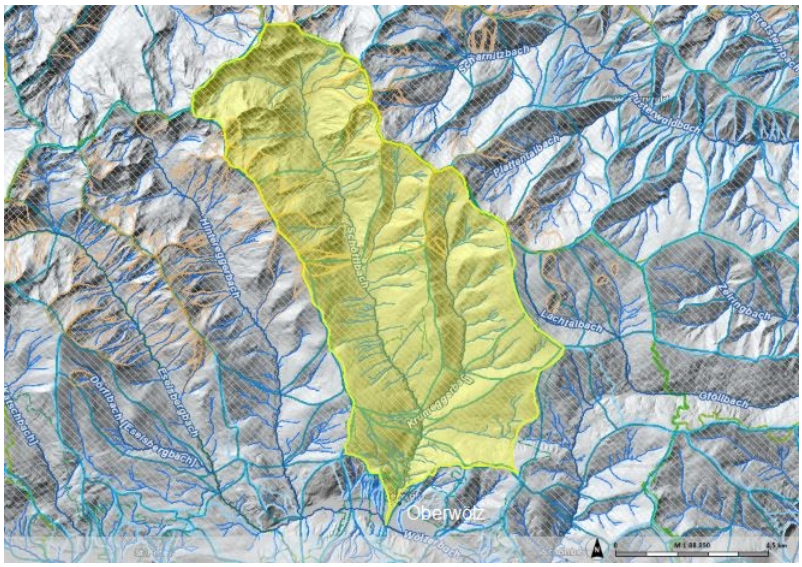

Figure 2.1: *Project area in Oberwölz (GIS-Steiermark (2018))*

2.2 Hydrology of the Project Area

As Langer, Stoisser (2016) already described in their work, the Schöttlbach has a total length of around 16 km. With its average inclination of 2.4^o, the annual sediment transportation comes to a total of 50.000 m^3. The torrent catchment area is divided into several sub-basins as listed in Table 2.1.

Table 2.1: *Sub basin on Schöttlbach torrent catchment area*

Sub-basin	**Lenght [km]**	**Area [km^2]**
Schöttlbach	16.1	70.0
Hubnerbach	2.3	1.7
Hühnerbach	4.1	4.7
Krumeggerbach	5.7	16.1
Schmiedbognerbach	1.9	1.6
Salchauerbach	4.0	6.4

Though the Schöttlbach catchment is in total approximately 70 km^2, the catchment for the Schötllkapelle cross section, where a new set of sensors is installed, is only about half the size. The catchment area until the bridge at the Schöttlkapelle is 33.7 km^2 in size and can be seen in Figure 2.2 below.

Figure 2.2: *Catchment of Schötllkapelle cross section (Google (2018))*

The hydrological flood water values are given in Table 2.2. In a different flood water study conducted by the WLV[1], flood values of much higher magnitude can be found. In this study a 150-year-flood (HQ150) value of 165 m^3/s was calculated for the same catchment area. Possible reasons for this discrepancy can be, that in purely hydrological discharge calculations, as done by Sackl (2011), only clear water hydrography is calculated. Compared to the WLV calculations, where not only clear water, but also debris and sediment mass were included in the calculation. Considering these mass discrepancies, a HQ150 of 165 m^3/s (WLV) compared to a HQ300 of 150 m^3/s (Sackl (2011)) becomes more reasonable. For hydraulic research methods the clear water hydrography values shall be used.

Table 2.2: *Hydrology of the Schöttlbach (Sackl (2011))*

	Discharge [Q]
HQ30	80 [m^3/s]
HQ100	125 [m^3/s]
HQ300	150 [m^3/s]

Recent studies from Sass et al. (2015) in 2015 mention, that in this century, precipitation in combination with global warming will reduce during the summer months and increase during winter months. This will result in fewer snowfall and advanced liquid precipitation during the cold season. Potential hazardous rainfall events, with a daily precipitation of 20-50 mm, will rise throughout this century, especially in the winter months. Nevertheless, high concentration rainfall is also expected for the warmer season on the sub-daily scale. For defined flood events with a significant return period, the interval will be shortened. This means, that a 50 year flood event (HQ50) will be 30 mm higher at the turn of the century than it is now (2018). Considering this, an increased sediment transport can also be expected and needs to be researched thoroughly.

2.3 Geology and Geomorphology of the Project Area

The project area is situated in the ”Wölzer Kristallin” of the Eastern-European covers in the middle-eastern alpine old crystalline (”Altkristallin[2]”), as seen in light pink in Figure 2.3. The ”Wölzer Kristallin” is mainly composed of mica schist, also called ”Wölzer

[1] German: Wildbach und Lawinenverbauung; English: Torrent and avalanche control.

[2] Geologists, before the turn of the century, created this name for a pre-Paleozoic material consisting of Gneiss and Mica Schist (Scharbert, Schönlaub (1980)).

Glimmerschiefer". The northern part of the catchment, as well as parts along the Schöttlbach are covered in the occasional Pleistocene moraines, shown in Figure 2.3 in bright yellow (Niederl (1990)).

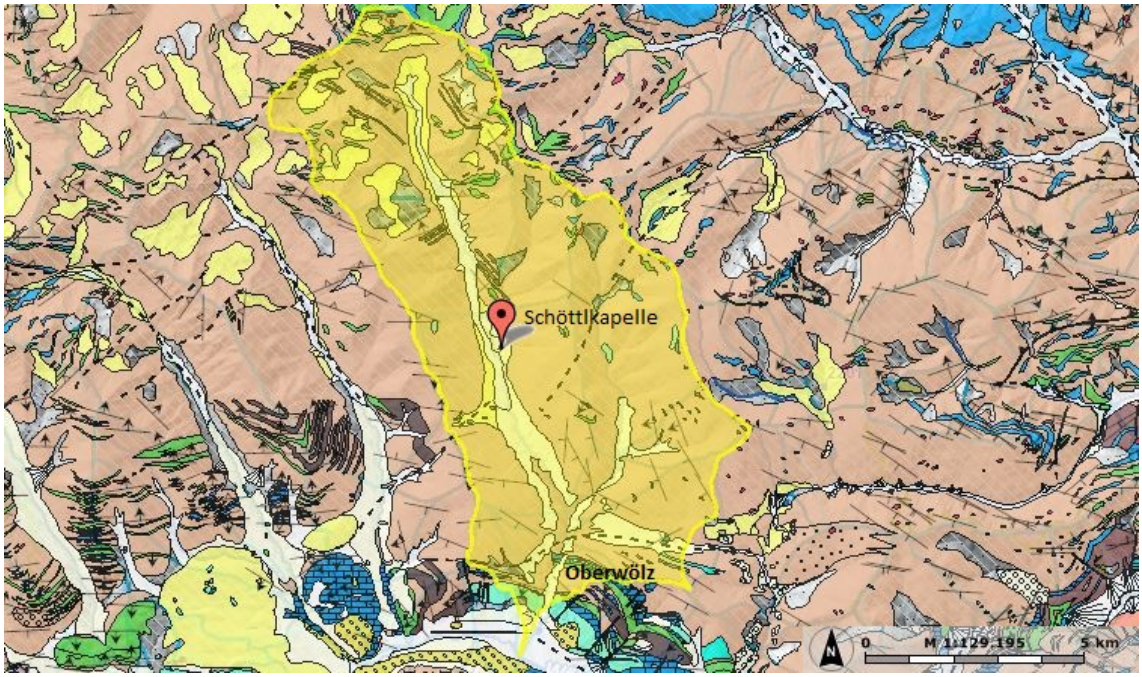

Figure 2.3: *Geology and catchment of the project area (GIS-Steiermark (2018))*

These Pleistocene moraines were formed after the last ice age, when the glaciers of this region started to retreat into higher altitudes. What is left now, are moraines with step slopes, with virtually endless amount of sediment to feed the Schöttlbach cascade.

2.4 History of Flood Events

Over the last decades, the municipality of Oberwölz and the surrounding regions have been hit by a significant number of thunderstorms, and thus heavy flood events which caused damages not only along the river, but also in the inhabited areas in and close to Oberwölz. In the following paragraphs a chronological list of recorded events from 1995 to 2011 and their magnitude can be found for the region and the catchment area of the Schöttlbach (Hübl et al. (2011)).

Schöttlbach Over the Years

In the Figure 2.4 the events are listed and shown with a magnitude scale where "fair" means minor damages on the one hand and "severe" on the other hand, classifies events that caused for heavy destruction of infrastructure, buildings and harm to human life in between the years 1935 until 2017 (Hübl et al. (2011)).

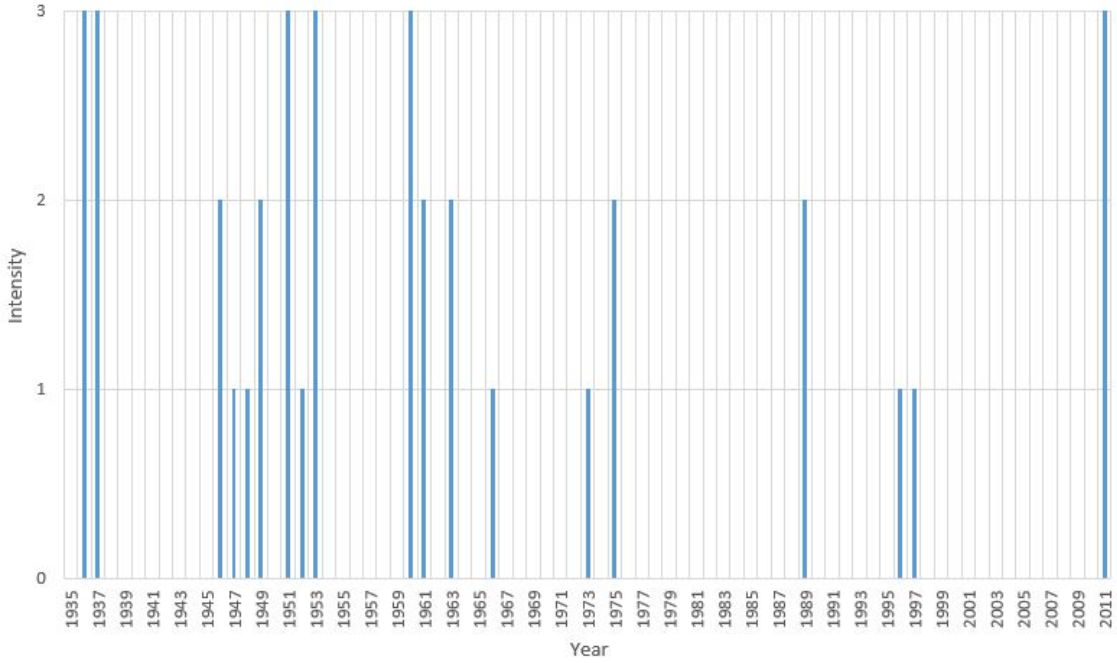

Figure 2.4: *Overview of known significant flood events from 1935 until 2011 in the catchment area of the Schöttlbach (Hübl et al. (2011))*

1765: A flood event, without magnitude, was first mentioned in the cities chronic. Further Information was not given.

18.07.1936: To this date the heaviest rainfalls recorded. In combination with hail, debris flow along the slopes of the river occurred that reached down into the valley. A cottage (Schlitterer Hütte) got destroyed and took the lives of a mother and her child. Downstream all bridges were demolished and the valley, as well as the channel, were ruined.

24.07.1937: Heavy Thunderstorms destroyed fields and forests in and around Oberölz.

13.06.1946: Heavy rainfalls concluded in a flood that lead to damages at the ”Sagmüllerwehranlage” , which was used for electricity production.

1947, 1948: In the years 1947 and 1948 three flood events caused damages at the construction site of the sediment and debris dam (German: Bogensperre).

16.08.1949: Cloud-burst-like rainfall caused colmation of the riverbed with gravel and sand. The dam at the channel bottom could hold back most of the debris.

02.08.1951: Thunderstorms in combination with hail in the upper reaches demolished the dam at a height of 36.77 m and completely filled it up at a height of 24.09 m.

19.07.1953: Heavy rainfalls occurred and lasted the whole day. Debris and driftwood was stored in the river up to a height of 3 m. Agricultural land was covered with sediments at

the confluence of the Hühnerbach into the Schöttlbach.

20.07.1960: Heavy downpours caused damages on municipality lands, as well as bridges, agricultural fields, forests and buildings. Parts of the town were cut off from the outside world. Numerous bridges were torn away, the town of Oberwölz was flooded. Landslides caused destruction of 20 ha of forestry land.

05.09.1960: Another heavy rainfall in September of the same year caused flooding at the upper catchment of the Hühnerbach.

20.06.1961: In the rear catchment a cloud-burst-like rain event together with hail caused landslides and mudflows, of which some are covering private land plots. In the suburban area river slopes slid away and electrical poles collapsed.

22.08.1961: In the area of Hinteregg until Schöttleck, Rossalpe and Alpl heavy thunderstorms in combination with hail took place. This caused flooding and mudslides in these areas.

12.-13.12.1961: Due to heavy rain fall in combination with thaw, respectively melting snow, some 100 m of municipality road were damaged close to Schmiedbognerbach.

1973, 1974, 1989, 1996, 1997: In these years heavy rainfall and thunderstorms caused flood events that damaged or destroyed bridges and roads.
Additionally, in 1974, a number of fields, private lands and municipality roads in the town were overflown by mud and debris (Hübl et al. (2011)).

07.07.2011: Heavy rainfall caused for extreme flooding of the valley especially in the city with roughly 90.000 m^2 of transported sediment. Houses and roads were destroyed. This was the start of the research program ”ClimCatch” for sediment transport in mountain streams and torrents (Barbas (2014)).

05.08.2017: Heavy rainfall occurred during the night and caused flooding of the valley of Oberwölz until Niederwölz. More than 200 people were evacuated due to dangerous landslides (ORF-Steiermark (2017)).

2.5 ClimCatch

After a severe flood event in July 2011 in Oberwölz, the project ”ClimCatch - Impact of climate change on the sediment yield of alpine catchments”, funded by the Austrian Climate Research Program (ACRP) was created.

The catastrophic event showed, that it is of utmost importance to investigate how possible changes in precipitation, precipitation distribution and the reduction of the glaciers and

snow pack due to global warming, affect the balance of Alpine catchment areas. Proper investigation measures to understand the sediments load of the torrents and their changes, as well as to optimize technical protective measures and research, require a variety of measuring stations spread over the research area. However, bed load measuring stations are generally scarcely positioned in Austria. In Styria the first were only implemented with the start of this project altogether (Sass et al. (2015)). Therefore, the main objectives of the project were (i) to get an understanding of the Schöttlbach catchment, its sediments sources and depositional areas; (ii) the quantification of sediment transport in the catchment area and sub-basins and (iii) to assess the impact of on-going climate change on the frequency, intensity and distribution of the precipitation events (Sass et al. (2015)).

The project was completed in 2015. Parts of the outcome of ClimCatch are mentioned throughout this thesis.

2.6 RunSed-CC

More recently, a new research project was initiated by the Department of Geography and Regional Science at the University of Graz in cooperation with the Institute for Hydraulic Engineering and Water Resources Management at Graz University of Technology after successfully finishing the ClimCatch research tasks.

"RunSed-CC- Modelling future runoff and sediment transport in alpine torrents", funded by the ACRP, was created to continue the research of previous studies. Generally, even though severe damages occur due to sediment transport and movement in very steep mountain torrents and streams, only little research or data collection has been carried out in the Austrian and Swiss alps so far (Universität Graz (2018)).

"RunSed-CC will address these knowledge gaps. The project's components are: (1) numerical modelling of current and future runoff based on spatially highly resolved climate scenarios considering a scenario coming close to the "well-below 2.0 ^{o}C" threshold aspired in the Paris Agreement and of contrasting high-end climate change conditions (rcp8.5 emission scenarios); (2) numerical modelling of current and future sediment transport based on modelled runoff and sediment availability; (3) validating the modelling results using the existing data and infrastructure from the pre-project ClimCatch and (4) the transfer of the results to other eastern Alpine torrential catchments. This will lead (5) to the development of future management strategies to tackle the effects of climate change. Furthermore, uncertainties regarding precipitation, runoff, sediment availability and sediment transport will be addressed (Universität Graz (2018))."

2.7 Installed Measuring Systems

Over the course of the years, between 2011 and 2018 (on-going), numerous measuring methods were researched and, if applicable, installed and evaluated. The following paragraphs include information about the measuring cross sections and the technical (hydraulic) methods in use.

A large variety of methods are used in order to investigate the catchment area comprehensively and to grasp the process of this complex project area. These methods were implemented by the team of Sass et al. (2015) during the ClimCatch research project and new methods are added for the research project RunSed-CC:

- Regular geomorphological mapping and Airborne Laser Scans (ALS) are carried out to record the sediment cascades in the catchment area.
- Photogrammetric analyzes and laser scans are used in the Schöttlbach retention basin to measure the total sediment and debris discharge from the catchment area.
- Terrestrial Laser Scans (TLS) are used on a regular basis to quantify geomorphological processes in the project area.
- Colored tracer stones, telemetry stones, MEMS[3] Accelerometer sensors , Sediment Impact Sensors (SIS)[4] and a multiparameter sensor, including a nephelometric turbidity probe, are used to observe the sediment transport.
- Gauging stations are installed to measure the flow and water level of the torrent at several cross sections. Tracer fluids have been in use as well.

The map of the project area in Figure 2.5 shows the measuring methods, that are installed.

In the following paragraphs the three main cross sections for the project area and the installed measuring systems are summed up. The information and facts were gathered from the publications of Barbas (2014), Langer, Stoisser (2016) and Spreitzer (2014). A detailed description of the used measuring methods as well as additional methods will be given in Chapter 3.

[3]MEMS: Micro Electromechanical System accelerometer Sensors

[4]Whilst the operation of the Sediment Impact Sensors is temporarily paused, the MEMS accelerometer have been installed in July 2018. More information is given throughout this thesis.

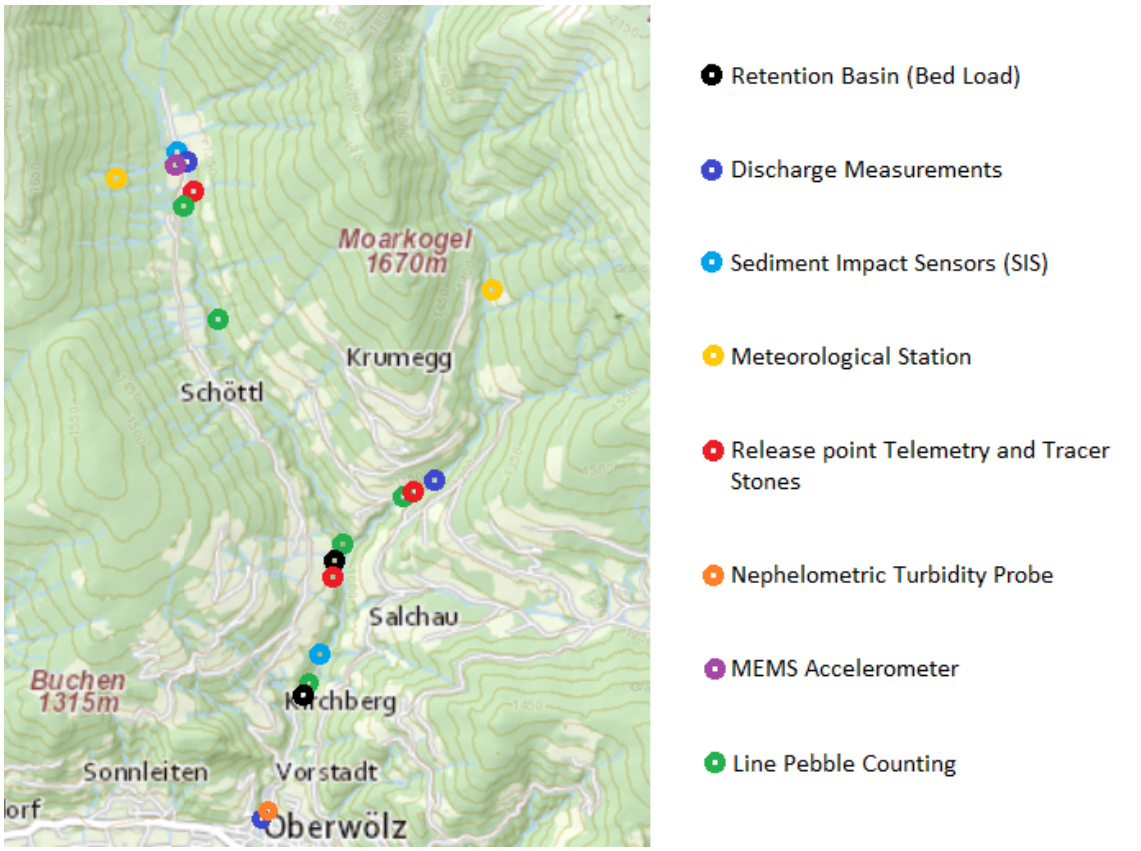

Figure 2.5: *Map (GIS-Steiermark (2018)) of installed measuring methods in the project area (modified from Barbas (2014))*

2.7.1 Hintereggertor - Schöttlbach

When ClimCatch was first initiated, the Hintereggertor cross section was the outlet of the project area, with the most diverse measuring methods. The river reaches rectangular shape and the hardly changing riverbed, thus the crossing bridge provided an appropriate space for long time measurements.

On the bridge (Figure 2.6), a radar gauging station, which measures the flow velocity (Doppler principle) and the water level (Impulse-radar technology), is mounted. Furthermore, a multiparameter sensor, that measures not only the nephelometric turbidity but also the temperature and the conductivity of water, is installed. All measured values are automatically forwarded to a central data collector, which collects the information and transmits it to an FTP server.

Recent gauging, turbidity and conductivity data sets for the period of April 2018 to September 2018 are analyzed in Chapter 5.

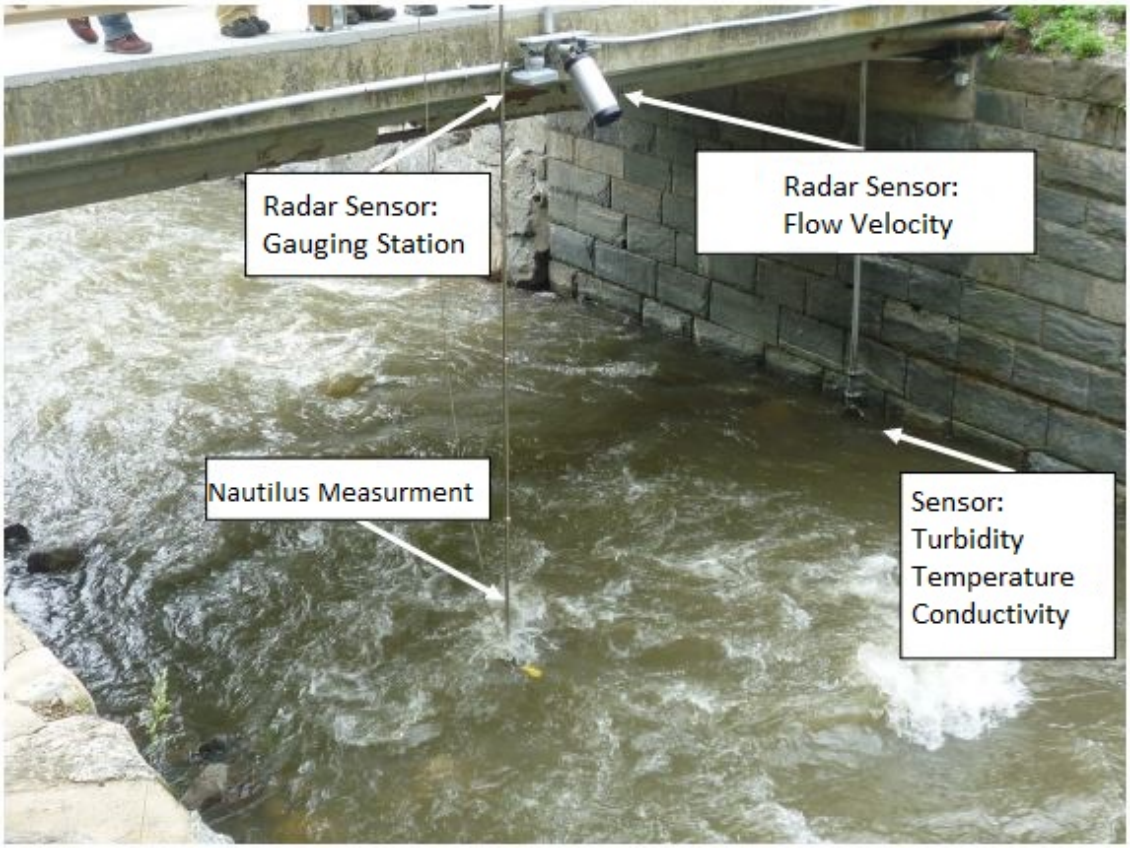

Figure 2.6: *Measuring cross section at the Hintereggertor (modified from Barbas (2014))*

2.7.2 Schöttlkapelle - Schöttlbach

Roughly 7.5 km upstream of the city of Oberwölz, at an elevation of 1195 m a.s.l., the measuring station at the Schöttlkapelle was erected. This location was chosen due to the excellent mounting conditions of the equipment at the bridge, which crosses the Schöttlbach to the other side of the valley, as well as the power supply and accessibility. In Figure 2.7, the cross section can be seen before the construction of a submerged weir and installation of the new set of sensors (MEMS Accelerometers). Just 150 m upstream of this cross section, a meteorological station and a number of Sediment Impact Sensors (SIS) were mounted onto rocks into the river. These sensors were in use for ClimCatch but are not collecting data for RunSed-CC at the moment.

The cross section includes a pressure probe that is mounted on the bridge abutment for water level measurements. Data can easily be transmitted via a contactless infrared transmitter. In consequence of the rather steep stream section and therefore continuously changing riverbed, the gauging station did not work perfectly. Therefore, a threshold was constructed into the riverbed in July 2018. Due to its stable concreted profile, it

Figure 2.7: *Measuring cross section at Schöttkapelle*

shall make discharge measurements more accurate and additionally provides space for ten MEMS Accelerometer Sensors for measurements of sediment transport.

2.7.3 Krumeggerbach

The Krumeggerbach cross section provides the same discharge measurement method as at the Schöttlkapelle. A pressure probe, identical to the Schöttlkapelle probe, is installed at the left bridge abutment. The data can also be transmitted via contactless infrared interface. In 2016, two Sediment Impact Sensors in combination with bed load samplers were installed in the cross section to measure the sediment transport rates. Therefore, a threshold was concreted into the profile. After a severe flood event, however, the left part of the threshold, holding one SIS sensor, was demolished and washed away (see Figure 2.8).

The ever changing riverbed of the Krumeggerbach makes it almost impossible to make valid discharge measurements and calculations due to the constantly shifting rating curve.

Figure 2.8: *Measuring cross section at Krumeggerbach*

3 Research Methods

This chapter gives an overview of the definitions used in this thesis, to explain general measuring methods, basic hydraulic calculations and to get an understanding of the project area and the measuring methods in use in more detail.

3.1 Classification of Rivers

In Austria and in the surrounding alpine regions a river with high inclination, rapidly and strongly changing discharge, thus, a high transport rate of sediment is usually categorized as a mountain torrent, or simply torrent.

The main characteristics of these torrents are a rather small catchment area, flood water events that are caused by heavy rainfall and thunderstorms, a high inclination of the riverbed and tributaries as the main source of debris and sediment input into the system. The main characteristics during a heavy rain event are presented with an increasing discharge in shortest time, vertical erosion of the slopes and the riverbed, transport of large quantities of solids (sediment, debris), frequent mudflows and alluvial deposition of these solids in lower parts of the valley (Barbas (2014)).

In general, a river can be divided into three sections (Figure 3.1) which are described below (GKG-Schweiz (2004)):

- Upper reaches: precipitation is collected in this section of the catchment area and the sediment and debris is mobilized. Due to the steep and elongated river reaches, high flow velocities occur and vertical erosion along the riverbed can happen.
- Middle reaches: also called sediment transport sections or the sediment highways. Due to the decreasing inclination the flow velocities reduce. In the middle reaches the sediment deposition and erosion balance each other out. Gradually, the depth erosion is replaced by the lateral erosion of the riverbed. The river begins to meander and sandbanks can form.

- Lower reaches: the section of sediment deposition. Often, these are the areas where severe damages happen in populated ares due to flooding. Low inclination in the river results in low flow velocities. Therefore, also the grain size of the transported sediment decreases.

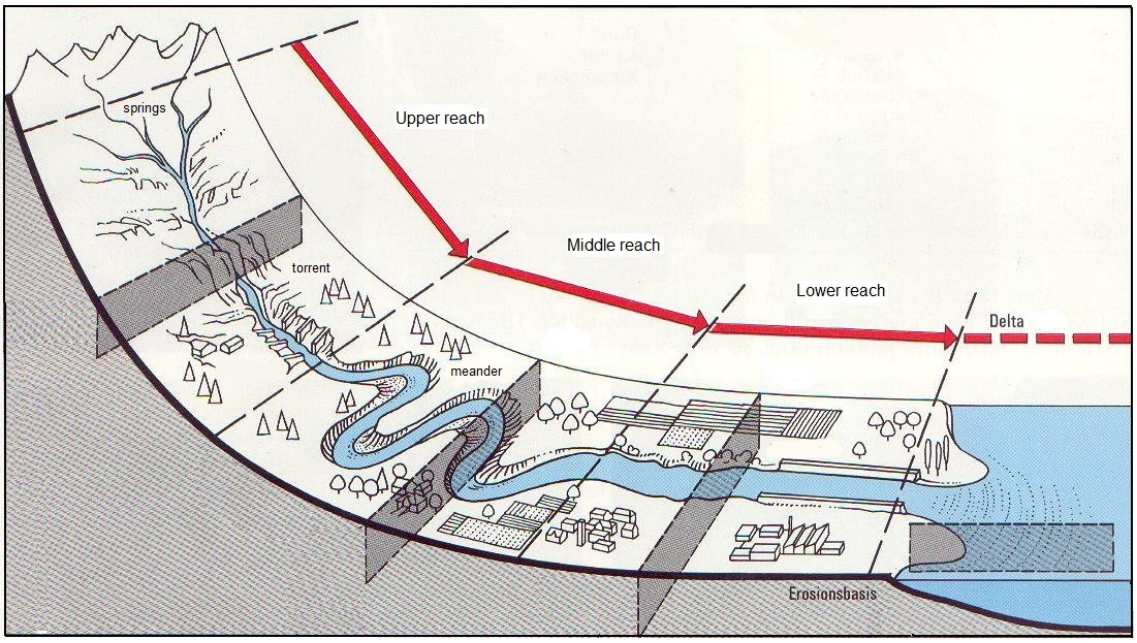

Figure 3.1: *Course of a river (GKG-Schweiz (2004))*

3.1.1 River Morphology

The aim of every river, stream and creek is to transport water downwards a riverbed with a balanced and steady inclination. Since this is almost never present due to the tectonic structure and the different geologies, the river has to shape the landscape with the help of three processes: erosion, transport and deposition (GKG-Schweiz (2004)).

As mentioned in Section 3.1, erosion processes define the course of a river by eroding the riverbed or the slopes. This vertical erosion effect is dependent on the inclination of the riverbed, the discharge and the geology of the riverbed and the to be transported material.The lateral erosion is the removal of the material resulting from weathering, erosion and slope erosion. If the lateral erosion is stronger than the vertical erosion, the river is not able to transport the entire mass of the deposited material of the slopes.

Erosion in a river can only take place if there is a sufficient amount of material that can be transported. Additionally, when the flow velocities are low, sediment mass is deposited and instead of erosion, sediment accumulation occurs (GKG-Schweiz (2004)).

The project areas valley form can be described as a V-shaped valley (German: Kerbtal). Its typical V-shape can be seen in Figure 3.2. The GKG-Schweiz (2004) says, that in a V-shaped valley, the erosion of the valley slope is about the same due to the downward rushing water as due to the vertical erosion of the riverbed. This erosion process leads to a uniform removal of material and gives the valley its typical cross section.

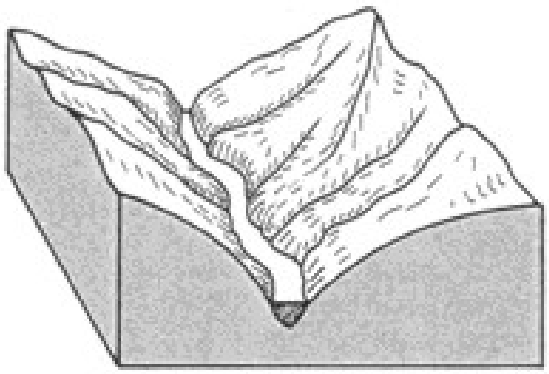

Figure 3.2: *V-shaped valley (GKG-Schweiz (2004))*

3.1.2 Alpine Mountain Rivers and Torrents

Rickenmann (2016) found that a distinction between mountain river and torrents can be made. In Figure 3.3 the torrent and mountain river characteristics are shown.
In general, they can be differentiated by the processes of either debris flow or fluvial sediment transport, the inclination and the morphology of the riverbed, the sediment storage in the bed as well as the lateral sediment input of the river. The light gray areas show the increasing and decreasing importance of the sediment storage in the riverbed and the lateral input of sediment.

Due to this comparison the project areas river is classified as a torrent from its spring in the mountains to the Schöttlkapelle and some 2 km downstream with approximately 6% of inclination, boulders and bedrock in the river. It can be compared to a mountain river from there on downwards to the Hintereggertor with its more stable and uniform geometry and occurrence of pools and bars and a decreasing inclination.

3.2 Sedimentological Parameters

Sediment transport in alpine water courses are highly influenced by the shape, geometry and proportion of the grain as well as the distribution of the grain size. Considering the large variability of grain size distribution in a stretch of a river reach and over a course

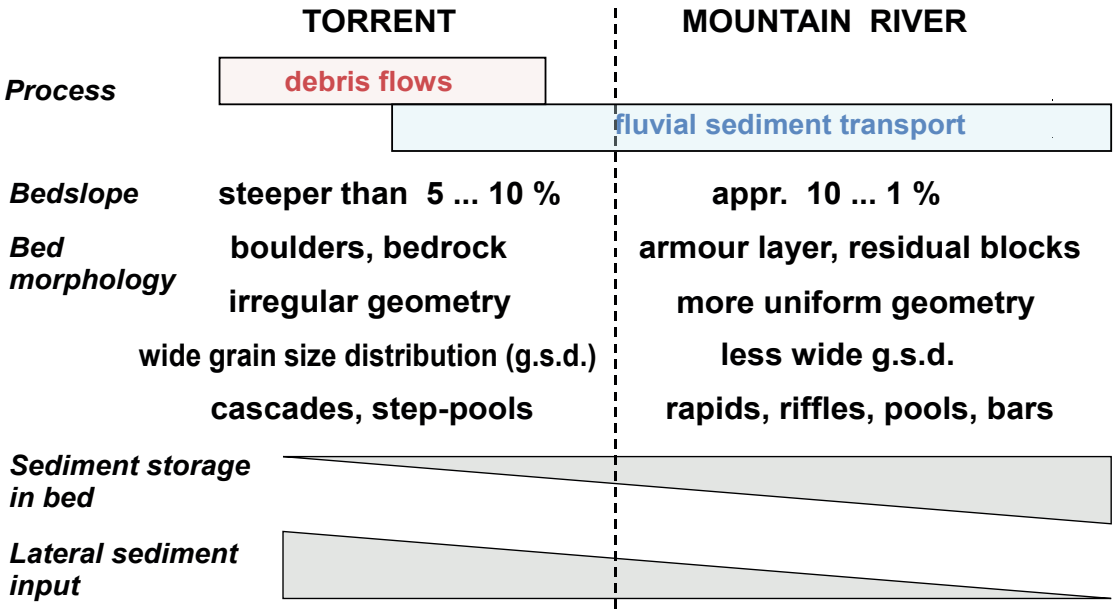

Figure 3.3: *Distinction between torrent and mountain stream. (Rickenmann (2016))*

of time, making an accurate statement for a representative grain size distribution is a challenging task.

For the computation of sediment transport and the discharge in a river, information about characteristic grain diameters are required. These diameters are needed for evaluating the flow resistance, the efficiency of the transport and the start of mobilization, the latter benefiting also from information about the grain shape. When researching a cross section, the information that is gained is very limited in its spacial and temporal accountability. The resulting grain size distribution as well as the hydraulic conditions and bedload transport information represents only a very limited, almost static, time span. The dynamic changes of the sedimentological conditions in a riverbed are only shown partially and for a very limited time (Rickenmann (2016)).

3.2.1 Grain Size Distribution

As explained by Rickenmann (2016) and mentioned before, the grain size distribution measured in a cross section is only of spatial and temporal accountability. To reduce the error of the grain size distribution of the surface layer and to reduce spacial variability, it is important to divide the to be assessed river reach into the river bed and banks. Additionally, it is advised to investigate morphologically important elements such as occurring pools, steps, rapids and gravel banks in the adjacent area (proportional relevant area).
The variability over time is dependent on the process dynamics over the course of a trans-

port event. An appropriate conclusion can only be made after comparing several transport events and by using a combination of measuring techniques.

3.2.2 Grain Shape

The grain shape, amongst other factors, influences the transport of sediment to a great extent. Not only is the start of mobilization of the grain affected by it, it also influences the transport process itself (Rickenmann (2016)). Dependent on the mineralogy and the rock stratum of the grain and the prevailing transport and weathering conditions, different grain roundings are to be expected. A spectrum of sediment distinguished by sphericity[1] and roundness can be seen in Figure 3.4. Despite the categorization below, grain shape can also be determined by the axis ratio (long-, middle-, short axis). This results in e.g. platy, stalky or globular grains (Petrograph (2014)).

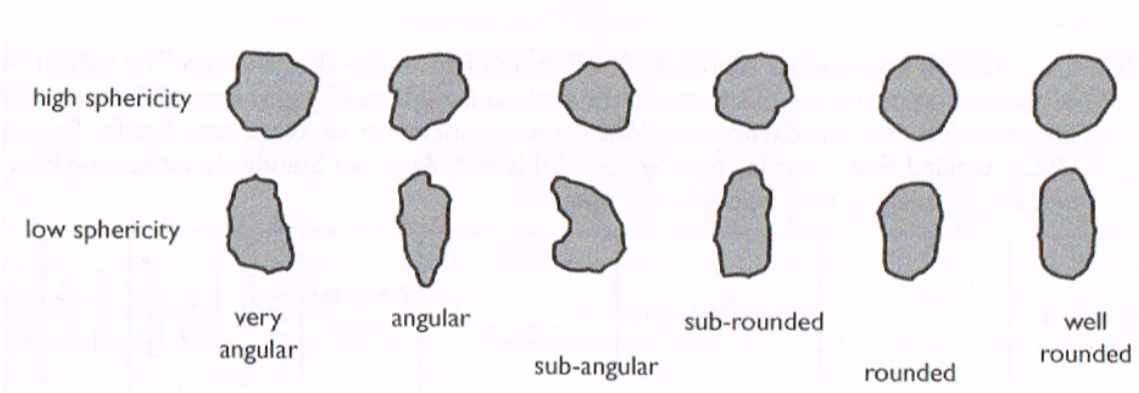

Figure 3.4: *Grain shape divided by roundness and sphericity (Rickenmann (2016))*

For example, with a plate-like shape of the grain in the fluvial-formed bed, a structure comparable to a roof-tile surface, is able to develop. This leads to a reduction of the effective grain roughness and allows for more sediment transport to happen (Rickenmann (2016)).

3.3 Suspended Sediment

Suspended sediment (suspension load) is flowing in the water, since either the density of the solid particles is lower than that of the water, or due to turbulence, respectfully the particle shape, a lowering of these solids onto the riverbed is not possible (Spreitzer (2014)). This means that a large amount of sediment is transported in the flowing water, that does not settle onto the riverbed, where most bed load and sediment transport measurements

[1] Sphericity is a measure of how spherical a grain is.

are done. In general, natural waters contain a vast variety of material. This transported material can lead to turbidity of the water. This includes, but are not limited to clays, silts, organic water, inorganic matter, vegetation and even living organisms that produce a large variety of particle sizes and optical obstructions. These solids hinder the transmittance of light through the water body, which gives the basis for turbidity measurements. Naturally, turbidity can therefore not be defined universally, but rather has to be calibrated for all water bodies separately (Bartby (2015)).

3.3.1 Principles of Turbidity Measurements

Turbidity can be measured by using an electric turbidity meter or a turbidity tube and is usually measured in Nephelometric Turbidity Units (NTU). Apart from that, many other units including Formzin Nephelometric Units (FNU) and Formazin Attenuation Unit (FAU) are frequently used. The table below shows all the common measuring units and the description of technology that is in use.

Table 3.1: *Units for traceability of technology (Sadar (2002a) modified)*

UNIT	**Name**	**Description of compliant technology**
NTU	Nephelometric Turbidity Unit	White light, 90 degree detection only
NTU$_R$	Ratio Nephelometric Turbidity Unit	White Light, 90 degree detection with additional correction detectors
FNU	Formazin Nephelometric Unit	860 nm Light (near IR) with 90degree detection (ISO7027 compliance)
FNU$_R$	Formazin Nephelometric Unit	860 nm Light with 90degree detection and additional interference correction detectors
FNU$_{2B}$	Formazin Nephelometric Unit Dual Beam Detection Technology	4 beam IR Detection utilizing 2 light sources and two detectors
FNU$_{BS}$	Formazin Nephelometric Unit– using Backscatter Detection	860 nm detection angle with a backscatter detector (270 –285) degrees angle relative to the incident beam
FAU$_{xxx-nm}$	Formazin Attenuation Unit using a defined wavelength	The detection angle is 180 degrees of the incident light beam

3.3.2 Principle of the Turbidimeter

As light gets directed into a fluid with suspended particles, its intensity is reduced due to scattering and absorption of rays. Depending on the system that is used, detectors collect the back-scattered light, which results in qualitative turbidity measurements. These measurements do not necessarily express the quantity of suspended solids, but are rather an aggregate measure to detect the amount of light that is either scattered or transmitted through by the particles in a body of water (Sadar (2002b)).

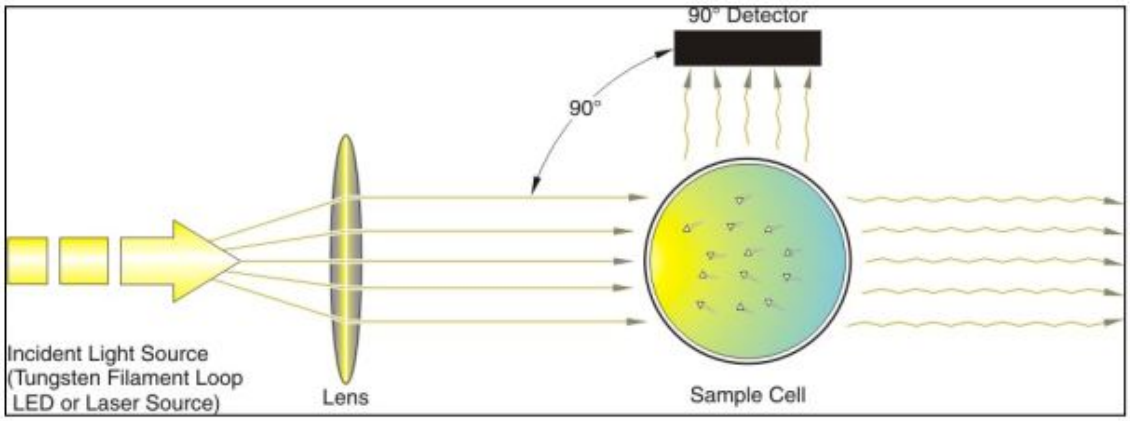

Figure 3.5: *Optical Geometry as used for the nephelometric turbidity measurements (Sadar (n.A))*

The schematic drawing in Figure 3.5 illustrates the structure of a nephelometric turbidimeter with a 90^o detector and a light source. This setup is used in most nephelometric turbidity sensors because of the sensitivity to the wide range of particle sizes due to the 90^o angle of the detector.

Instrument technology is advancing fast for some decades now, resulting in a large number of measurement techniques and sensor designs. Most of these improvement strategies address interferences and other inconveniences that occurred with previous systems. New approaches, like a change of light source and detector designs, have been tested. In Table 3.2 common turbidimeter design criteria can be found. The main goal is to reduce or eliminate the impact of confounders in the water such as bubbles, color, path length, absorption and stray light on the measuring result.

3.3.3 Calibration and Evaluation Process

As mentioned above, due to the unique composition of water, the resulting evaluation curves for proper readings have to be defined independently for each body of water. In

Table 3.2: *Design criteria for turbidimeters (Sadar (2002b))*

Incident Light Sources	• Incandescent light source • LED (Light Emitting Diode) • Laser-based light source
Detection Angle	• 90 degree detection angle • Attenuated detection angle (180 degree) • Backscatter detection angle
Number of Detectors	• Multiple detection angles • Dual light source detector

addition, turbidity values can vary in between river reaches, so it is advisable to take probes in the area of your sensors stationing and start the calibration process accordingly. For an accurate calibration Sadar (2002b) advices to verify the conducted test with either the same or similar technology (at least light source and detector angle).

More on the calibration and evaluation process and measurement readings for the project area can be found in Section 4.2.

3.4 Discharge Measurements

The aim of the discharge measurement is to determine the quantity of water Q that flows through a selected cross section (measuring cross section) of a watercourse per time unit. The discharge of a river, stream or any body of water can be assessed in a high number of ways. Two possible ways to categorize them is by the measuring methods as listed below (Dyck, Peschke (1995) and Pertl (2004)).

- Direct measurements
  - Volumetric or vessel measurement
- Indirect measurements
  - Pitot pipe
  - Venturi pipe
  - Measuring weirs

  - Dilution measurements with tracer fluids
  - Measurements of cross section and velocity
    * Magnetic inductive
    * Current meter
    * Ultrasonic measurements
    * Water level measurements at fixed hydraulic conditions
  - Others

The ever changing riverbeds of mountain torrents provide only a few possible cross sections to install a gauging station (measuring station) for discharge measurements. Ideally, the cross section should be trapezoidal in shape and the riverbed should be stable against erosion. If none of these requirements can be met, a compromise with the least possible impact on the measurements accuracy shall be chosen (Dyck, Peschke (1995) and Pertl (2004)).

As some of these principles were used in the project area during previous studies or during this thesis a more detailed explanation will be given about the technology and theoretical background. Furthermore, the data that has been collected for the Schöttlbach during 2014 and 2016 will be summed up for each measuring device.

3.4.1 Dilution Measurements with Tracer Fluids

Particularly in alpine areas, especially in mountain torrents, meteorological limits are encountered when using certain measurement devices in the often very rough waters with turbulent outflow conditions. Alternatively, so-called ”tracer dilution methods” are available.

Basically, the tracer systems can be distinguished by the type of tracer material used and the way the material is induced into the water. The most commonly used tracers in practice are sodium chloride (common salt) and fluorescent dyes as well as radioactive materials. Should any other tracer be chosen, Fürst, Jugovic (2009) advices to consider the following key aspects:

- No risk to health
- High water solubility
- Not present in natural waters, or only in low concentrations

- Chemical and physical stability
- Detectable in the lowest concentration
- Time-saving and simple measuring technology
- Low price

As mentioned before the inducing process plays a significant role as well. The tracer solution can be added continuously in a constant amount and concentration or momentarily, by adding the total amount of tracer solution at once (integration procedure).

Continuous Addition of Solution: A constant tracer flow $[q]$ of known concentration $[C_1]$ is added to the flowing water until a constant concentration $[C_2]$ is established in the measuring cross-section after complete mixing with the water.

Momentary Addition of Solution: The total amount of tracer solution m (m = volume times concentration) is added at once to the flowing water with the initial concentration $[C_0]$. After complete mixing with the water, the desired flow rate is given by the integral of the change in concentration $[C_t - C_0]$ over the time interval $[t]$ of the tracer cloud through the measuring cross-section (Fürst, Jugovic (2009)).

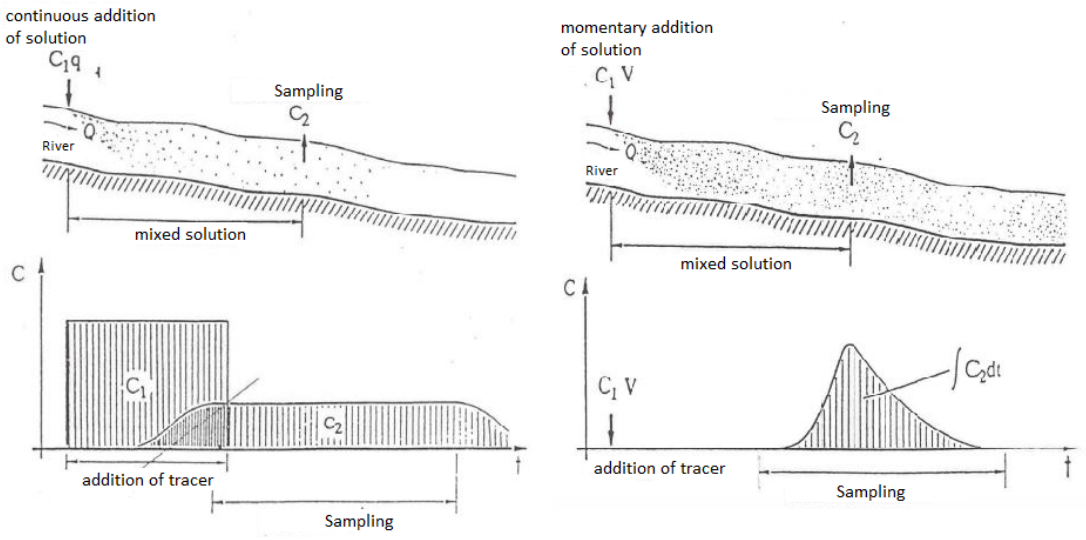

Figure 3.6: *Inducing tracer solution. Left: continuously; Right: momentary (Fürst, Jugovic (2009) modified)*

3.4.1.1 Application of the Tracer Method in Oberwölz

Unless otherwise noted, the following paragraphs refer to the tracer measurements done by Spreitzer (2014) during the research for his master thesis.

For the measurements a common salt tracer was used and the solution got induced momentarily into the river Schöttlbach. First, the flow had to be estimated to calculate the concentration of the tracer solution. It is recommended to add approximately 0.5 kg of salt to 0.1 m^3/s of water. In a second step the measuring device with the measuring probes was calibrated to fit the conditions of the river, since every body of water has a different ground conductivity.

Generally, it can be said, that the purer the water, the lower the electrical conductivity. After a successful calibration of the probes, weights were attached to the probes and they were placed into the river. The appropriate amount of salt, which is adjusted to the flow of the river, should first be dissolved in a bucket approximately 100 m upstream of the measuring point (position of the measuring probes) and then at once ”momentarily” added to the river. At this point the measuring device is activated and it registers an increase in the conductivity of the water and can therefore draw conclusions about the discharge via the entered flow path and salt concentration. When the salt concentration has completely vanished in the river and the conductivity values have reached their initial values, the measurements can be stopped and the device will issue the flow values instantaneously.

Figure 3.7: *Salttracer equipment (Spreitzer (2014) modified)*

Unfortunately, the results from the tracer measurements did not correlate well with the values from the flow rate curve of the Schöttlkapelle from 2014. This could be due to flood events that changed the morphology of the riverbed after the rating curve was created and shows again that flow rate curves for mountain torrents need to get adjusted very frequently to receive useful information.

3.4.2 Measurements of Cross Section and Velocity

In general, this measurement method is used to determine the mean flow velocity in an associated cross section. The number of vertical measuring paths, as well as the measuring points per path, depend on the desired accuracy, the shape of the channel, the water width as well as the velocity ratios (super-critical, sub-critical flow). The measuring time per to be evaluated point should be chosen between 15 and 60 seconds. Figure 3.8 figuratively shows the cross-section of the river reach, as well as the velocity distribution at the measuring paths (Dyck, Peschke (1995)).

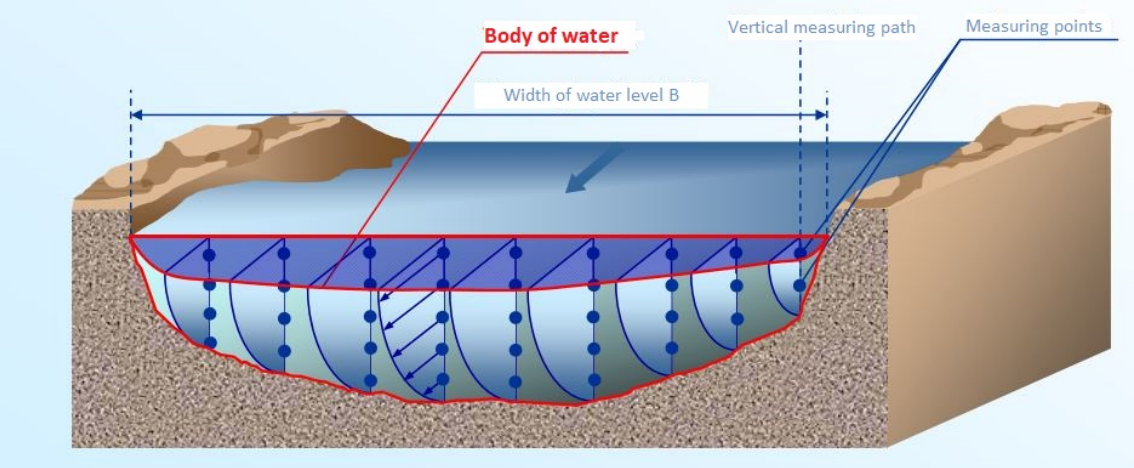

Figure 3.8: *Sketch of the velocity distribution in cross section (Fürst, Jugovic (2009))*

Measuring the mean velocity can be done with a magnetic inductive device, a current meter or by using ultrasonic measurement devices such as the ADCP (Doppler principle). Technically, all of them except the ADCP can be used in mountain torrents and are described in the following paragraphs.

3.4.2.1 Magnetic Inductive

Early records date back to 1939, when the first magnetic-inductive flow meter has been used. The discoverer of this physical phenomenon was the English physicist Michael Faraday (1791 - 1867). It was his discovery, that in a conductive metal rod with a length L, that is moved at a certain velocity v through a magnetic field B, electrical charges are shifted and thereby an electric voltage U_e of a few millivolts is generated between the ends of the metal rods. The size of the induced measurement voltage is directly proportional to the movement speed, the strength of the magnetic field and the length of the metal rod as seen in Eq. 3.1 (Pertl (2004) and Altendorf, Stauss (2003)).

$$U_e = B \times L \times v \tag{3.1}$$

U_e = Induced Voltage
B = magnetic field
L = Length of Conductor respectively distance of electrodes
v = Velocity of the Conductor, in correspondence to the flow velocity of water

With the geometry of the measuring cross section A, the discharge can be calculated using the equation for Continuity as shown in Eq. 3.2.

$$Q = v \times A = \frac{U_e}{B \times L} \times A \tag{3.2}$$

For the assessment of the velocity and discharge at the project area in Oberwölz a Nautilus probe is used. More about the measuring aspects and results are described in Section 4.1.

3.4.2.2 Current Meter

When using a current meter (Figure 3.9), vertical paths with measuring points along them are chosen in a frequent distance over the whole width of the river. In this process the water depth and flow velocity are measured at each point. Therefore, the sensors head is turned into the flow direction and the current meter records the number of revolutions, which represents the measure of the flow rate (Fürst, Jugovic (2009), Pertl (2004), Altendorf, Stauss (2003) and OTT Hydromet GmbH (2018)).

Figure 3.9: *Current meter (OTT Hydromet GmbH (2018))*

Depending on the application, it is possible to guide the wing on a measuring rod or, when mounted on a load weight such as a stationary cable crane or measuring vessel, as a floating wing. Current meter measurements are suitable for small creeks, shallow rivers as well as deeper bodies of water with flow velocities of up to 10 m/s. However, water depths over two meters shall be avoided (OTT Hydromet GmbH (2018)). When applying current meter measurements in mountain torrents, ideally, a measuring rod is used either by a person standing in the river holding the rod or, if possible, lowered from a bridge (Langer, Stoisser (2016)).

3.4.2.3 Ultrasonic Measurements

Since the beginning of the 70s, the ultrasound method has been used to determine the flow in water. This method is based on the principle, that a sound signal in the flowing water propagates faster with the flow, than against the flow (Dyck, Peschke (1995)). Generally, ultrasonic flow measurements are done by sending high-frequency sounds waves through a fluid. This can be done by Doppler method or through transit time method, which will be described below (Altendorf, Stauss (2003)).

When using the Transit Time Method Altendorf, Stauss (2003) say, that two sensor simultaneously transmit and receive ultrasonic pulses or acoustic signals. Dependent on the flow, the ultrasonic waves require different transit times in order to reach the other sensor in flowing water. Considering, that the sensor distance is known, the measured transit time difference of the pulse is directly proportional to the flow velocity. With the aid of a transmitter, the ultrasound sensors are stimulated to emit ultrasound and in addition, this measures the transit time difference.

The Doppler Method to determine flow is based on the ”Acoustic-Doppler-Effect”. Most commonly used for flow measurements nowadays are the Acoustic Doppler Current Profiler (ADCP). The ultrasonic pulses emitted by the ADCP are reflected by particles in the water and then received back as an echo. The movement of the particles is determined by the frequency shift between the transmitted and received signal. The ADCP Boat (OTT Q Liner2) from OTT Hydromet GmbH (2018) is suitable for bodies of water of up to 20 m in depth.

The ADCP (Figure 3.10) is mounted on a small boat, which can be guided from one side of the river to the other, the path can be chosen freely, however, the slower the boat is guided the more data is collected, thus the more accurate are the results. When guiding the sensor over the river, the flow velocity, the velocity of the boat and the water depth are measured (OTT Hydromet GmbH (2018))

The flow calculation is then based on measurements of vertical flow velocity profiles (Compare: Current meter and magnetic inductive) and is done with a software directly at site. This give results for the profile of the riverbed, flow velocity distribution and discharge in a very short time.

Figure 3.10: *Acoustic Doppler Current Profiler*

3.4.2.4 Water Level Measurements at Fixed Hydraulic Conditions

Barbas (2014), Altendorf, Stauss (2003) and Pertl (2004) say, that the water level can be measured analog as well as digital with fixed gauges in the river profile, with sensors of different technologies such as radar, ultrasonic or with pressure probes. These measurements build the basis for the calculation of a function for the rating curve. Generally, the rating curve shows the relation between the water level and the discharge in a river. To receive a fitting rating curve it is of importance to choose a cross section in the river where the riverbed is stable, the hydraulic conditions do not change and easy accessibility is given. The accuracy of the rating curve is also dependent on the number and preciseness of single reference measurements (e.g. Nautilus measurements, wing measurements). Through inter- and extrapolation and hydraulic as well as geometric information a rating curve can be created either manually or with the aid of computer programs such as the bed load analyzer[2] (Fleissner et al. (2014)) or similar.

More information on the radar sensor at the Schöttlbach can be found in Section 4.3.

[2]Program download link `https://www.tugraz.at/fileadmin/user_upload/Institute/IWB/Lehre/Software/BedLoadAnalyzer/BedLoadAnalyzer2.1_build_win.zip` or go to `https://www.tugraz.at/en/institutes/iwb/studying/software/bedloadanalyzer/` for more information.

3.5 Bed load Measurements

Measuring bed load can result in a large number of possibilities, but not every method is suitable for the task. Assets and drawbacks can be found in every system. When choosing a suitable method for measuring bed load movement, factors like the river morphology, the results the system delivers, the available budget or the duration of measurements have to be taken into account. In many cases a combination of measuring systems are advisable (Habersack et al. (2012)).

These measuring systems must meet numerous requirements, particularly when being installed in an alpine mountain torrent where it has to withstand drastic climatic conditions.

Barbas (2014) categorizes the measuring systems as listed below:

- Direct Measuring Systems
  - Bed load sampler
  - Sediment traps
  - Sediment slots
- Indirect Measuring Systems
  - Hydrophone
  - Geophone
  - Tracing or telemetry stones
  - Sediment Impact Sensor (SIS) measurements
  - Accelerometer (MEMS)

which will be described in short detail below. It is important to understand, that the natural flow and sediment transport should not be disturbed by the measurement in any way, otherwise the results will be tampered and unrealistic.
Generally, it is possible to measure the whole sediment load with direct measuring systems. For that to happen, big dam-like structures have to get dredged and analyzed.

Each measuring method has its qualities and limits, which makes it even more necessary to find a combination between indirect and direct measuring techniques (Habersack et al. (2012)).

3.5.1 Direct Measuring Systems

Direct measuring systems describe techniques that actively collect sediment with the help of bed load samplers, containers and submerged chambers acting as sediment traps in thresholds. For these systems the biggest transported grain size in the investigated river reach should be considered for dimensioning purposes (Barbas (2014) and Turowski (2011)). Direct measuring systems are used selectively and provide an insight into sediment transport and grain size distribution over a short period of time (Habersack et al. (2012)).

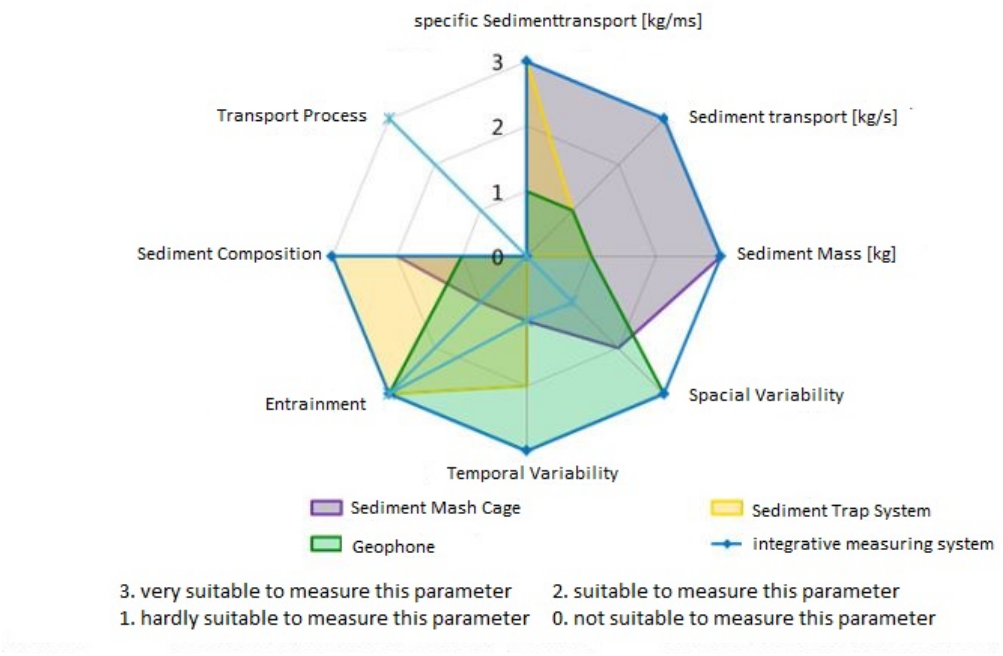

Figure 3.11: *Assessment sediment measuring systems- integrative system (Habersack et al. (2012) modified)*

Figure 3.11 shows the need of an integrative measuring system. Only when a combination of sediment measuring systems are in place, good quality data can be collected and used for further studies and calculations (Habersack et al. (2012)).

3.5.1.1 Bed Load Samplers

Depending on the catchment area and predominant local conditions, different bed load samplers are to be used. In Figure 3.12 and Figure 3.13 some construction types can be seen. These cages are lowered onto the river bed or floating can be stabilized with ropes and sediment is collected over a certain time interval.

These measurements result in grain size distribution and transport rate (Turowski (2011)). The main advantage of bed load samplers is their high flexibility and movability. A drawback can be, that bed load samplers cannot be used for high discharges, as flood events in alpine torrents carry wooden logs and big, heavy rocks, that can destroy them (Habersack et al. (2012)).

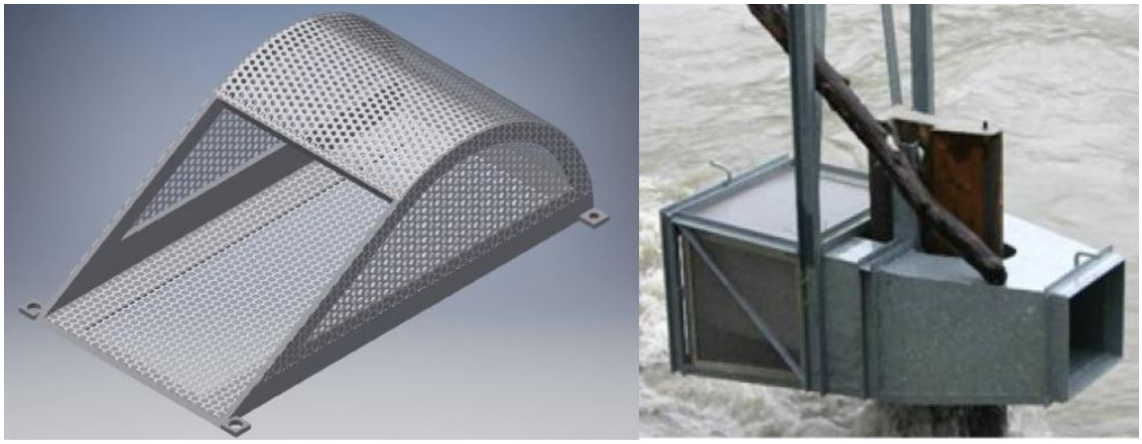

Figure 3.12: *Left: Bed load sampler design Oberwölz (Langer, Stoisser (2016)); Right: TIWAG collector (Habersack et al. (2012))*

Bed load samplers, like the Helley-Smith collector as seen in Figure 3.13, still play an important role in today's sediment measurements. Due to the conical expansion of the collecting cage a suction effect is produced, which balances the resistance that is produced by the collecting cage. The velocity of the entering suspension is therefore almost equal compared to the flow velocity of the stream (Habersack (1997)).

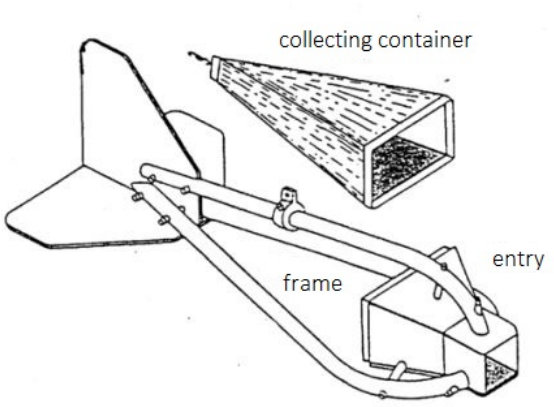

Figure 3.13: *Large Helley-Smith collector (DVWK (1992) modified)*

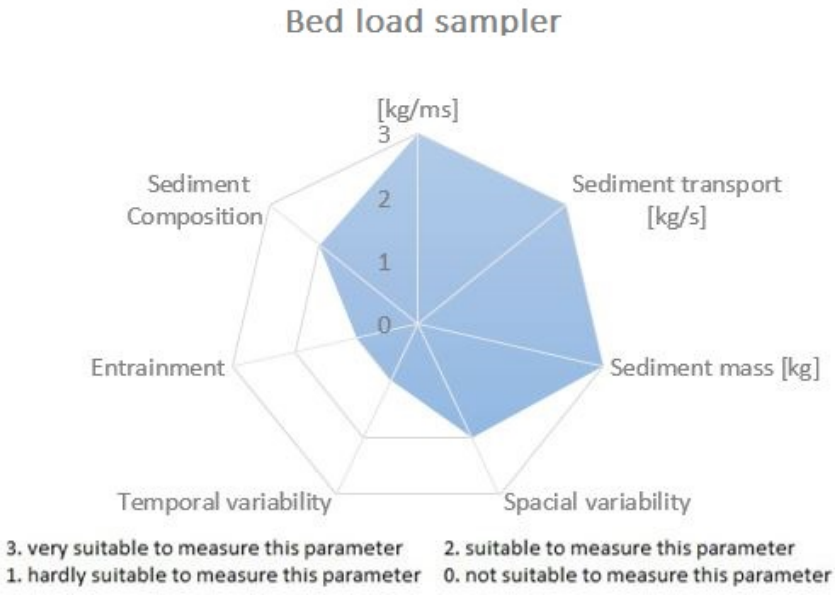

Figure 3.14: *Assessment sediment transport system- sediment bed load sampler (Habersack et al. (2012) modified)*

3.5.1.2 Sediment Trap System

Generally, fixed sediment traps are understood to be collecting bins or slots, that are submerged into the bottom of the river bed or built into concrete thresholds into rivers. They need to be emptied manually after a period of time. For the design it is crucial to know the sequence in which the pebbles and stones bounce along the riverbed. Additionally, these systems need to be flush cast into the riverbed so the natural flow remains undisturbed (Habersack (1997)).

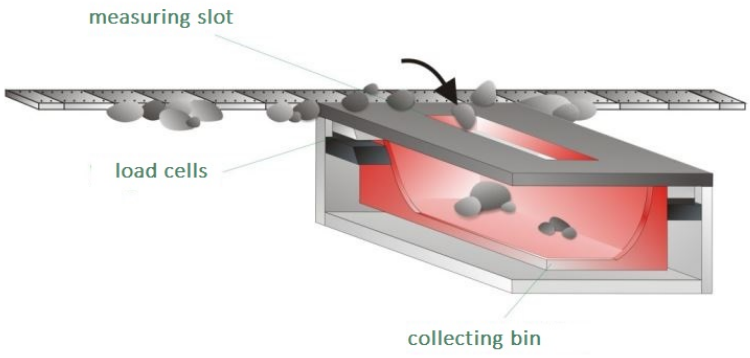

Figure 3.15: *Sketch of a sediment trap system (Habersack et al. (2012))*

Modern bin trapping systems as seen in Figure 3.15, are equipped with load cells, which measure the weight of the collected mass in [kg] as well as hydraulic mechanisms, that

automatically opens slots in the cover in case of an event. Over the course of the flood event, the sediment mass is then measured and logged.

In Figure 3.16 below an incident log of mass (under buoyancy) over time can be found as an example. This log was part of the sediment transport study in Dellach, on the River Drau in 2009 (Habersack et al. (2012)).

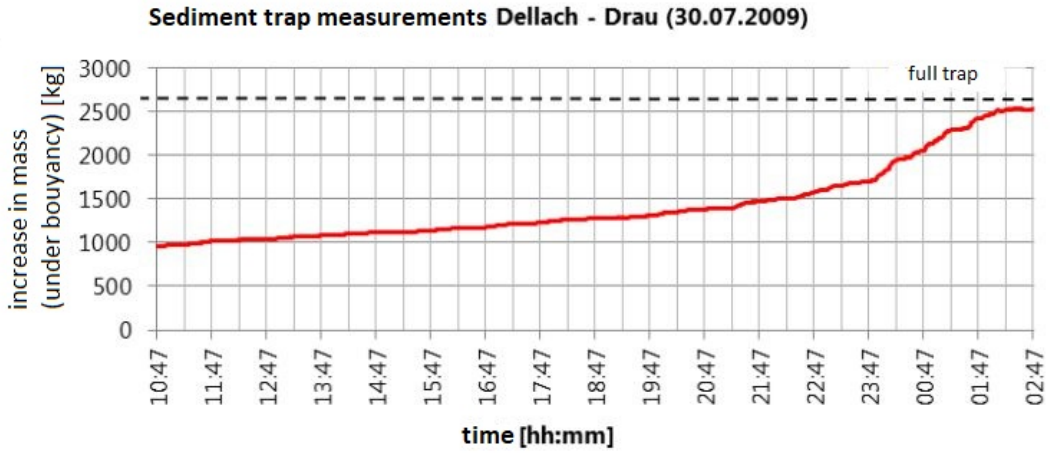

Figure 3.16: *Example log for a fixed sediment trap. (Habersack et al. (2012))*

Sediment slots as shown in the system sketch Figure 3.17 need to be constructed over the whole cross section of the river bed. Unfortunately, this is only possible for small rivers and streams and only partly suitable for mountain torrents (Barbas (2014)).

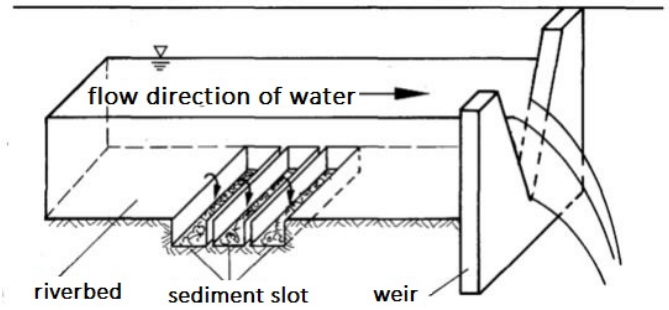

Figure 3.17: *Sketch of sediment slot system (DVWK (1992) modified)*

The main advantages of the sediment trap systems include automated measurements over a longer period of time and that, compared to the bed load samplers, measurements are possible even for high discharges. Apart from receiving information about sediment drift over the whole cross section of the river, the sediment trap also produces insight on texture of the material, as well as the entrainment of the sediment.

Due to the stationary location of the traps the sediment drift can only be measured for this spot, therefore, sediment transport and mass cannot get evaluated with this system alone. A net chart below in Figure 3.18 shows the fields in which the sediment traps are most useful (Habersack et al. (2012)).

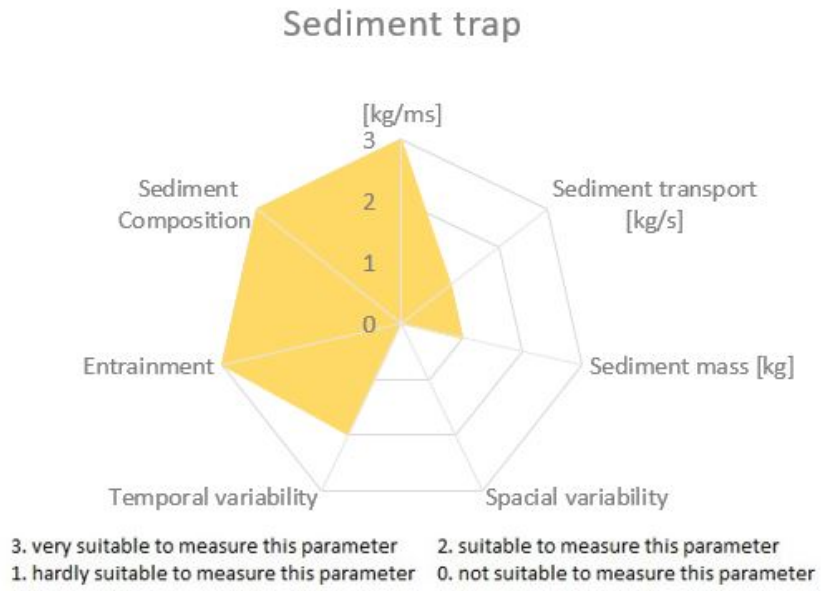

Figure 3.18: *Assessment sediment transport system - fixed sediment traps. (Habersack et al. (2012) modified)*

3.5.2 Indirect Measuring System

Indirect methods for sediment measurements use non-invasive techniques to minimize the disruption in sediment and water flow. These techniques are not comparable to direct measuring systems as they measure the transport itself, when indirect methods, measure the activity of the transport. The activity of the transport has been studied numerous times over the last decades, but the main background can be divided into four measuring groups (Turowski (2011)).

Turowski (2011) claims, that indirect measurements can be divided as follows:

- Acoustic system (sound)
- Impacts
- Noise in a field (magnetic)
- Echo (sonar)

In the following paragraphs a description of functionality for some frequently used systems can be found. The experience and lessons learned from previous studies conducted in the project area, as well as similar indirect measurements in different project areas are described.

3.5.2.1 Hydrophone

A hydrophone is a typical acoustic measuring system and measurements can either be done in an indirect or passive manner (Belleudy (2015) and Langer, Stoisser (2016)).

- When measuring indirectly, impacts caused by collision of sediment onto a steel plate are being monitored by high-sensitivity microphones and later recalculated into sediment mass.
- Passive measuring methods use the sound that is produced by the sediment and record the data with high-resolution in the gauging station. This method is and excellent tool for measuring sediment mass in rivers, however, the installation in mountain torrents is not advisable, due to high bed load transport an overlay of noise signals can occur.

Both techniques require thorough calibration measurements with sediment traps or bed load samplers, otherwise useful information about sediment transport is hard to gain (Langer, Stoisser (2016)).

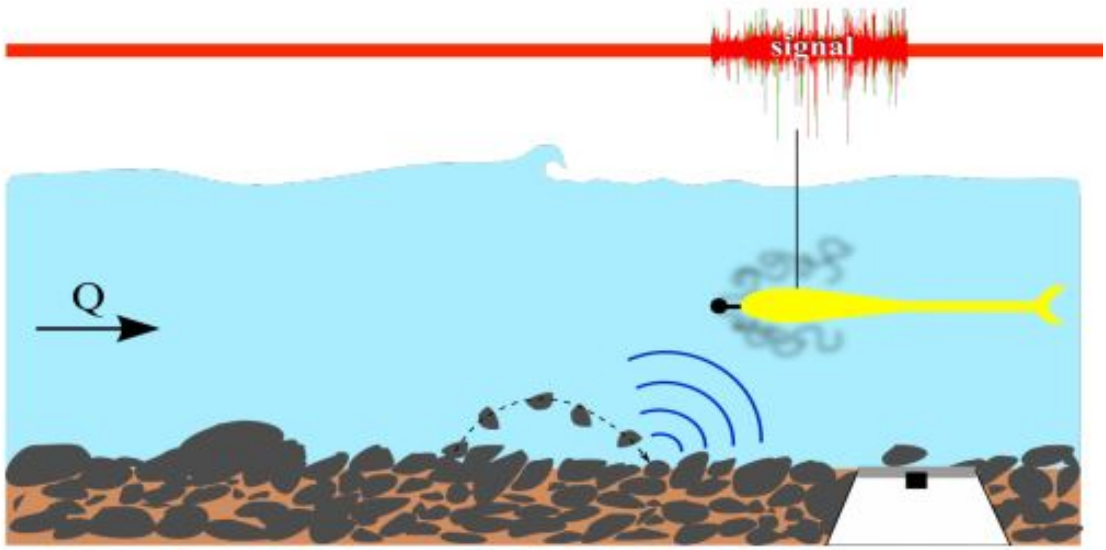

Figure 3.19: *Schematic setup of a hydrophone with sediment traps (Belleudy (2015))*

A main advantage of the hydrophone is, that measurements can be recorded continuously and it is fairly feasible during floods. It can be placed anywhere in the cross section due to the integrative system. A drawback is the sophisticated calibration with direct measuring systems and that small particles cannot be registered. A schematic graph for a hydrophone measurement is shown in Figure 3.19 and Figure 3.20 (Belleudy (2015)).

3.5.2.2 Geophone

Another main component of the indirect measuring systems are the geophones. Geophones can be mounted onto steel plates and submerged into the riverbed, periodically, over the whole cross section of the river. Sediment that is being transported over the steel plates create vibration, which is then recognized by the geophone (Turowski et al. (2008)).

The geophones interior is based on the physical principle of forced oscillation with a coil and a magnet (Langer, Stoisser (2016)). In Figure 3.20 the sensor is shown with a typical impact graph.

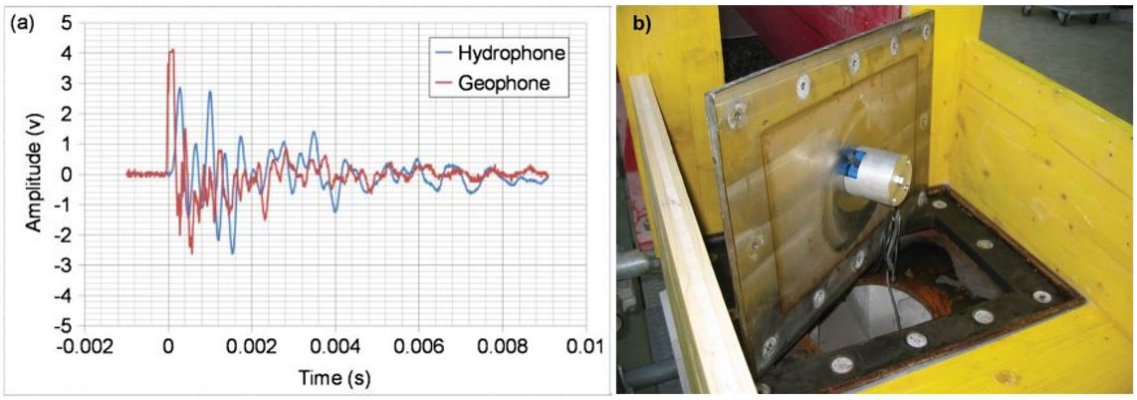

Figure 3.20: *(a)Geophone for Erlenbach and (b)sample graph. (Rickenmann et al. (2012))*

Whenever sediment or debris is transported over the steel plate, the magnet is being taken out of its initial position either lengthening or compressing the coil, which results in a shift in the sensor, thus electrical energy, proportional to the impact, is being produced. When an impact occurs on the steel plate, vibrations are recorded. The produced signal is transformed into a fluctuation of voltage. If a threshold value is reached an impulse will be registered and recorded on a data logger (Turowski et al. (2008)).

Similar to the hydrophone, a thorough calibration with direct measuring systems, such as a sediment trap system or bed load samplers, needs to be done to gain data with high quality (Turowski et al. (2008)).

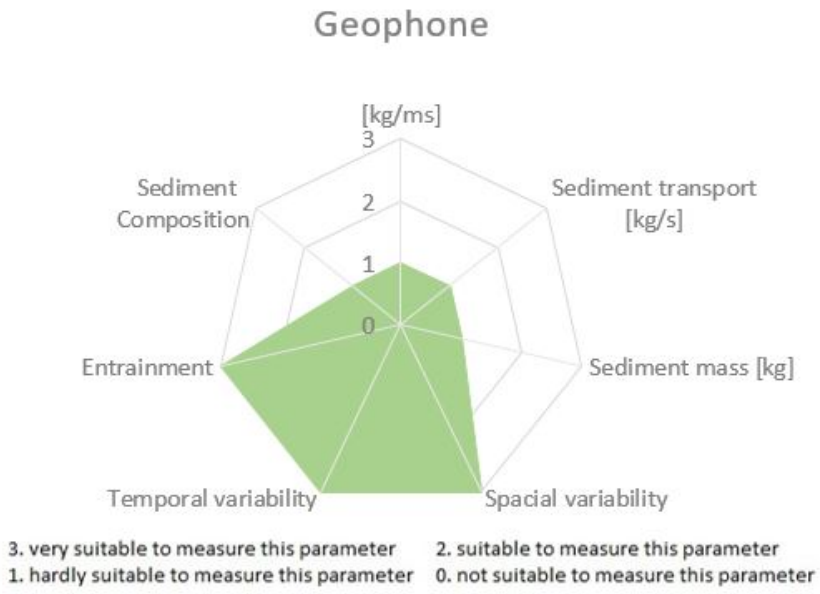

Figure 3.21: *Assessment sediment transport system - geophone (Habersack et al. (2012) modified)*

As can be seen in Figure 3.21 there are some areas where the geophone is appropriate as a measuring device on its own. Further advantages of the geophones include a continuous record of the intensity, the use of a threshold value, sturdy technology and relatively little cost in production. The drawbacks of the system can be summarized with a mandatory need for calibration and the minimum particle size that can be detected, which are far bigger than for the hydrophone (Langer, Stoisser (2016)).

The application of geophones in mountain torrents has been thoroughly studied by Rickenmann et al. (2012) in the alpine stream ”Erlenbach” in Switzerland, where the sediment transport is studied for more than 30 years now. Since 1986 in addition to geophones also piezo-electronic impact sensors are in use to record a continuous sediment transport in the river. In 2008 and 2009 the measuring system in the Erlenbach was equipped with automated sediment bed load samplers.Studies in the laboratory had shown, that geophones can recognize stones and pebbles with more than 10 mm grain size, therefore bed load samplers were installed to cover the remaining mass. A rail system as seen in Figure 3.22 with a scale allows an easier filling, emptying and recording process of the bed load samplers. Once a flood event is registered by the Sensors, the measuring system automatically sends an empty baskets to the channel and logs the weight until it is full. When the maximum level of sediment is reached the system automatically sends an empty basket in exchange to the full one. Once these cages are emptied, the sediment is transported into the laboratory, where it is dried and grain size distribution charts are produced. A connec-

tion between discharge of the river, sediment transport and grain size can be gained as a result (Rickenmann et al. (2012)).

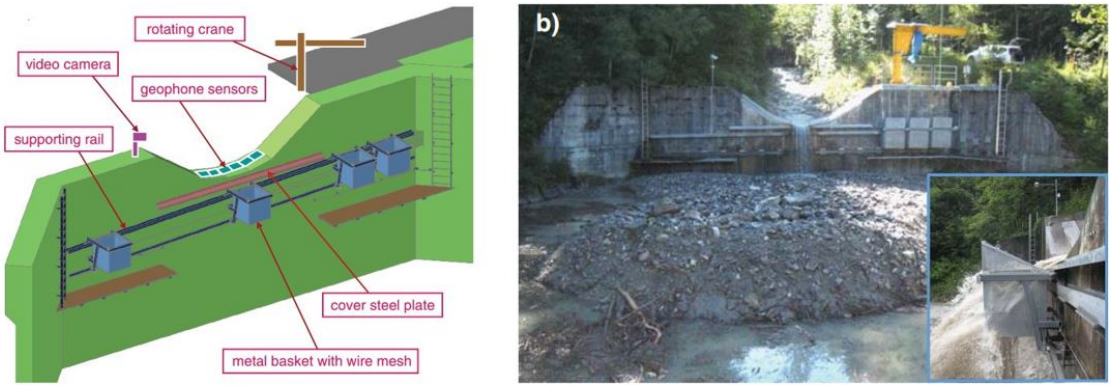

Figure 3.22: *Schematic setup versus implementation at the Erlenbach (Rickenmann et al. (2012))*

3.5.2.3 Tracer Stones and Telemetry Stones

Tracer and Telemetry Stones are roughly based on the same principle. For both concepts, stones are randomly taken out of the riverbed of the project area and brought to a laboratory where their geometry and weight is measured. The stones are then handled differently. The main aim of theses systems is to record the transport of the sediment for a flood event.

The tracer stones are marked and painted thoroughly. Conditions in the mountain torrents are rough and the stones color coat has to be enduring against strong abrasion forces. Therefore, before painting them in bright neon colored varnish, the stones need to be thoroughly washed and coated with primer. The finishing touches are done with coating of wax layer or epoxy varnish before they are placed back into the riverbed.The telemetry stones are handled similarly to the tracer stones, but instead of painting them and making them stand out in the riverbed, these stones are equipped with a transmitter that is incorporated into the stone, padded with foam material and closed up with body filler. Each stone is marked with the assigned frequency number and colored, which is used to detect the telemetry stone with a hand held scanner after the flood event (Barbas (2014), Spreitzer (2014) and Langer, Stoisser (2016)).

Tracer and telemetry in the Schöttlbach 2016

In July and August 2016 Langer, Stoisser (2016) placed 45 colored tracer stones and 8 telemetry stones in the Schöttlkapelle cross–section. In the first run 25 tracer and 2 telemetry stones were put into the river and shortly after, the highest flood event of the

year 2016 with a discharge of 11.30 m^3/s was measured. The first walk-through of the river left 17 tracer stones to be found. The 8 stones that were found got marked in a map with the help of a GPS device. The distance of the stone that was transported the most was 412 m and had a mass of 8.65 kg.

In the second run 20 tracer stones and 6 telemetry stones were placed in the cross-section and roughly 1 month after that another flood event with a discharge of 7.31 m^3/s was measured. During this attempt it was found, that stones between 9 to 15 kg did not get transported, which concludes in a result for the start of entrainment. For the third test 9 tracer were placed in the river and only 3 of them (possibly covered by sediment) could not be found by the end of the research period (Langer, Stoisser (2016)). Transport distance of the trials can be found in Figure 3.23. However, results from Barbas (2014) differentiate as the start of mobilization for a stone with approximately 35 kg was during a calculated discharge of 7,77 m^3/s.

Considering, that the reretrievability of the tracer stones declines over time due to algae growth and overburden of sediment tracing the stones gets more complicated. For these field tests the tracer stones had a probability to be found of approximately 20–35 %. The telemetry stones, however, had a chance to be found of roughly 50 %.

The **transport distance** of the tracer and telemetry stones is dependent of the mass of the stones and was therefore divided into four weight categories. These categories were unified with Barbas (2014) system:

- XS: 0.0-0.5 kg
- S: 0.5-3.0 kg
- M: 3.0-8.0 kg
- L: 8.0-16.0 kg

Considering, Barbas (2014) findings about transport distance in relation to the sediment mass, the results differ significantly compared to those from Langer, Stoisser (2016). In Figure 3.24 a comparison of the results for a discharge of approximately 7 m^3/s was made.

According to Langer, Stoisser (2016) the differences from these studies occurred due to the placement of more stones in each category by Barbas (2014), thus a higher retrieval of the tracer stones followed.

When looking at the **entrainment of sediment** mass, the connection between sediment mass and discharge of the river are the front running factors. Mobilization of the different

Figure 3.23: *Transport distance of tracer stones for 22.July-29.September 2016 (Langer, Stoisser (2016))*

categories vary between the above mentioned studies. Whilst a stone of category ”L” was mobilized during a discharge of 7.77 m^3/s in Barbas (2014) study, a stone with 15.6 kg remained unmoved during a similar discharge of 7.31 m^3/s in the Langer, Stoisser (2016) study.

3.5.2.4 Sediment Impact Sensor (SIS)

If not otherwise noted the facts of the following paragraphs are taken from Spreitzer (2014) and Langer, Stoisser (2016).

Sediment Impact Sensors are high resolution sensors (piezoelectric technology) that are mounted on a steel plate (sensor plate) to to get a qualitative judgment regarding bed load

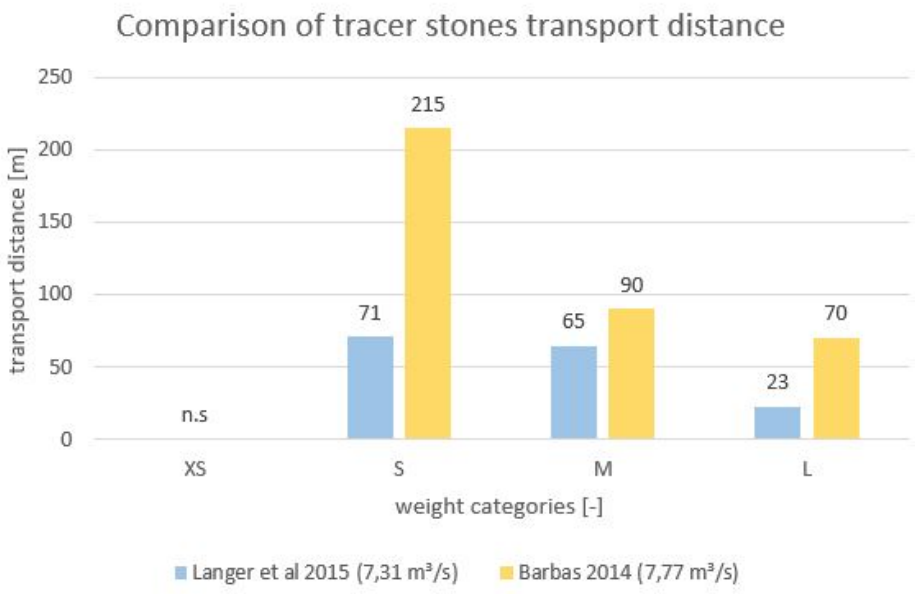

Figure 3.24: *Comparison of transport distances 2014 and 2016*

transport. These steel sensor plates are incorporated into the river by either submerging them into the riverbed or by installing them in a concreted threshold in the riverbed. When sediment particles are flushed over the sensor an electrical voltage is generated in the core of the sensor (piezoelectric impulse). The generated voltage is dependent on the size of the particles as well as the impact velocity of the particles. The signal is then recorded with an Arduino (small portable mini computer) and an amplifier circuit. Due to the installation of the SIS in rough terrain the power supply is given by 12 volt car batteries. To ensure a steady power supply these batteries must be replaced frequently.

Figure 3.25: *Installed SIS and bed load sampler (Spreitzer (2014))*

The sediment impact sensors (Figure 3.25) discussed in the publication of Spreitzer (2014) were already models of the 3^{rd} generation. Problems occurred with previous designs and kept continuing. For example the error prone cables connecting the sensors to the data logger were guided to the data logger underground after the openly laid wires were damaged by heavy stones in the river. Secondly, the mounting techniques of the sensors in the river was upgraded. At first impact anchors and safety nuts were used to mount the sensors onto big rocks in rivers. This technique proved to be very unsuitable. The forces in the river, caused by larger rocks during flood events, bent the anchors and damaged them severely. At a later stage the sensor plates were concreted into a submerged weir to improve their durability.

Calibration of SIS

For calibration purposes bed load sampler (design of TU Graz) were submerged into the river after each Sediment Impact Sensor to collect the sediment that was transported over the sensor plates during an event. The bed load sampler have to get emptied and analyzed frequently as they fill up fast. Over the course of the ClimCatch project different designs for these bed load samplers were built and tested. The version of Langer, Stoisser (2016) as seen in Figure 3.12 prove to be more durable against damages and more stable in their mounted position than previously used bed load samplers.

Results for Oberwölz

In Figure 3.26 from Langer, Stoisser (2016) some results of the sediment impact sensors at the Schöttlkapelle cross sections can be seen.

This shows only the results of one out of three sensors that are mounted in this cross section. What can clearly be seen is, that the start of mobilization of sediment that is recorded by the SIS occurs at a discharge of about 1.8 - 2 m^3/s. Similar values could be seen for all sensors.

A more detailed evaluation and summation of the impacts during the measuring period showed, that daily peaks differed from sensor to sensor. A reason for these different results can be that all of the sensors were mounted using different techniques and technology (torque of screws, etc.). For future sensor installation, the initial conditions shall be the same.

Furthermore, as mentioned above, the impacts can only be recorded at a discharge of more than 2 m^3/s. A discharge lower than this threshold value does not conclude in any information about the bed load.

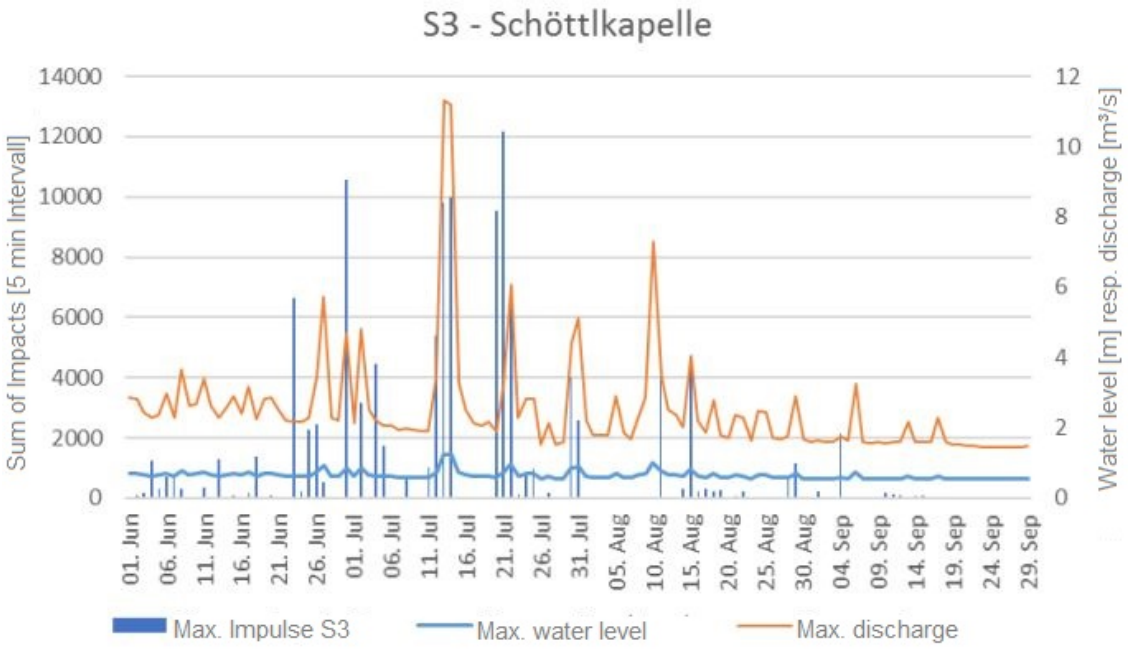

Figure 3.26: *Sediment Impact Sensor, gauging station and discharge June-Sept 2016 (Langer, Stoisser (2016))*

After a series of research trials, the measurements with SIS were paused until further notice. With lessons learned applied, a new sensor series called MEMS was developed. Chapter 4 provides more information on these sensors.

4 Methodology

This chapter includes all necessary information about the measuring techniques and methods that were in use over the course of this thesis or were developed during this thesis.

4.1 Discharge Measurements - Nautilus Probe

In order to determine flow velocities, the nautilus probe (MF Pro) from the company OTT was used. The Nautilus MF Pro is used when doing measurements in open channels, particularly in streams, creeks, small rivers and channels. Measurements in super critical flow conditions as well as in weedy riverbeds and low flow can be handled without any problems. Figure 4.1 shows the measuring device and all the needed equipment of the Nautilus probe (OTT Hydromet GmbH (2018)).

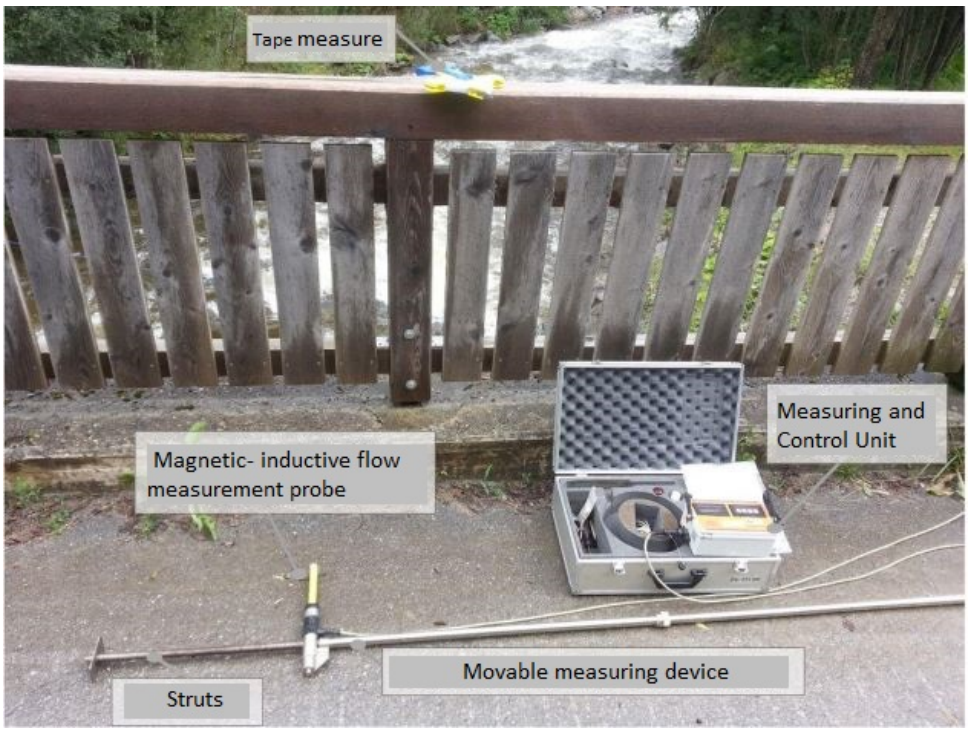

Figure 4.1: *Nautilus probe from the company OTT (Spreitzer (2014))*

In combination with the semi-graphical runoff determination method, the discharge for the individual partial areas of the cross section are calculated separately and summed up at the end. Therefore, the cross section is divided into several measuring sections. Generally, the more segments the more accurate the result. The Hintereggertor cross section got divided into 11 sections as shown in Figure 4.2. Each vertical measuring path has approximately one to six measuring points in a vertical distance of some 10 - 15 cm.

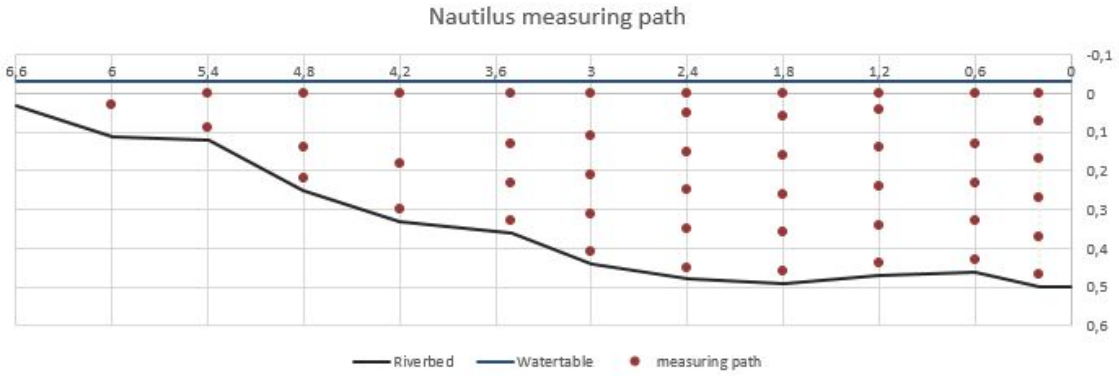

Figure 4.2: *Nautilus measuring path for the Hintereggertor cross section*

In order to conduct these measurements the nautilus probe has to be stationed at the paths mentioned above, the yellow part (see Figure 4.1) of the Nautilus probe facing against the streams flow direction. Due to the measuring devices setup, recordings of the flow velocity can only be done as low as 3 cm above the riverbed and approximately 3 cm below the water level. Otherwise, the measuring results will be falsified. Once the probe is set up, the measurements can start. At each vertical point, measurements were executed for 30 seconds and the average velocity, given by the probe, was logged. Afterwards, the discharge and mean flow velocity calculation for the Schöttlbach was executed. As said in 3.4 the calculation is based on the continuity equation, where the sections are added up accordingly and a mean value is created.
The results of the flow calculation for the 10^{th} of April 2018 can be found in Section 5.1.

4.2 Nephelometric Turbidity Measurements for Schöttlbach

A multi-parameter sensor from the company OTT was installed to find out how much suspended sediment is transported during a high water event. Before the Sensor at Schöttlbach was stationed, probes were taken out of the riverbed some 5-10 m upstream of the selected cross section Hintereggertor and taken to the laboratory to dry. The cross section that was chosen for the stationing lies in the city center, underneath a bridge, with good accessibility for maintenance purposes, as well as for visual inspection during high water events via the bridge.

Evaluation Curve Schöttlbach

As mentioned in Section 3.3.1 the sensor produces NTU values, which have to get converted into grams of sediment in 1 liter of suspension. Therefore, an evaluation curve had to be defined in the laboratory.

In the first step the extracted sediment from the Schöttlbach was taken to the laboratory to dry. After a week the sediment was weighed and packed into bags of 20, 50 and 100 grams and taken to the calibration point. A bucket was filled with 20 liter of clean water.

Figure 4.3: *Preparation of sediment for calibration*

To be able to construct this curve three tests were conducted. Unfortunately, the first test was performed when the sensor was not properly calibrated. This resulted in an NTU value for clean tap water of 60.7 instead of 1. After the first attempt the Sensor had to undergo a two-point calibration process. In this process two measurements with known values are carried out. The first measurement is done in tap water where the value is set to 1. For the second calibration point the probe is filled with formazin fluid (see supplier for details) of 20 NTU turbidity and the measured value is replaced by the fluids known value. After this calibration more realistic measurements were performed. Nonetheless, the results for the first evaluation attempt can be found in Figure 4.4 marked in gray. After the proper calibration of the sensor, two more sets of measurements were carried out. In the first step the sensor was placed in the bucket and the readings started. In regular time intervals and under constant motion of the water (no air bubbles were produced) the bags of sediment were pored into the bucket individually.

Table 4.1: *Sediment per step in evaluation curve*

Unit														
g/l	1	2	3	4	5	7.5	10	12.5	15	17.5	20	22.5	25	30
g/b	20	40	60	80	100	150	200	250	300	350	400	450	500	600

Table 4.1 lists the steps and gram intervals for the evaluation curve in grams per liter [g/l], and total amount of grams in the 20 liter bucket [g/b].

The results of the second and third measurement are marked in orange and blue in the graph below. For the generation of the evaluation curve a mean value of the two valid measurements was added in red. On the basis of these data sets, linear regression analysis was done.

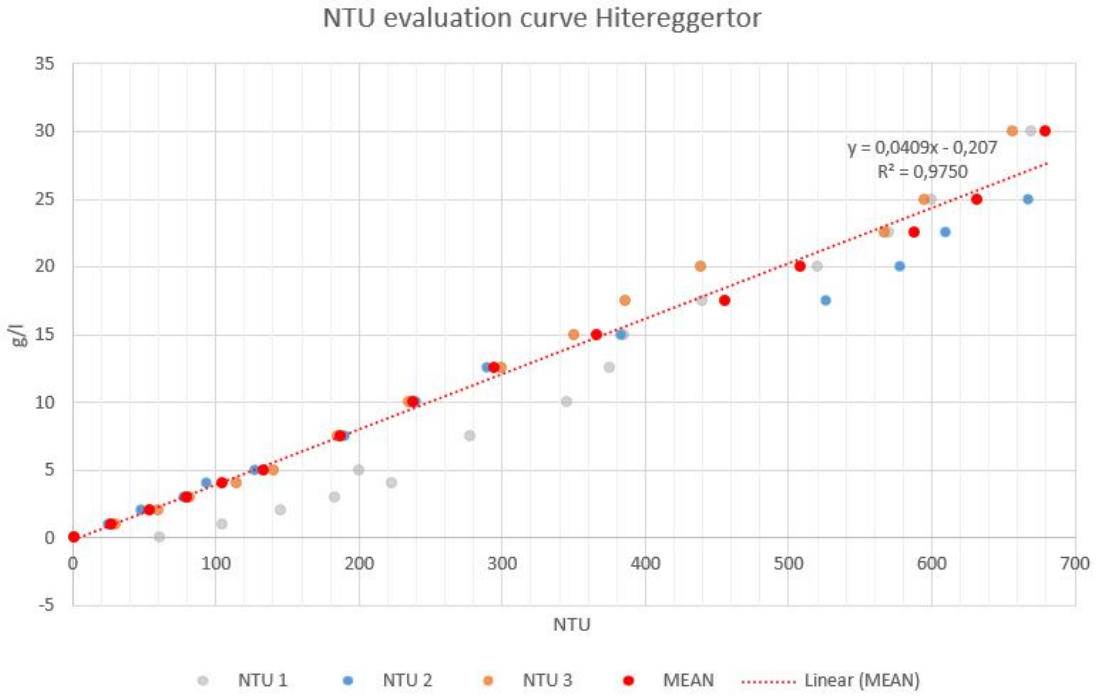

Figure 4.4: *NTU rating curve for Schöttlbach*

4.3 Gauging Station Hintereggertor

The water level in a river can be measured in different ways. For the project in Oberwölz a radar sensor and two pressure probes are in use. The pressure probes will not be discussed in this thesis, as the output of the sensor is not valid due to the constant change of the riverbed.

The radar sensor at the Hintereggertor is mounted in the middle of the bridge facing down towards the water surface. The sensor uses radar impulse technology. A transmitter sends out short radar pulses in the 24 GHz ISM band and a separate receiver collects the reflected impulses coming from the water surface. Simultaneously, the distance between the water level and the sensor is determined (Barbas (2014)).

These water level measurements are used to determine the discharge in the river in combination with a rating curve. Additionally, the profile of the river as well as the inclination of the river reach was measured in a survey to receive accurate information. More information on the rating curve as well as the discharge for the period of April 2018 until September 2018 can be found in Section 5.2.

4.4 Micro Electromechanical System Accelerometer (MEMS)

A Micro Electromechanical System accelerometer, also called MEMS, is a sensor that measures acceleration forces or proper acceleration[1] in three axis and can therefore be described as a 3-mass-oscillator. Figure 4.5 shows the directive of the three preferred directions (Reichenbach et al. (2003)).

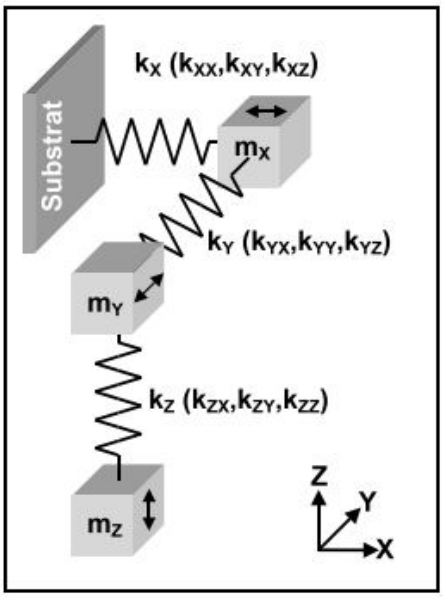

Figure 4.5: *3-mass-oscillator (Reichenbach et al. (2003))*

[1]The acceleration felt by objects, as opposed to the coordinate acceleration. For instance, the acceleration of objects at the Earths surface is measured as 9.81 m/s^2 upwards, but without coordinate acceleration. The free fall of an object towards the Earths core would reduce the acceleration to 0 m/s^2 but coordinate acceleration would exist (Definitions.net (2018)).

In general, the mechanical structure of the sensor is positioned in an electrical conductive layer and on a silicon plane. It consists of a seismic mass (m_x, m_y, m_z) and a suspension system per axis (k_x, k_y, k_z) that is mounted movable in a plane and parallel above the substrate. The distance between the whole structure and the substrate is defined by the thickness of the sacrificial layer, which will be removed after the fabrication. Figure 4.6 shows the setup of the structure (Reichenbach et al. (2003)).

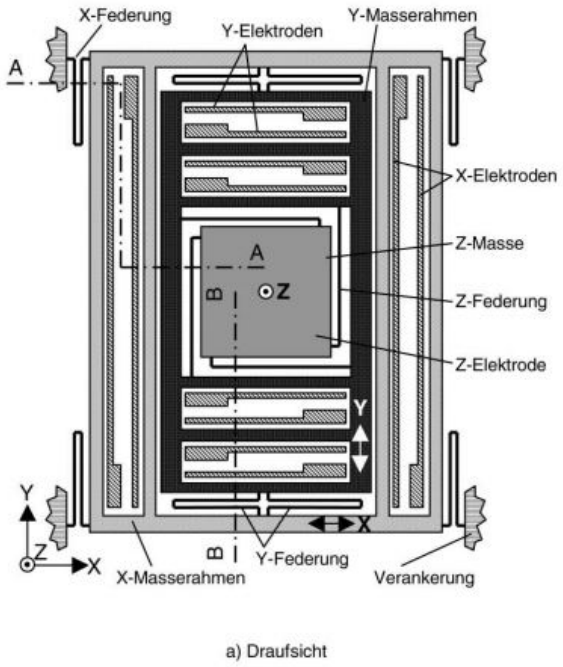

Figure 4.6: *Setup of an accelerometer in top view. (Reichenbach et al. (2003))*

The suspension system allows an elastic displacement of the masses, from an inoperative state in defined manner, in the three orthogonal axis. The displacements are produced by the inertia of the masses as compared to an acceleration that is acting on the element from the outside. These motions produce displacement changes in the plate capacitors between the fixed electrodes and the structure itself, so that in comparison to impacting acceleration, proportional changes in capacity occur (Reichenbach et al. (2003)).

4.4.1 Development of MEMS

MEMS sensors are used in a wide range since the late eighties. They were first implemented in 1987 into airbag systems as crash sensors. Non-MEMS crash sensors that had been used in earlier stages were designed with a more mechanical system where a metal ball is retained by a rolling spring as well as a magnetic field. The simple and less expensive method relies on the movement of the ball in response to a fast car deceleration and

two contacts that shorten inside the sensor. This mechanism is quite sensitive to errors as the contacts can get contaminated or the ball can get blocked. A MEMS device, however, can be equipped with a self-test feature that will check the state of integrity at every engine start.

Development of the sensors continued during the nineties in which time MEMS got incorporated into cameras and binoculars for image stabilization purposes. Later on, the technology was further improved and sized down even more. After being built into smart phones in 2005, game controllers followed in 2007. The range in which the sensor technology developed is shown in the schematic graph in Figure 4.7 (Chollet, Liu (2016)). The Runsed-CC research programs hopes are high, that another circle for monitoring purposes will be added to the graph in the future.

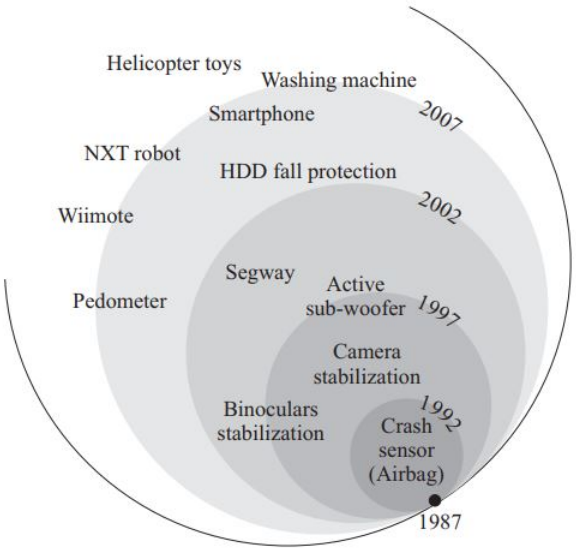

Figure 4.7: *Application progress of MEMS accelerometer (Chollet, Liu (2016))*

Most recently accelerometer of this kind were made available to the average costumer. When being connected with an USB port, data can be read with the help of a simple logging tool. The companies selling these sensors advertise them with a field of application ranging from motion detectors, gaming and pointing devices, burglar detection, sleep quality monitor, seismography, mechanical vibrations analysis (spectrum analyzer) and even as baby movement detector or baby monitors (Chollet, Liu (2016)).

4.4.2 SerialPlot Software

SerialPlot (Free Software Foundation (2018)) is an open source software that allows for readings of data from a serial port in the binary data formats (u)int8, (u)int16, (u)int32

and float. Users can define a frame format for a robust operation. Furthermore, ASCII format input is supported. Important for the cause of this thesis was, that synchronized multi-channel plotting (x-, y- and z- direction of sensor) is possible. Sending commands to the sensor in binary format and ASCII is possible, the latter was used during the tests. Especially useful is the option for the recording of data and the snapshot option of the current waveform. In the software the bit range can be modified from (signed and unsigned) 8 to 24 bit.

With the aid of this software all tests during this thesis were recorded and later analyzed. Output of the software was done with simple text files, including columns for each channel (x-, y- and z- direction of sensor).

Working with SerialPlot

The following steps describe the installation and settings needed to gain sensor data:

- Download and install *SerialPlot* from *https://bitbucket.org/hyOzd/serialplot/downloads/*. This is possible for Linux as well as Microsoft.
- Connect the sensor via USB-cable and load the port by clicking the *reload port list* sign in the *port*-tab of the software.
- In the *data format*-tab select ASCII and add 3 channels. As a channel separator use a comma.
- Open the *plot*-tab and select all 3 channels; Check the box for *Auto Scale Y- Axis* and select *signed 10 bits -512 to +511* for *Select Range Preset*.
- The *Commands*-tab allows for input of commands. E.g. FREQ 3200 for 3200 Hz setting or RANGE 8 for 8 g of range.
- When clicking the *Open*-button, the sensor and computer are connected and readings can be made.
- In the *Record*-tab a storage location for the data can be defined. Tick *Windows Style Line Endings*.
- Click the button *Record* at the beginning of the recording and at the end.
- The saved files can be found in your chosen directory.

Sensor Data

Data that is collected with SerialPlot does not seem to be very informative at first. It has to get converted into acceleration. This conversion is dependent on the range and frequency setting that has been made for the measurement log. The sensor output, values between -512 and +511, are transformed into acceleration of the axis with (Tindie Inc. (2018)):

$$a_{x,y,z} = \frac{S \times R}{510 \times g} \quad for\ positive\ values \tag{4.1}$$

$$a_{x,y,z} = \frac{S \times R}{511 \times g} \quad for\ negative\ values \tag{4.2}$$

a = acceleration
S = sensor output
R = range
g = gravitational acceleration 9.81 m/s^2

The available frequency values of the MEMS Accelerometer in Hertz [Hz] are: 3200, 1600, 800, 400, 200, 100, 50, 25, 12.5, 6.25, 3.13, 1.56, 0.78, 0.39, 0.2, 0.1. Meaning, that as many as 3200 measurement values can be collected in a second of time. (Tindie Inc. (2018))

The range of an acceleration sensor is the span of gravitational acceleration in [g = 9.81 m/s^2] that can be measured with it. Tindie Inc. (2018) acceleration sensor offers a number of range settings starting at $\pm$ 2 g and going as far as $\pm$ 16 g.

4.4.3 MEMS Accelerometer in Rivers

MEMS accelerometer as a sediment measuring device, especially in rivers and in general is a pilot project and one of its kind. Therefore, a number of tests had to be made to guarantee that the developed sensor works under water and useful data is delivered. All test graphs can be found in the Appendix.

4.4.3.1 Laboratory Test - Design Phase

The sensor measuring unit was produced in the laboratory at the Institute for Hydraulic Engineering and Water Resources Management at Graz University of Technology in co-

operation with the Department for Geography and Regional Science at University of Graz. The basic design for the sensor is inspired by the SIS sensor design by Spreitzer (2014). Earlier works with the SIS sensors mentioned irregularities in measuring results due to some technical details. Therefore, a number of design test were conducted. Furthermore, some specific design tests for measuring with the MEMS accelerometer had to be made. These included:

- Screw torque
- Choice of padding material
- Wet tests
- Range
- Frequency

For the characteristic settings and test results of each design test see Chapter 5. When spheres 1 to 4 are mentioned for design test, steel spheres of different size and weight are referred to (1 = 1.1 g, 2 = 5.5 g, 3 = 21.8 g, 4 = 32.7 g).

4.4.3.2 Construction Manual

The basic design and setup of the sensor emerged from the SIS sensor design by Spreitzer (2014). Merely a few changes were made due to the size and geometry of the new sensor dongle (MEMS) itself. In the following paragraphs the setup of the measuring device and its components is described.

Acceleration Sensor

The acceleration sensor is the heart of the measuring device. The sensor in use is a *ADXL345*, which is a rather small, thin, ultra-low power, 3 axis accelerometer. High resolution measurements in a range up to $\pm 16g$ can be performed. It measures not only static acceleration of gravity but also dynamic acceleration that result from shock and motion. Due to the high resolution of the sensor, inclination changes measurements of less than 1.0^o are possible (Analog Devices Inc. (2015)).

The accelerometer is programmed to send gravitational forces in 3 axis. When the sensor is placed flat on a surface, simple g values (gravitational force $1g = 9,81m/s^2$) for each axis (Figure 4.8) are delivered. Considering a flat surface, values as shown in Figure 4.9 should be received (Analog Devices Inc. (2015)).

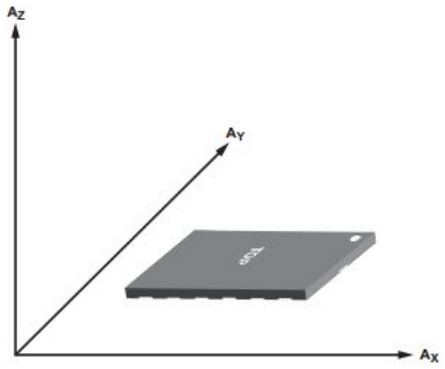

Figure 4.8: *Axis of acceleration sensitivity (Analog Devices Inc. (2015))*

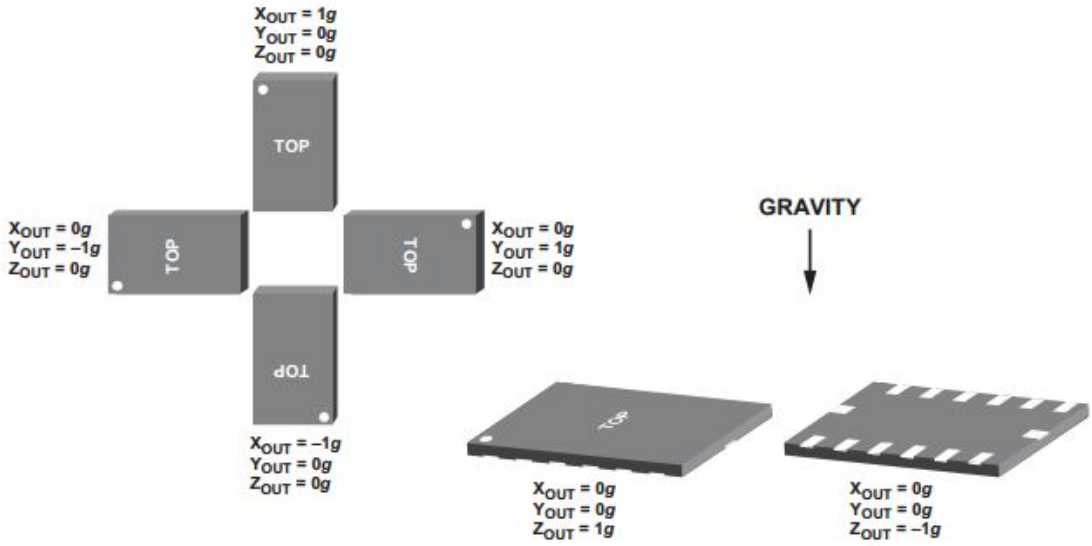

Figure 4.9: *Output response versus orientation to gravity (Analog Devices Inc. (2015))*

When the sensor is irritated or disturbed in its position, acceleration changes in all axis can occur. For example, if the sensor gets purely vertically tapped on, the z-axis experiences an acceleration change and the amplitude of the graph peaks. This can be seen in the Figure 4.10 (Analog Devices Inc. (2015)).

For the test conducted at the laboratory only the z-axis values are looked at, as it is assumed, that the vertical displacement due to sediment impact causes more amplitude on the z-axis than on any other.

Accelerometer Dongle

The used dongle as seen in Figure 4.11 is produced by a Polish electrical engineering group. The ADXL345 is mounted onto a circuit board and is equipped with a micro USB port. Due to the lack of space in the sensor casing it was necessary to solder the USB

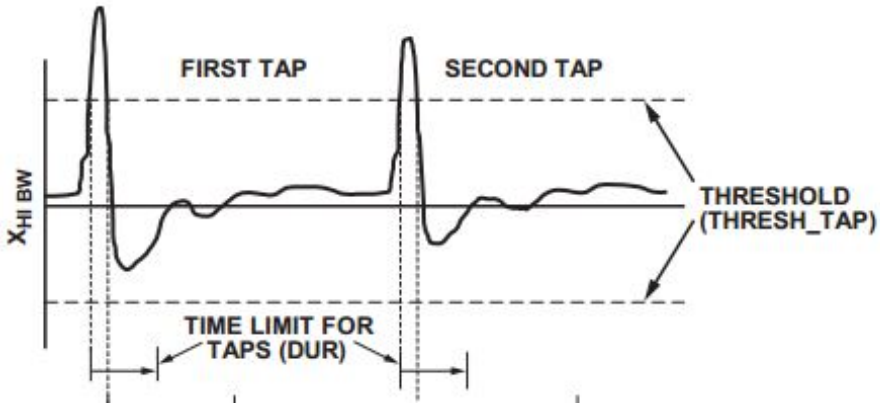

Figure 4.10: *Sensor tap interruption (Analog Devices Inc. (2015))*

cable directly onto the port, rather than using the provided Micro USB slot. The dongle has a size of 49 x 26 mm and is equipped with an integrated LED light for display of acceleration measurements and its velocity, as well as for power indication. The product can be purchased for roughly 40 $ via their platform Tindie Inc. (2018).

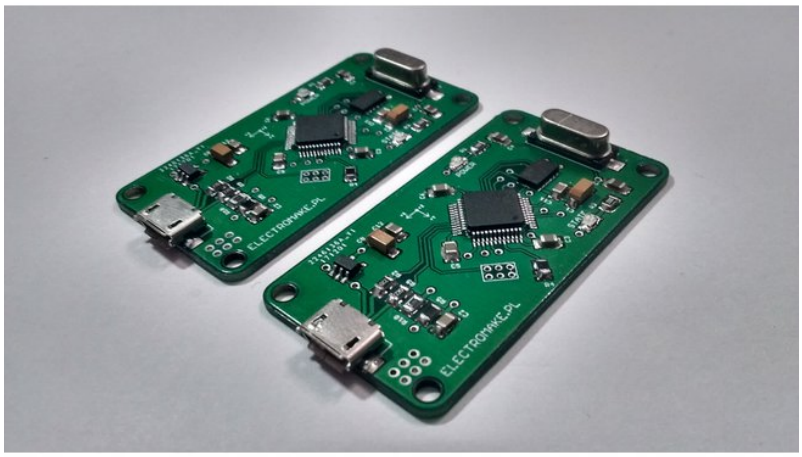

Figure 4.11: *3-axis USB accelerometer (Tindie Inc. (2018))*

Sensor Plate and Casing

The sensor plate and casing was originally designed for the SIS sensors and customized to fit our needs. Especially the mounting of the dongle onto the steel plate needed adjustment.

The steel plate as seen in Figure 4.12 below is 150 x 150 mm in size and 10 mm thick and has a steel grade of 235. These proportions and material have proven sufficient during the SIS field tests. The dongle is glued into a form pipe of 80 x 50 mm with epoxy resin,

which secures the electronic parts of the dongle against infiltration of water. The epoxy resin is transparent, so inspections of the power light can still be made.

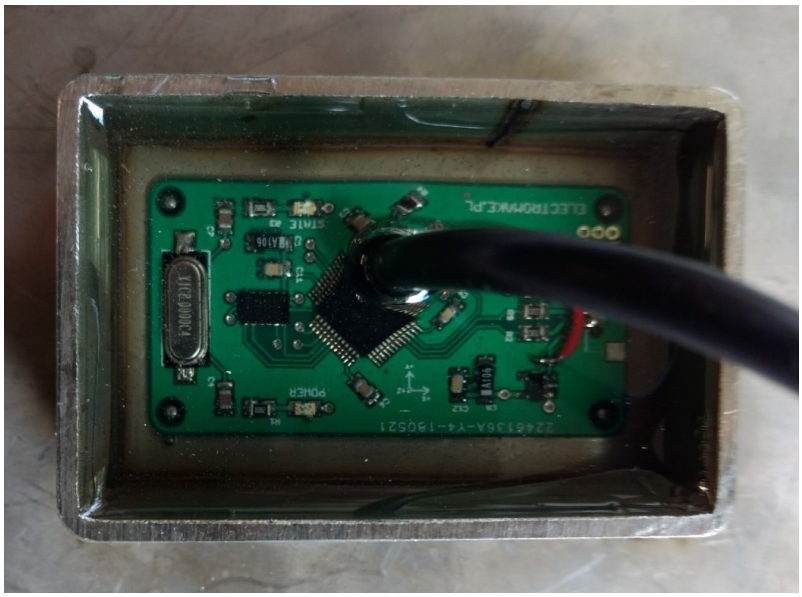

Figure 4.12: *Dongle in epoxy resin on sensor plate*

The steel plate is mounted into the steel casing with four bolts on a rubber plate with a thickness of 5 mm. The steel casing has a bottom outlet for the USB cable of the sensor. The connection between the sensor casing and the measuring station shall be made watertight.

Wiring

To connect the sensors to the measuring station and computers, water prove wiring is required. USB A cables are used for this project. To secure the connection of the USB cables against penetrating water, the connectors are coated with epoxy resin and covered with shrinking tubes. This has proven sufficient in a 72 h wet test as described in 5.

In Figure 4.13, the finished sensor plates can be seen.

Axis Transformation

Since the installation of each sensor is different, an axis transformation is needed when evaluating the data of each sensor. This is necessary, because it cannot be guaranteed that each sensor is mounted in the same position and height. To gain data that can be compared, an axis transformation, where the z-axis is transformed to ± 9.81 m/s^2 and the x- and y-axis are set to 0.0 m/s^2 is necessary. *(Note: This was not done for the laboratory test so far as only one sensor was in use and no cross referencing with a second sensor was needed.)*

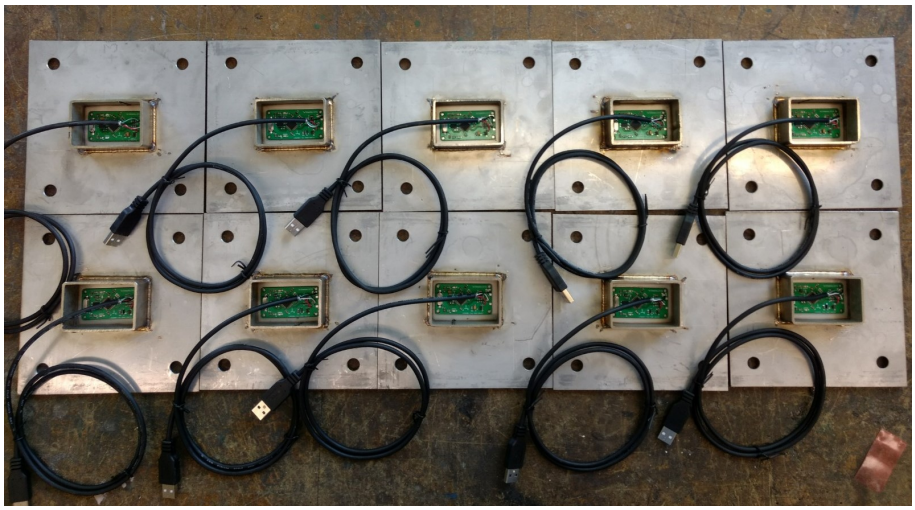

Figure 4.13: *Setup of the finished sensor plate*

4.4.4 Installation in the River

The installation of the MEMS accelerometer in the river Schöttlbach is the first of its kind. In the beginning of the development of the sensors, the Austrian Torrent and Avalanche Control and the project coordinator agreed, that the location for the installation at the Schöttlkapelle would be most suitable. Due to the design and placement of the measuring station, interference with flora and fauna would be limited and natural flows in the river would not be disturbed. For the installation of the sensors in the river, a submerged weir was constructed by the WLV as seen in Figure 4.14. On top of the submerged weir big stones and boulders (slopes) can be seen, they were concreted into the top to gain a nature like surface and to reinstall the natural roughness of the channel. Furthermore, a number of black tubes can be seen on the bottom of the picture. These empty ducts go from underneath each sensor, through the submerged weir, to the surface, where they will be connected and guided to the measuring station.

The location for the submerged weir was chosen due to the rivers natural flow direction, the easy accessibility and the connection to the electrical grid. The concept for the spacing in between the sensors was established on the basis of natural flow and intensity. The submerged weir holds ten sensors in total, five sensors per row, arranged in two rows. The construction drawings can be found in Figure 4.16. The goal was to guide low water through a deeper channel on the right outer third of the river. If this channel would not exist, sedimentation in low water season would occur over the whole profile of the Submerged weir and the sensors might get blocked. The location for the low water channel was chosen due to the natural flow direction of the river. In this rather small section four

Figure 4.14: *Submerged weir under construction July 2018*

sensors were mounted. A higher density of sensors was chosen due to the shape of the low water channel and the expected additional flow in it. The six remaining sensors were mounted on the left side of the river with a distance of about 1 m between the sensors.

Figure 4.15: *Back-filled and finished submerged weir*

Figure 4.15 shows the back filled submerged weir in the river. The section for the low water flow can be seen on the lower half of the picture. Measurements are possible at this point, however, the software package to handle the data is not yet ready for use.

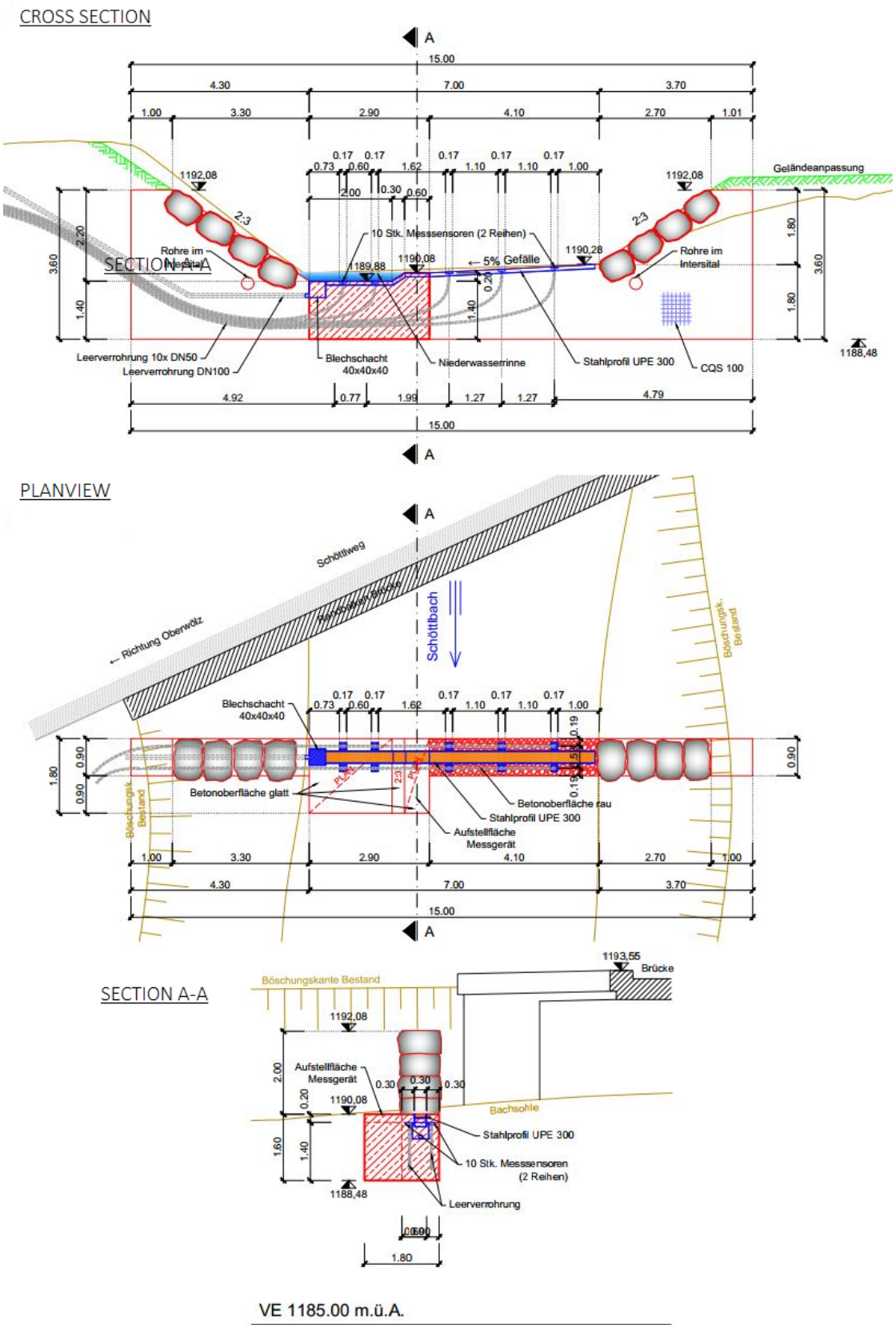

Figure 4.16: *Submerged weir design construction drawings (WLV, 2018)*

5 Data Evaluation and Validation

The following sub-chapters discuss the evaluation and, if given, the validation of the measurements and their results. Since the operation of the MEMS sensors did not start yet, the chapter will include evaluation and validation of the tests conducted in the laboratory before the sensors were mounted into the river.

5.1 Nautilus Measurements

Figure 5.1: *Measuring cross section Hintereggertor*

Data for the evaluation of the mean velocity and discharge were executed on the 10th of April 2018. Therefore, the team of the Institute for Hydraulic Engineering and Water Resources Management from the TU Graz set up the Nautilus probe at the Hintereggertor cross section. The flow velocity was measured in 11 vertical paths with 1 to 6 measuring points per path. In each point the velocity was measured for 30 seconds and a mean value was produced by the sensor unit.

Teststrecke: Schöttlbach

Aufnahmedatum: 10.Apr.18

Bemerkung: Messbeginn 10:30
Messende 11:30

Messprofil: Hintereggertor

Messzeit: 30 sec
Breite B = 6,60 m

Messlotrechte		1	2	3	4	5	6	7	8	9	10	11
Abst.v.l.Ufer [m]		0,20	0,60	1,20	1,80	2,40	3,00	3,50	4,20	4,80	5,40	6,00
Wassertiefe [m]		0,47	0,43	0,44	0,46	0,45	0,41	0,33	0,30	0,22	0,09	0,08
Abstand von der Sohle [m]		0,47		0,44	0,46	0,45						
		0,37	0,43	0,34	0,36	0,35	0,41					
		0,27	0,33	0,24	0,26	0,25	0,31	0,33				
		0,17	0,23	0,14	0,16	0,15	0,21	0,23	0,30	0,22		
		0,07	0,13	0,04	0,06	0,05	0,11	0,13	0,18	0,14	0,09	
		0,00	0,00	0,00	0,00	0,00	0,00	0,00	0,00	0,00	0,00	0,03
	v [m/s]	0,89		1,11	1,31	1,05						
		1,02	1,08	0,96	0,79	0,75	0,71					
		1,00	1,17	0,75	0,98	1,01	0,68	1,23				
		0,56	0,52	0,76	1,11	0,89	0,89	0,97	0,98	0,65		
		1,17	0,68	0,78	1,06	0,92	0,85	0,80	0,75	0,51	0,33	
		0,43	1,03	1,46	0,86	1,36	0,57	0,96	0,17	0,43	0,30	0,10
f_{vi} [m^2/s]		0,416	0,367	0,386	0,464	0,420	0,312	0,312	0,186	0,112	0,028	0,004
v_{mi} [m/s]		0,886	0,854	0,878	1,008	0,934	0,762	0,945	0,620	0,509	0,313	0,050

A = 2,019 m^2

v_m = 0,811 m/s

Q = 1,637 m^3/s = 1637 l/s

Figure 5.2: *Calculation sheet with the results of nautilus measurement at Hintereggertor*

As seen in the table in Figure 5.2, the mean velocity was calculated to $v_m = 0.811\ m/s$ with the corresponding discharge of $Q = 1.637 m^3/s$.

5.2 Gauging Data - Rating Curve

Gauging data has been collected continuously by the radar sensor on the Hintereggertor bridge. Normally, these water level measurements are used to calculate the discharge with the help of a pre-designed rating curve and a corresponding function, where the height of the water level is put into the equation and the discharge is returned. As the geometry and profile of the riverbed change after almost every high water event, these rating curves needed to be adjusted and recalculated. Usually, this task includes multiple flow measurements (current meter or nautilus) in the river to calculate the discharge at a certain water level. With inter-and extrapolation a rating curve can be generated.

Unfortunately, an update of the rating curve was not possible due to the lack of reference measurements. However, the relative measured water level in combination with the flow velocity of the radar sensor data is shown in Figure 5.3. All values shown are measured values of the radar sensor. Faulty measurements can be included, since a cross check with the second gauge could not be made due to the lack of data.

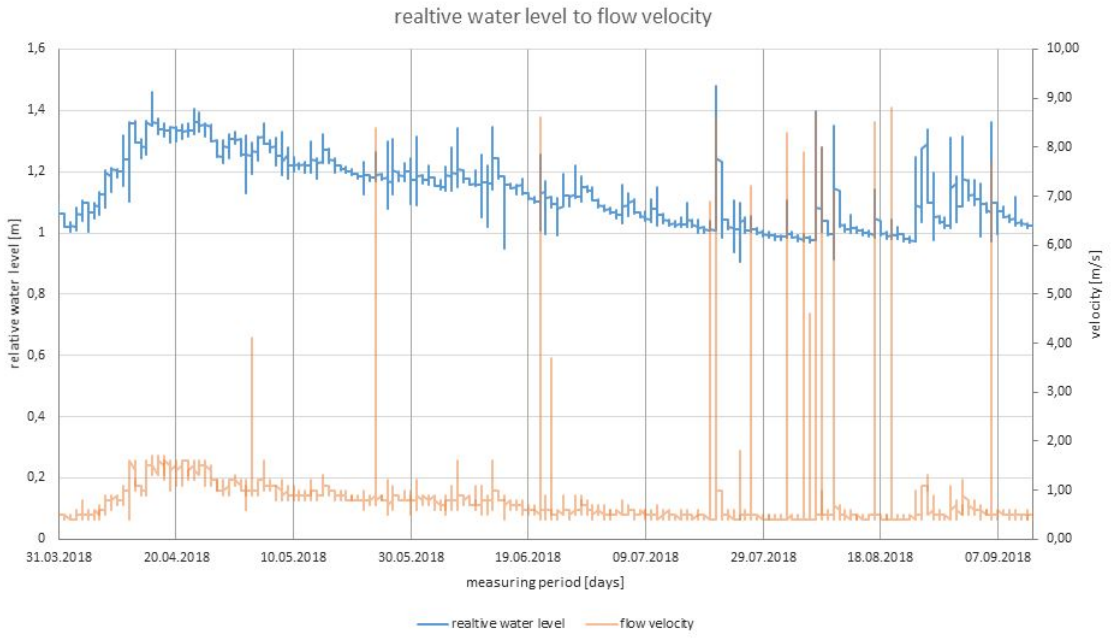

Figure 5.3: *Relative water level and velocity at Hintereggertor from April to September 2018*

Generally, the flow velocity increases when the depth of the river rises and the hydraulic radius increases. Therefore, a clear connection between the relative water level and the

flow velocity in the Schöttlbach should be able to be made. However, a clear connection can only be recognized in the months of July until September 2018, where the water level rises and therefore also the flow velocity. In the months between April and June, this connection is harder to make as an increase in water level does not necessarily conclude in a higher flow velocity. Possible reasons for these irregularities cannot be named.

5.3 Turbidity Measurements

The installed multiparameter sensor at the Hintereggertor can easily be used for readings of turbidity measurements with the curve as seen in Figure 4.4 in Section 4.2. In case of a flood event, the values can get extracted from the computer log and compared with the curve. As an example, if the turbidity reaches a value of 420 NTU, about 17 g/l of sediment were transported in the suspension.
It is expected to receive more detailed information about fine sediment transport during floods, as they form a large part of the overall transported mass.
Even though the sensor was installed in late July 2017 no valid measurements can be used for data validation and evaluation, due to an error in the sensor. A possible reasons for this could be the installation of the sensor in the river or an error in the sensor itself.

5.4 MEMS Accelerometer

The MEMS accelerometer allows for simple programming and configuration by sending signals or rather commands via the program SerialPlot (Free Software Foundation (2018)) to the sensor. These commands include frequency manipulation and the extension or reduction of the range, in which it can measure the acceleration. In the following section, the choice for both of the above's setting is described. Additionally, the design tests for the screw torque, choice of padding and the wet tests are described.

For the selection of these settings, the sensor structure was mounted into a channel (discharge possible) at the laboratory of the Institute. Therefore, the sensor casing was concreted into a block providing space for the steel plate with the fixed sensor. After assembling it with a sheet of padding rubber and four screws (equal torque) the tests began. The same metal spheres were used for the test as for the material test before.

5.4.1 Screw Torque

Spreitzer (2014) mentioned in his master thesis on Sediment Impact Sensors, that due to different screw torque when mounting the sensors in the river, it was not possible for them to compare the results of the tests. In addition, the team behind the MEMS

accelerometer had reasons to believe, that the screw torque has influence on the measuring results. Therefore, two settings of torque were used on the 4 screws in the sensor plate and test were executed.
The first series was screwed in with a torque of 10 Nm and the second series with 20 Nm.

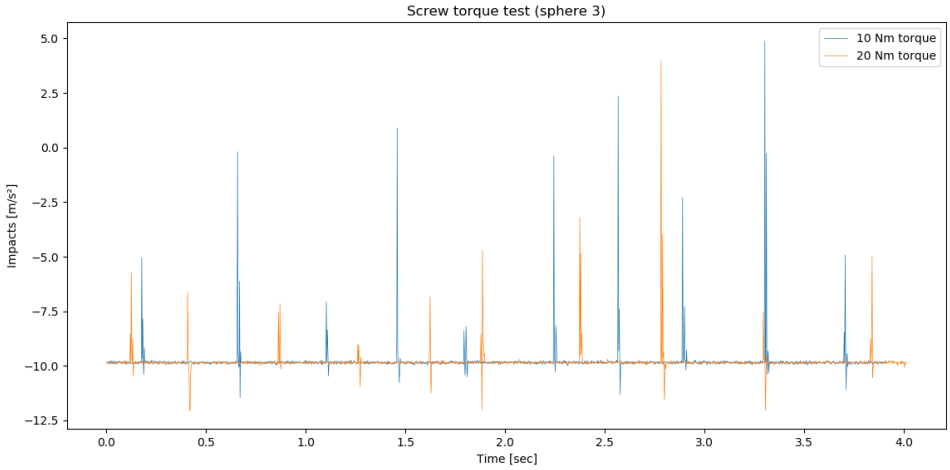

Figure 5.4: *Torque test, 50 mm dropping height of sphere*

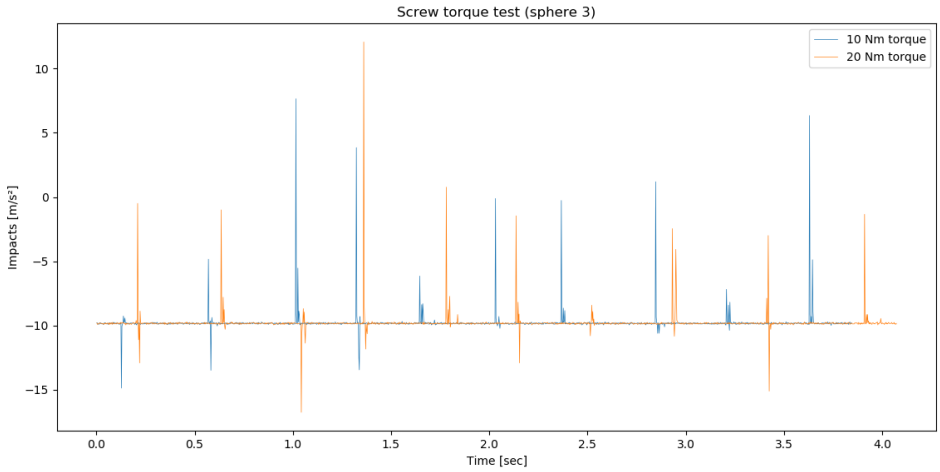

Figure 5.5: *Torque test, 100 mm dropping height of sphere*

A comparison of the torque settings can be seen in Figure 5.4 and Figure 5.5. Both graphs show impacts of a steel sphere (sphere 3) onto the sensor plate from a vertical dropping distance of 50 mm and 100 mm with a torque setting of 10 Nm (blue) and 20 Nm (orange).

Both graphs show impacts of different magnitude for both torque settings. In the first graph the 10 Nm setting seems to allow for higher impacts, but when looking at the second graph the 20 Nm setting delivers higher impacts. When comparing the graphs it is hard to distinguish between a more suitable torque setting, even when looking at additional graphs of other sphere sizes. Therefore, it can be said, that the torque setting of the screws has no influence on the measuring result. However, each set of screws per sensor must be fixed with the same torque setting to guarantee proper measurement results. Additionally, all sensors in a measuring cross section shall be mounted with the same torque setting.

5.4.2 Choice of Padding Material

For the choice of padding material between the sensor steel plate and the counter steel box, two different types of rubber were available. These rubber plates are put in between the steel construction to mitigate the impact on the sensor as it is quite sensitive.
The first trial was conducted with rubber of 60 $\pm$ 5 (shore A) hardness that was also used for the SIS sensors and the second trial with rubber of 40 $\pm$ 5 (shore A) hardness.

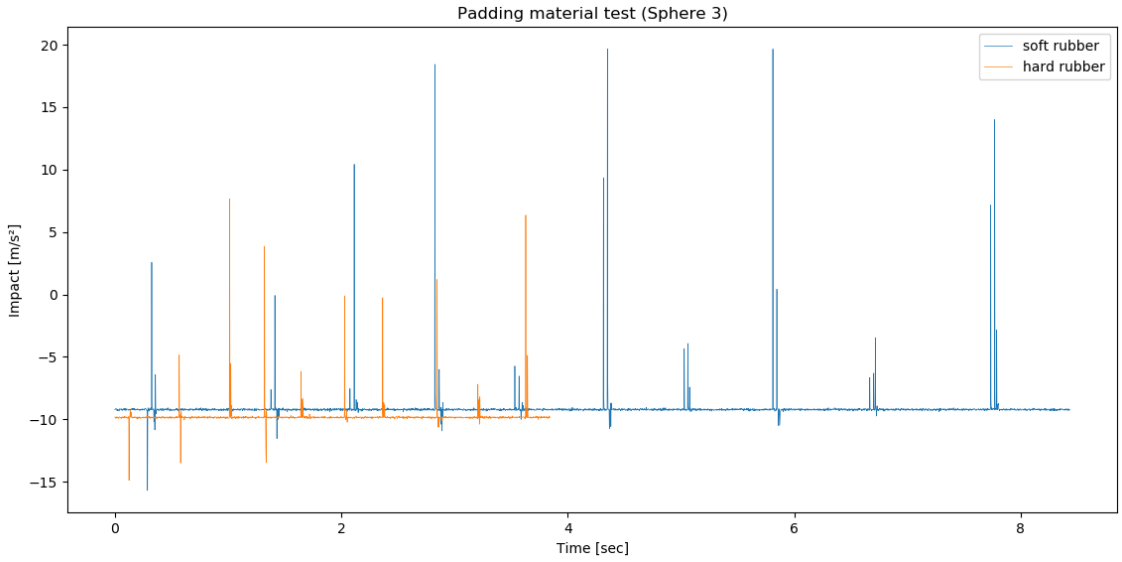

Figure 5.6: *Padding material test, sphere 3*

In both Figure 5.6 and Figure 5.7 it can be seen, that the softer rubber delivers higher impacts. As the sensors are very sensitive to impacts, the rubber with a higher hardness was chosen, as the limits of the sensors measuring range will not be reached as fast as with the softer rubber. Note, that the offset of the two graphs occurs due to the rearranging of the sensor when installing the softer rubber and due to the slightly different thicknesses of the materials.

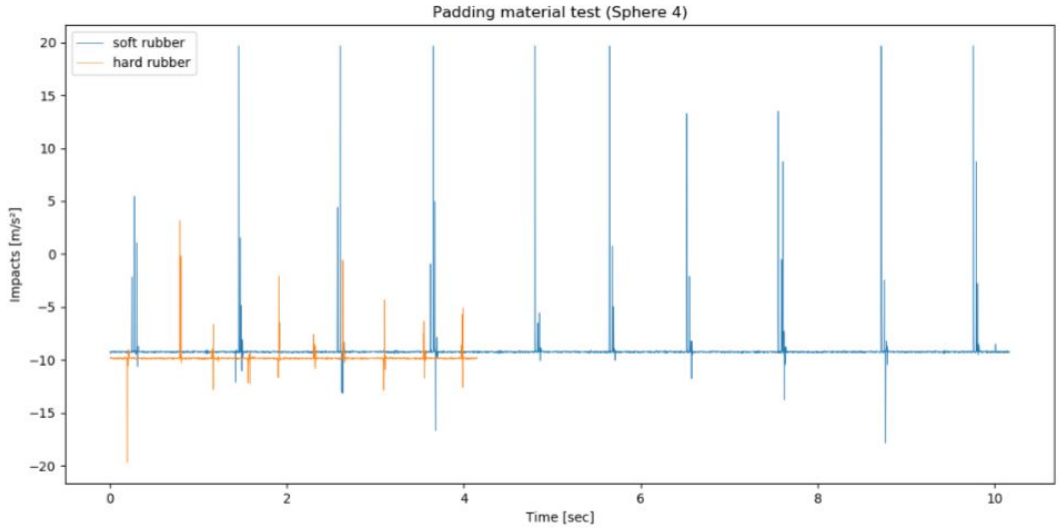

Figure 5.7: *Padding material test, sphere 4*

5.4.3 Wet Tests

After the assembling of the sensor (full construction manual in the paragraphs below), wet tests were needed as it will be installed in the riverbed. The sensor plate itself is glued onto the steel plate and filled watertight with epoxy resin. The connecting cables are coated with epoxy resin and mantled with shrinking tubes.
To guarantee that all sensors will be working in the field, they were submerged in a tank of water (Figure 5.8). After 72 hours the sensors were connected to the computer. All of the 10 sensors passed the test and were approved to be installed in the river.

Figure 5.8: *Wet test of the sensors at the laboratory*

5.4.4 Range

The first trial was conducted with the smallest sphere and lowest range (2 g) at a vertical height distance of 5 and 10 cm. The range soon had to be increased to 16 g, after the maximum values had been reached in the lower ranges. Even after increasing the gravitational span of the sensor, the drop of the steel spheres onto the plate occasionally reached the maximum value of 16 g or 156.96 m/s^2.
Even though these test represented extreme conditions, a later test under more realistic circumstances (stones of different sizes, impact height and direction, discharge in channel, etc..) showed, that even then extreme values could be reached. In Figure 5.9 a graph of a test with 3 stones (100-150 mm) can be found. While the first stone does not yet exceed the measurable value, the second and third do. These values were measured in the channel with 30 l/s of discharge and the stones were released into the water at a reasonable and realistic height.

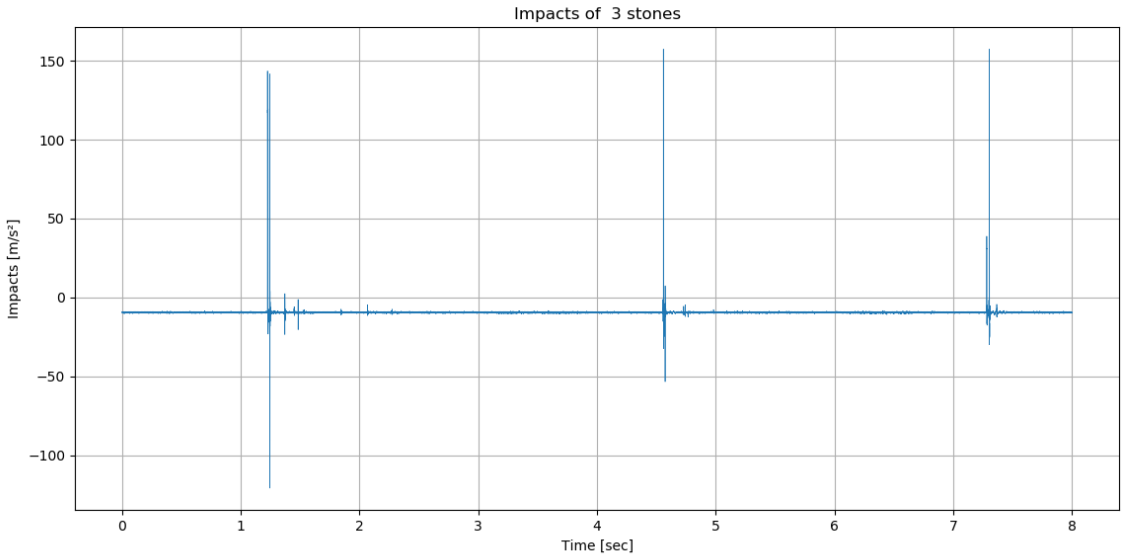

Figure 5.9: *Test with three stones (100-150 mm)*

Nonetheless, for the measurements in the field, the range of 16 g can be sufficient. Multiple test with buckets of 5 kg of rounded gravel (16/32 mm), rolling over the sensor, delivered measuring values of about half (80 m/s^2) of the possible maximum impact acceleration.

5.4.5 Frequency

At the beginning of the tests and at later stages, the amount of measuring data that would be collected with a 3200 Hz setting of the sensor caused for some discussions. Therefore, the goal was to reduce the frequency as much as possible and to still receive valuable data. For this cause, a measuring series with 2 different sized steel spheres and at a later stage with 5 kg buckets of (16/32 mm pebbles) were executed.
The first test with the steel spheres, as described in the Section 5.4.4, caused impacts that reached the maximum values already at a dropping distance of 50 - 100 mm. Figure 5.10 shows the graph of the comparison of the 5 g and the 20 g sphere, with 3200 Hz frequency and 100 mm dropping distance.

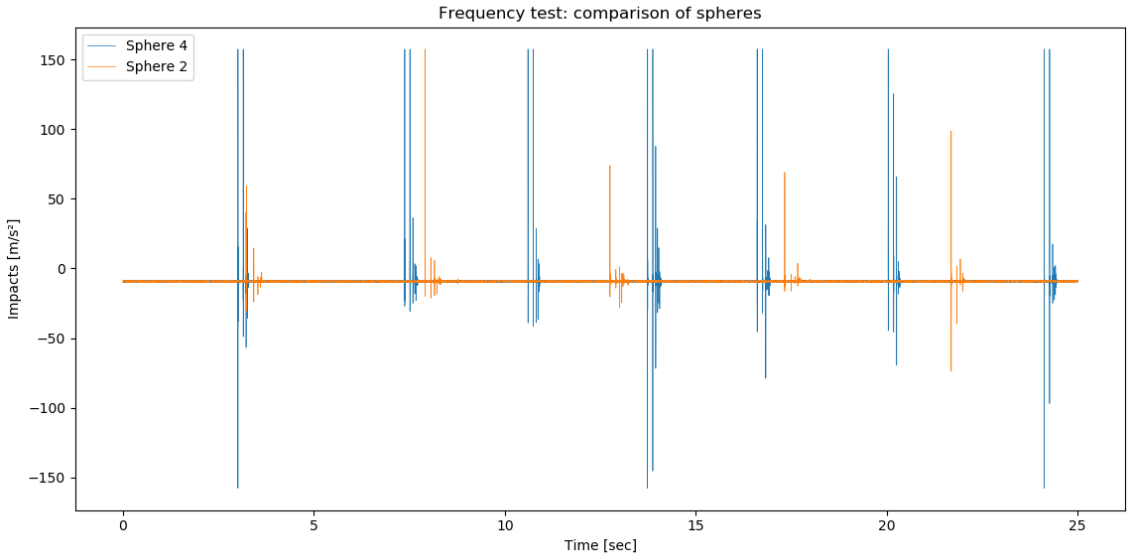

Figure 5.10: *Test with spheres, 3200 Hz, height of release 100 mm*

While sphere 4 clearly reaches the maximum acceleration values for the sensor during the whole test, sphere 2 does so only during the second drop. More tests with sphere 4 were not conducted, as the full amount of values could not be measured.
Tests with sphere 2 were done with frequencies of 3200, 1600 ,800, 400, 200, 100, 50 and 25 Hz.

In Figure 5.11 tests with frequencies of 3200 - 200 Hz are shown. It can be seen clearly, that with 3200 Hz maximum impact accelerations were measured. When looking at frequencies of 1600 Hz and below, lower impacts can be noted. The reason for these lower values (compared to 3200 Hz) is, that values are measured 1600 times per second or lower. After execution of the test with different frequencies, it appears that impacts happen in

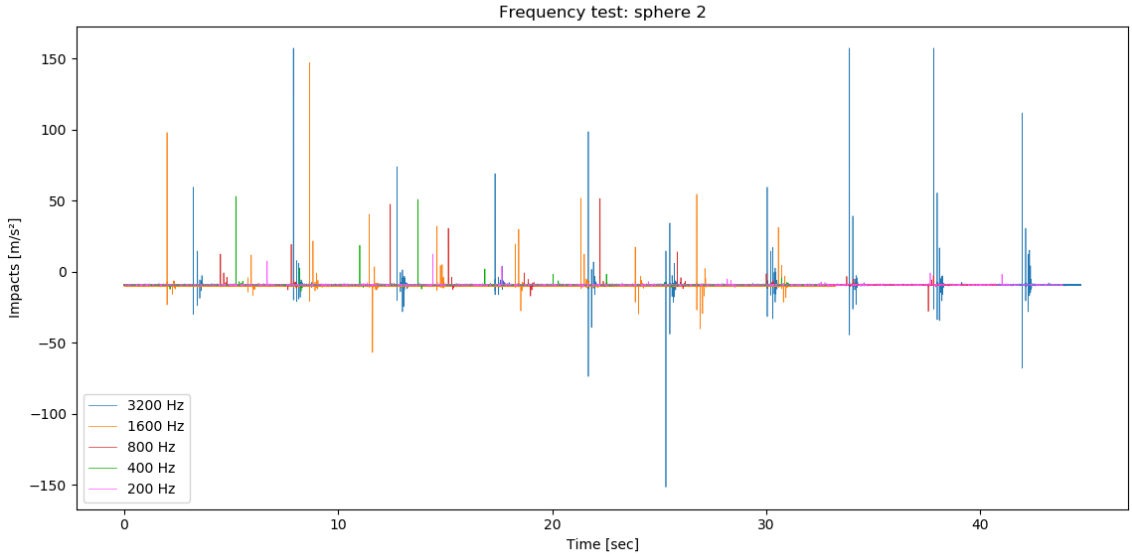

Figure 5.11: *10 drops of sphere 2 with different frequencies*

between measurements, even though 1600 measurements are done within the second. Considering this, it cannot even be guaranteed that measurements executed with 3200 Hz record all impacts to their full extent. However, this can not be said for certain, as the sensor is limited to 3200 Hz and cannot be tested at a higher frequency. The frequencies 100, 50 and 25 Hz are left out in the graph as it was not possible to do valuable measurements in this frequency ranges.

Due to an immense load of data storage that is needed for continuous measurements in a riverbed, further test were done to decide whether a lower frequency of 1600 Hz would be sufficient for the purpose. A sensor measuring with 3200 Hz produces approximately 27 GB of data per day, whereas 1600 Hz would lead to about 15 GB per day. Adding these values up for all 10 sensors would conclude in a daily storage of data of 270 GB respectively 150 GB.
Therefore, another series of tests were executed. Buckets of 5 kg of pebbles with diameters 16/32 mm were tipped into a channel were a sensor is mounted. The channel (approximately 60 cm wide) was additionally fed with 30 l/s of flowing water, for a nature-like experiment. Six test were done with 3200 Hz and six additional tests with 1600 Hz. Two graphs with results can be seen in Figure 5.12 and Figure 5.13, the whole set of graphs can be found in the Appendix.

A comparison of the impacts and therefore the acceleration of the impacts was done. For this cause, the positive and negative impacts caused by the pebbles of each bucket were

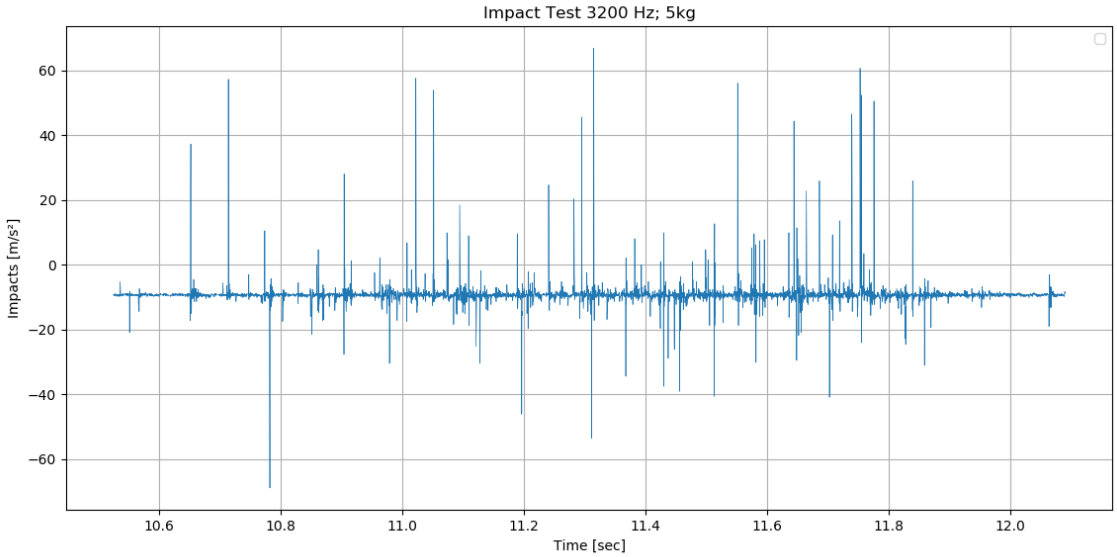

Figure 5.12: *Measurement of 5 kg bucket at 3200 Hz*

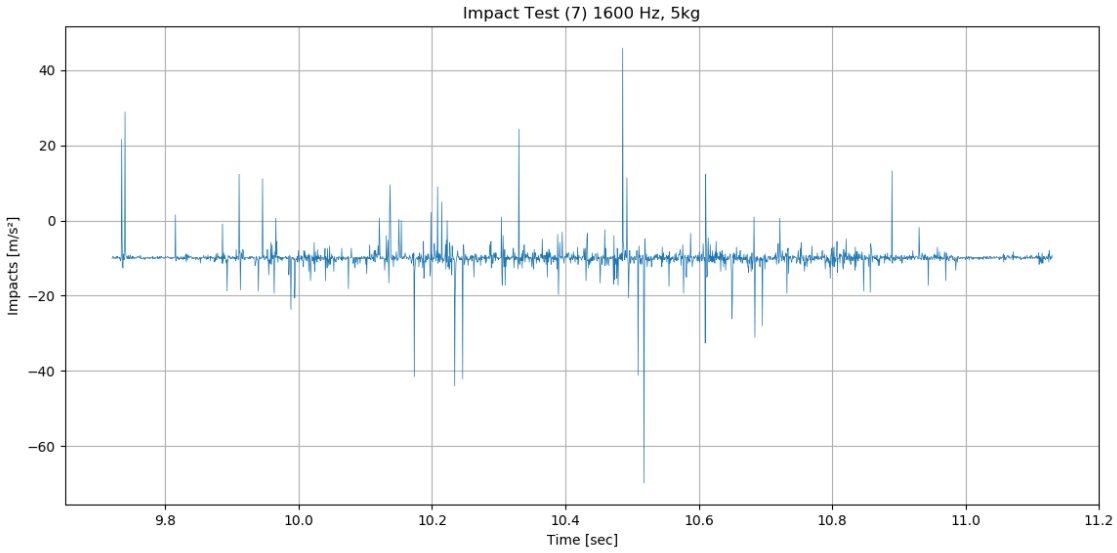

Figure 5.13: *Measurement of 5 kg bucket at 1600 Hz*

averaged over time. In Figure 5.14 a table of the tests and the results of the positive and negative impact sums for 3200 and 1600 Hz can be found. Out of 12 tests, one delivered faulty results and was not considered in the evaluation.

The measurements conducted with 3200 Hz clearly deliver more acceleration impact values and therefore higher impact sums over time, whereas measurements with 1600 Hz

	Time [sec]	Hz	Sumplus/t	Sumplus	Summinus/t	Summinus
1	1,565	3200	824,81	1290,83	-1100,34	-1722,03
2	1,485	3200	288,36	428,21	-1117,45	-1659,41
3	1,280	3200	810,84	1037,88	-1319,68	-1689,19
4	1,140	3200	1013,02	1154,84	-1431,81	-1632,26
5	1,350	3200	528,93	714,06	-1022,06	-1379,78
6	0,427	3200	494,31	211,07	-1065,49	-454,96
7	1,410	1600	209,40	295,25	-619,68	-873,75
8	1,779	1600	182,84	325,27	-544,84	-969,27
9	1,429	1600	281,18	401,81	-557,00	-795,95
10	1,190	1600	677,96	806,77	-662,23	-788,05
11	0,730	3200	309,17	225,69	-895,76	-653,90
12	1,660	1600	50,01	83,02	-509,39	-845,59

SET 1 (3200 Hz)	Summinus/t mean =	-1176,14
	Standarddeviation =	161,95
SET 2 (1600 Hz)	Summinus/t mean =	-578,63
	Standarddeviation =	61,40

Figure 5.14: *Positive and negative impact sum time averaging with mean values and standard deviation*

result in less values and a lower impact sum over time. Generally, it can be said that the correlation between the measurements of each frequency test are only matching to a small extent and that the deviation for Set 1 is higher than for Set 2. A reason for this deviation can be, that the larger impacts, during the tests for Set 2, were not measured due to the frequency setting of 1600 Hz. The variation of impact values in the Data Set 1 and Set 2 itself, could be explained by the number of tests for each frequency setting and, more generally, the execution of the experiment. First of all, the bucket was manually tipped into the channel. The height at which the bucket was emptied, as well as the alignment of the tipping direction varied. Furthermore, the sensor is mounted in a channel of approximately 60 cm of width. As the sensor is only 15 cm wide, the measurements cover only one fourth of the whole channel width. This means that it cannot be said how many stones went directly over the sensor and how many have passed by on either sides of the sensor. However, considering all of these factors a distinction between the two frequency measurements can be made when purely looking at the values for the total impact acceleration (Summinus/t).

In Chapter 6, a list of improvements for further tests as well as a recommendation for further tests is given.

6 Conclusion and Recommendation

This chapter includes recommendations, lessons learned and advice on measuring systems, techniques and future tests for the developed MEMS accelerometer.

6.1 Measuring Cross Section Hintereggertor

The measuring cross section Hintereggertor has all the needed devices to research flow velocity, water level measurements, turbidity of the water, conductivity and temperature. Additionally, it is easily accessible and therefore easy to maintain. However, the devices itself are of little to no use, if they are not delivering useful data. In the sections below some problems and how to resolve them are discussed.

6.1.1 Multiparameter Sensor

The multiparameter sensor collects information about the water temperature, conductivity and turbidity. When the probe was installed in July 2018 an error in the conductivity and turbidity sensor occurred and unrealistic values are returned. This error was not recognized until September 2018, when the evaluation of the data, during this master thesis was done. As these two parameters are key factors in the analyzation of the suspended sediment transport, field tests are suggested to ensure that the probe provides correct data. These field tests include a check of data of the probe outside of the river in fresh water and ensuring the data is reasonable, when putting the sensor back into the river, on site.

6.1.2 Gauging Station

The radar sensor gauging station generally delivers valuable data. However, the conversion of the values from relative water level to the discharge is problematic, as the rating curve needs to be updated. Therefore, multiple nautilus measurements shall be done to gain additional reference measurement. Only then, proper readings of the gauging station can be made. Cross checks with the data of the multiparameter sensor is advisable, as this data shall correlate.

6.2 MEMS Accelerometer

The first application of MEMS accelerometers has been during this master thesis. Therefore, a number of tests have to be made in the future to gain more information about the field of application, calibration tests and how to make readings of the data. Here is a short summary of the results, remarks, tips and suggestions for further testing of the sensor.

Laboratory tests

Screw torque tests for the fixation of the sensor plate with the casing were conducted with two different screw torque settings (10 Nm and 20 Nm). The results showed, that a differentiation between the two settings could not be made. However, the screw torque for all sensors shall be the same to guarantee the comparability of the results.

The laboratory tests for the choice of padding material showed, that the rubber used for the Sediment Impact Sensors proved to be very suitable for the task. For the new sensor setup laboratory tests have been carried out with rubbers of two different shore A hardness values (45 and 60). The results of the test showed, that the softer rubber (shore A hardness 45) allowed for much higher impacts, which is to be avoided due to the impact acceleration range of the sensor. The harder rubber allowed for an attenuation of the impacts. Additionally, the softer rubber was significantly compressed, even with the application of a low screw torque. The harder rubber did not show any signs of compression.

Wet tests, where the ten sensors for the Schöttlkapelle cross section were submerged into a tank of water over a period of 72 h showed, that all parts of the sensor are watertight and can be built into the submergerd weir.

For the setting of the sensors measuring frequency the tests showed, that measurements are only useful with a frequency setting between 1600 and 3200 Hz. Test conducted with frequencies below 1600 Hz delivered results, where impacts did not get recognized by the sensor and would therefore not be suitable for continuous measurements of the sediment transport and impacts. Additional testing for the distinction between test results for 1600 and 3200 Hz were done and showed, that with higher frequency more acceleration impacts can be recognized than with lower frequency. However, further tests are necessary to conclude, whether it is possible to gain similar results with 1600 Hz instead of 3200 Hz. Recommendations for further tests are given in the next paragraphs.

The range tests showed, that the maximum setting for gravitational acceleration of ± 16 g is necessary. Tests conducted with lower range settings delivered values, that reached the sensors peak with hardly any impact force. When increasing the range, the maximum

possible impact acceleration the sensor is able to recognize is about 156.96 m/s^2, which proved to be sufficient.

Recommendations

During the testing phase in the laboratory it was tried to unify the technique in which tests were conducted. For the first trials a steel construction was made that allowed for the test object to drop onto the sensor with fixed heights and into the same area of the sensor. The other tests in the bigger channel were set up differently. When emptying a bucket of sediment into the channel, human force is needed, thus irregularities can happen. These irregularities can be a change of alignment of the bucket when tipping the contents into the channel, but it can also include the height at which the bucket was emptied. Furthermore, the sensor width is one fourth of the width of the channel, which allows for sediment to pass on either sides of the sensor. This was problematic for the frequency design tests as there were only six trial runs per frequency setting. To gain reliable results more measurements for each setting have to be done.
Even though the discharge in the channel did not seem to have an impact on the sensor itself, it is advised to measure with the same flows for each trial test.

Figure 6.1: *Arrangement of the sensors in the river*

Future Tests and Measurements

For future tests and results that can be comparable, measurements on the sensor in the channel must be set up, so that no human error can occur and differences in the test result cannot be traced back to irregular handling of sediment. A conveyor band or a controlled tipping mechanism for the bucket shall be installed to reduce the error that can happen during the inducing of the sediment. Additionally, cross checks with a second sensor that is mounted in the alignment of the first sensor shall be made. This arrangement shall compare to the installation at the Schöttlkapelle measuring station as shown in Figure 6.1

Calibration tests shall be made with different mass and flow, once a correlation can be found in the first trial. Therefore, buckets of sediment mass or sediment mass on a conveyor band shall be induced in to the channel as described above at least 10-20 times. Once the tests with the first mass show similar results, more tests shall be made with different mass and discharges.

Bibliography

Altendorf M., Stauss T. Durchfluss-Handbuch: Ein Leitfaden für die Praxis: Messtechniken - Anwendungen - Lösungen. 2003.

Analog Devices Inc. . Data Sheet ADXL345 Digital Accelerometer Sensor. 2015. 1–40.

Barbas T. Masterarbeit: Untersuchung des Geschiebetransports in Wildbächen mittels Tracerverfahren. 2014. 1–185.

Bartby J. Progress in Filtration and Separation. 2015. 18th. 636–657.

Belleudy P. Bedload monitoring of rivers with hydrophone technique. 2015. 28.

Chollet Franck, Liu Haobing. A (not so) short introduction to Micro Electro Mechanical Systems. Sep 2016. 5.3rd. This is an electronic document published under Creative Commons Attribution-NonCommercial 3.0 License (`http://creativecommons.org/licenses/by-nc/3.0/legalcode`).

DVWK . Regeln zur Wasserwirtschaft. Geschiebemessungen. 1992.

Definitions.net . .STANDS4 LLC, 2018, Proper velocity. 2018. Accessed: 11.07.2018.

Dyck S., Peschke G. Grundlagen der Hydrologie: mit 72 Tafeln. 1995. 536.

Fleissner R., Dorfmann C., Aichinger S. Bed Load Analyzer V 2.1. 2014. Accessed: 25.10.2018.

Free Software Foundation . SeriaPlot Software. 2018. http://fsf.org, Free Software Foundation Inc., Accessed: 06.10.2018.

Fürst J., Jugovic C.J. Abflussbestimmungen in offenen Gerinnen. 2009.

GIS-Steiermark . Digitaler Atlas Steiermark: Gewässer und Wasserinformation. 2018. Accessed: 26.06.2018.

GKG-Schweiz . Fluviatale Kräfte in Ober-, Mittel- und Unterlauf. 2004. Accessed: 15.09.18.

Google . Image ©Digital Globe, Google Earth Pro. 2018. Accessed: 22.06.2018.

Habersack H. Wiener Mitteilungen Wasser Abwasser – Gewässer. Raum–Zeitliche Variabilitäten im Geschiebehaushalt und dessen Beeinflussung am Beispiel der Drau. 1997.

Habersack H., Aigner J., Kreisler A., Rindler R., Seitz H., Tritthart M. Geschiebemessungen an der Drau und Isel. 2012.

Hübl J., Eisl J., Hohl D., Kogelnig B., F. Mühlböck. Ereignisdokumentation und Ereignisanalyse Wölzerbach. 1. 2011. 80.

Langer B., Stoisser A. Masterarbeit: Erfassung des Sedimenttransports von Wildbächen in einem alpinen Einzugsgebiet mittels Sediment Impact Sensoren, Telimetrie und Radio Frequency Identification. 2016. 251.

Niederl R. Gefügeentwicklung der Wölzer Granatglimmerschiefer und der "Übergangsserie" bei Oberwölz (Steiermark). 120, pages 229–242. 1990.

ORF-Steiermark . Oberwölz: Aufräumen nach dem Unwetter. 2017. Accessed: 25.10.2018.

OTT Hydromet GmbH . OTT C31 Universal–Messflügel für die Abflussmessungen. 2018. Accessed: 12.08.2018.

Pertl A. Masterarbeit: Vergleich von Methoden und Messgeräten für die Durchflussmessungen an Oberflächengewässern. 2004. 80.

Petrograph . Sedimente und Kornform, Mineral – und Gesteinsbestimmungspraktikum an der Freien Universität Berlin. 2014. Accessed: 07.07.2018.

Reichenbach R., Schubert D., Reutlingen Robert Bosch GmbH, Gerlach G., Dresden Technische Universität. Dreiachsiger Beschleunigungssensor in Oberflächenmikromechanik. 2003. 225–232.

Rickenmann D. Methods for the Quantitative Assessment of Channel Processes in Torrents (Steep Streams). 2016. (IAHR Monographs).

Rickenmann D., Turowski J., Fritschi B., Klaiber A., Ludwig A. Bedload transport measurements at the Erlenbach stream with geophones and automated basket samplers. 2012.

Sackl B. Hochwasserdokumentation Wölzertal 07.07.2011. 2011. Vorabzug.

Sadar M. Turbidity Instrumentation – an overview of today‘s available technology. 2002a.

Sadar M. Turbidity Measurement: A Simple, Effective Indicator of Water Quality Change. 2002b. 1–5.

Sadar M. Making Sense of Turbidity Measurements– Advantages in Establishing Traceability Between Measurements and Technology. n.A. 1–10.

Sass O., Harb G., Truhetz H., Stangl J., Schneider J. Abschlussbericht Projekt ClimCatch. 2015. 1–40.

Scharbert R., Schönlaub H. Der geologische Aufbau Österreichs. 1980. 18.

Spreitzer G. Masterarbeit: Untersuchung des Sedimenttransports sowie des Abflussverhaltens von Wildbächen in einem alpinen Einzugsgebiet mittels Feldmessungen. 2014. 302.

Stadtgemeinde Oberwölz . Über die Stadt Oberwölz. 2018. Accessed: 06.06.2018.

Tindie Inc. . 3 axis USB accelerometer. 2018.

Turowski J. Geschiebetransport 2. Vorlesung für Hydro 1. 46 S., Vorlesungsunterlagen. 2011.

Turowski J., Badouy D. A. Rickemann, Fritschi B. Erfassung des Sedimenttransportes in den Wildbächen und Gebirgsflüssen– Anwendungsmöglichkeinten von Geophonanlagen. 2008.

Universität Graz Institut für Geographie und Raumforschung. RunSed-CC–Modelling future runoff and sediment transport in alpine torrents. Graz: Förderungsantrag A3 Klima Energie Fond–Modelling future runoff and sediment transport in alpine torrents – not published, 2018. 1–13.

List of Figures

List of Tables

Appendix

Content of the Appendix:

- Design test graphs (sphere tests)
- Frequency test graphs (sphere tests)
- Water test graphs (spheres and pebbles)
- Frequency test graphs (buckets)

Design test graphs (sphere test)

No.	Padding	Screw torque [Nm]	Height [mm]	Sphere	No.	Padding	Screw torque [Nm]	Height [mm]	Sphere
1	Hard	10	50	1	17	Soft	10	50	1
2	Hard	10	50	2	18	Soft	10	50	2
3	Hard	10	50	3	19	Soft	10	50	3
4	Hard	10	50	4	20	Soft	10	50	4
5	Hard	10	100	1	21	Soft	10	100	1
6	Hard	10	100	2	22	Soft	10	100	2
7	Hard	10	100	3	23	Soft	10	100	3
8	Hard	10	100	4	24	Soft	10	100	4
9	Hard	20	50	1	25	Soft	20	50	1
10	Hard	20	50	2	26	Soft	20	50	2
11	Hard	20	50	3	27	Soft	20	50	3
12	Hard	20	50	4	28	Soft	20	50	4
13	Hard	20	100	1	29	Soft	20	100	1
14	Hard	20	100	2	30	Soft	20	100	2
15	Hard	20	100	3	31	Soft	20	100	3
16	Hard	20	100	4	32	Soft	20	100	4

Frequency	200 Hz	Range	2

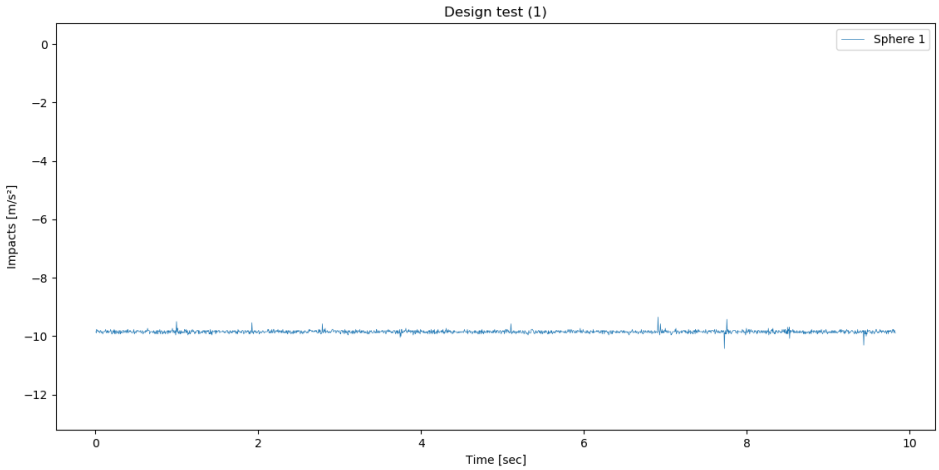
Design test (1)
Sphere 1
Impacts [m/s²]
Time [sec]

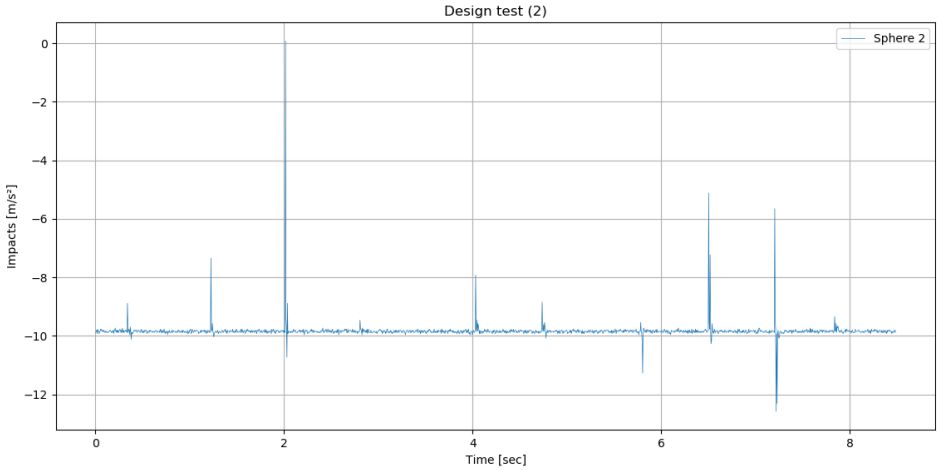
Design test (2)
Sphere 2
Impacts [m/s²]
Time [sec]

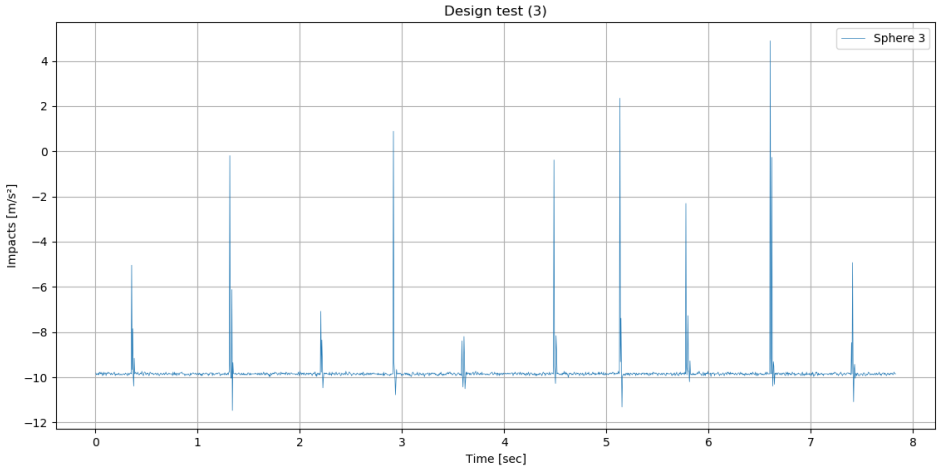
Design test (3)
Sphere 3
Impacts [m/s²]
Time [sec]

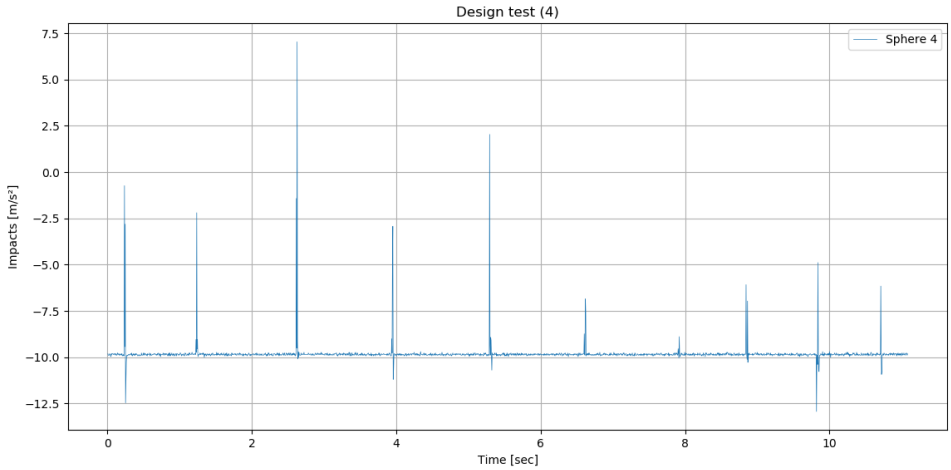
Design test (4)
Sphere 4
Impacts [m/s²]
Time [sec]

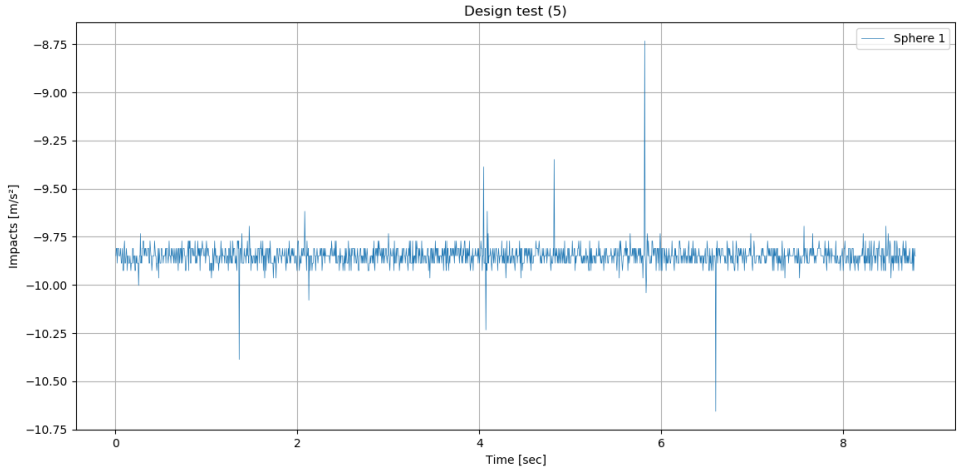
Design test (5)
Sphere 1
Impacts [m/s²]
Time [sec]

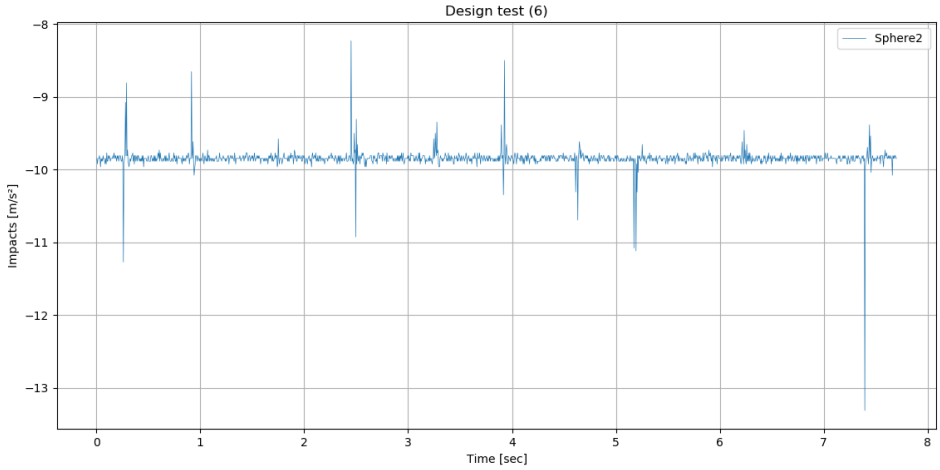
Design test (6)
Sphere2
Impacts [m/s²]
Time [sec]

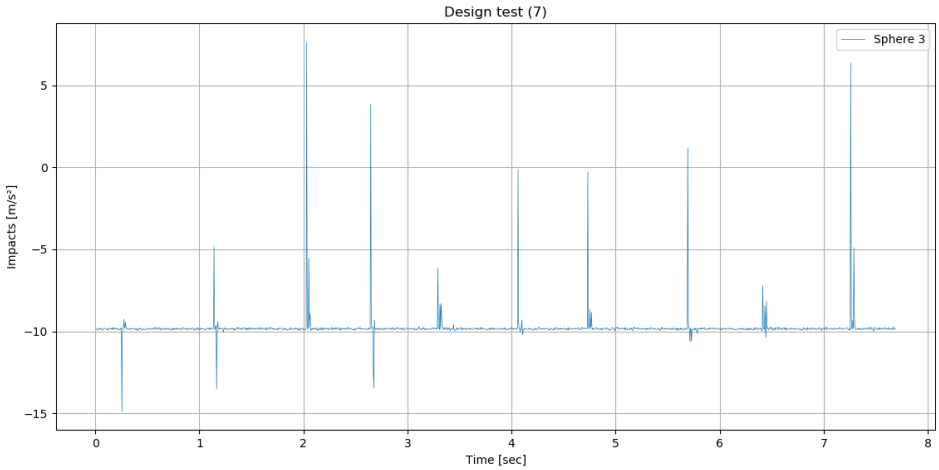
Design test (7)
Sphere 3
Impacts [m/s²]
Time [sec]

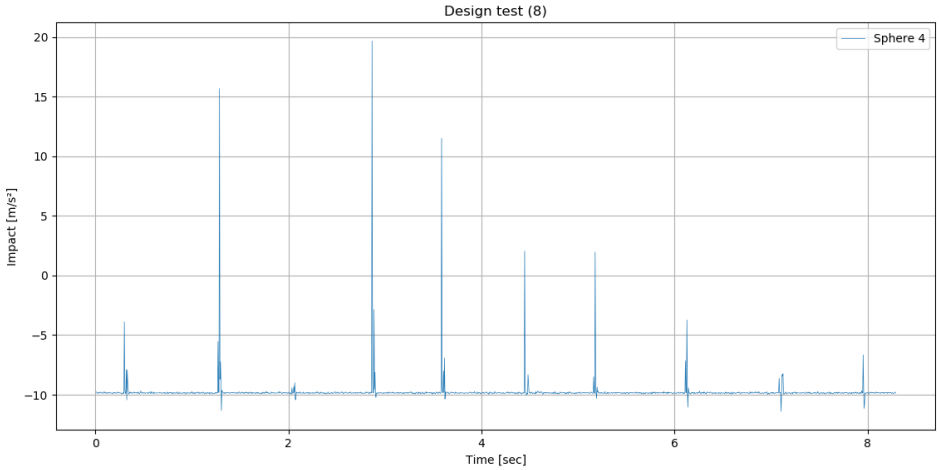
Design test (8)
Sphere 4
Impact [m/s²]
Time [sec]

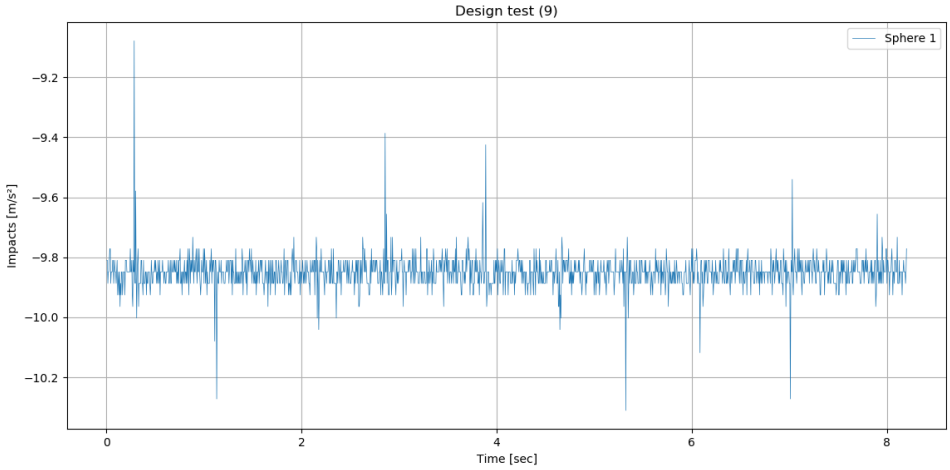
Design test (9)
Sphere 1
Impacts [m/s²]
Time [sec]

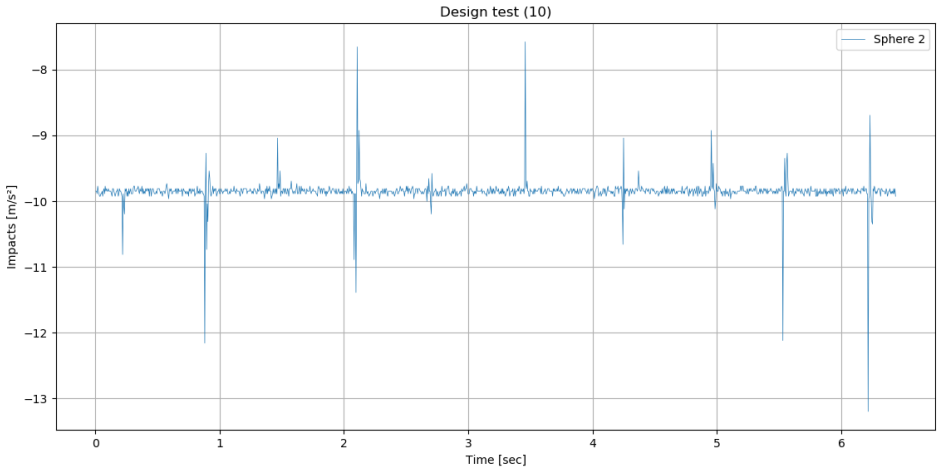
Design test (10)
Sphere 2
Impacts [m/s²]
Time [sec]

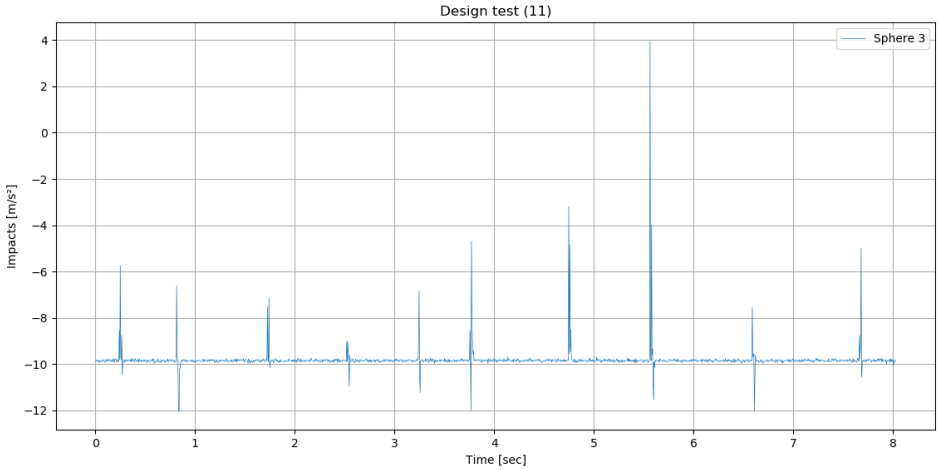
Design test (11)
Sphere 3
Impacts [m/s²]
Time [sec]

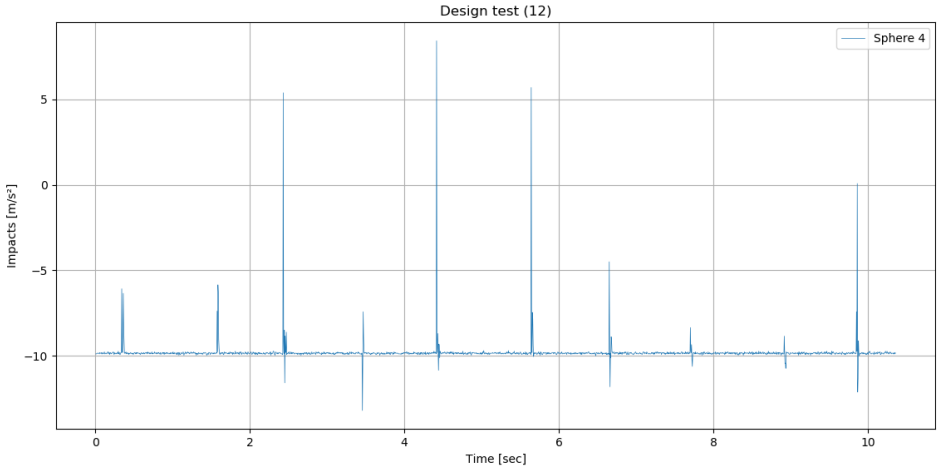
Design test (12)
Sphere 4
Impacts [m/s²]
Time [sec]

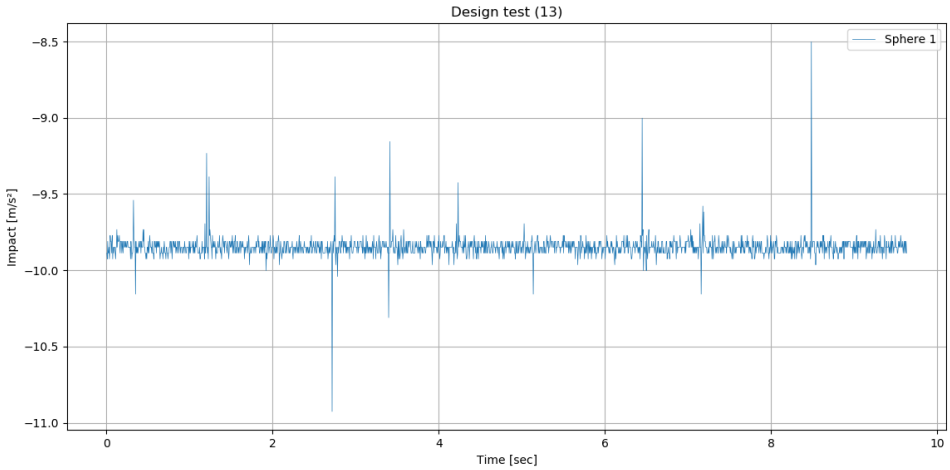
Design test (13)
Sphere 1
Impact [m/s²]
−8.5
−9.0
−9.5
−10.0
−10.5
−11.0
0
2
4
6
8
10
Time [sec]

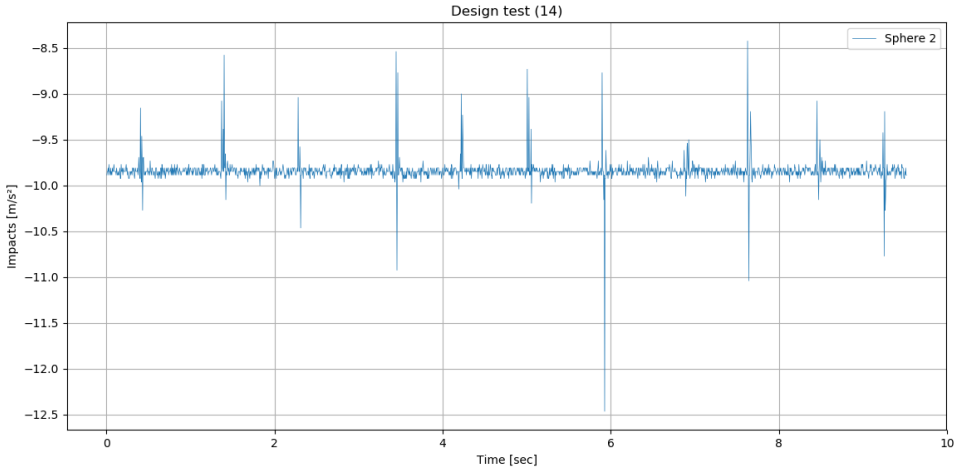
Design test (14)
Sphere 2
Impacts [m/s²]
−8.5
−9.0
−9.5
−10.0
−10.5
−11.0
−11.5
−12.0
−12.5
0
2
4
6
8
10
Time [sec]

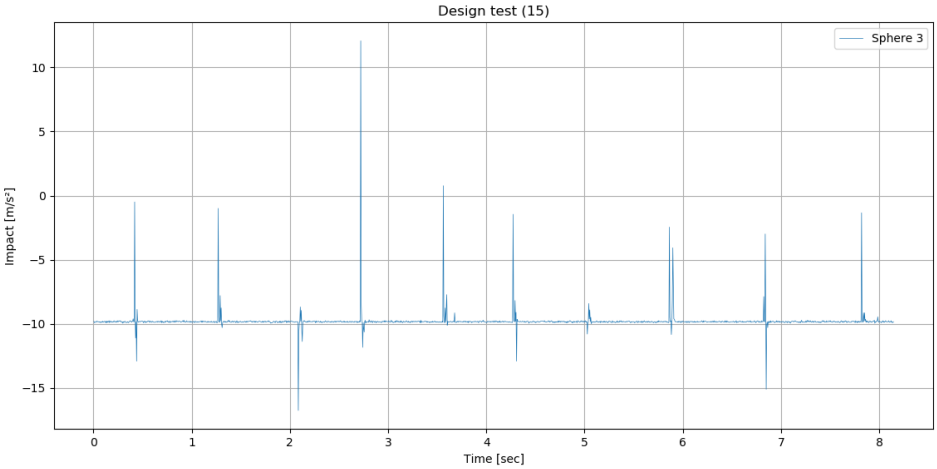
Design test (15)
Sphere 3
Impact [m/s²]
10
5
0
−5
−10
−15
0
1
2
3
4
5
6
7
8
Time [sec]

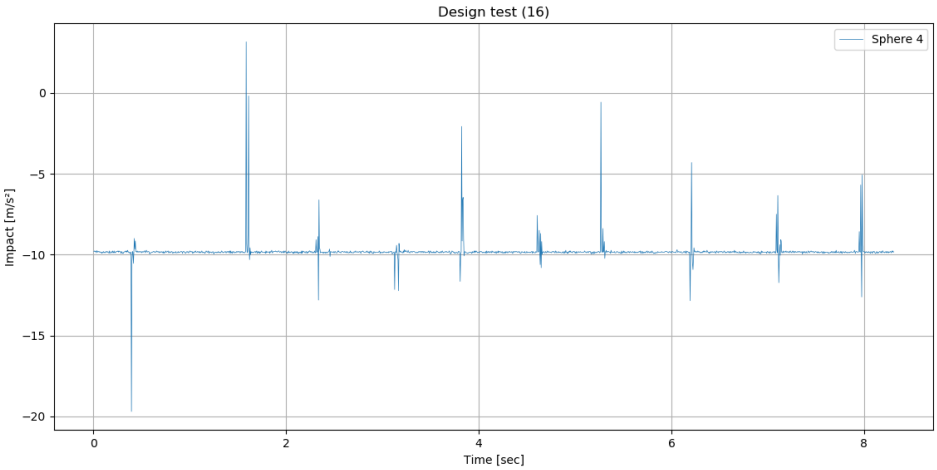
Design test (16)
Sphere 4
Impact [m/s²]
Time [sec]

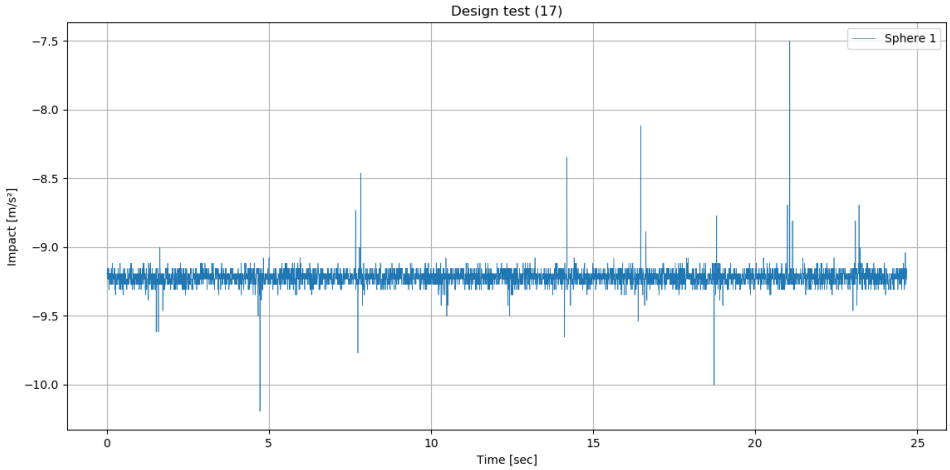
Design test (17)
Sphere 1
Impact [m/s²]
Time [sec]

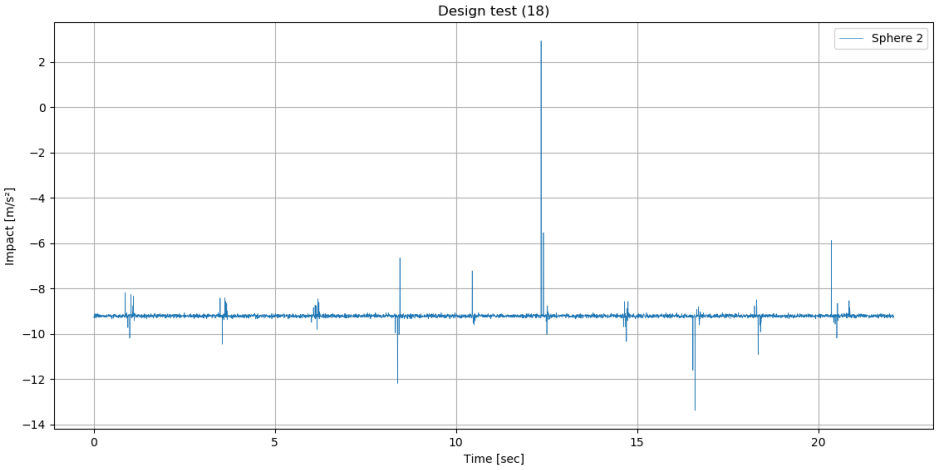
Design test (18)
Sphere 2
Impact [m/s²]
Time [sec]

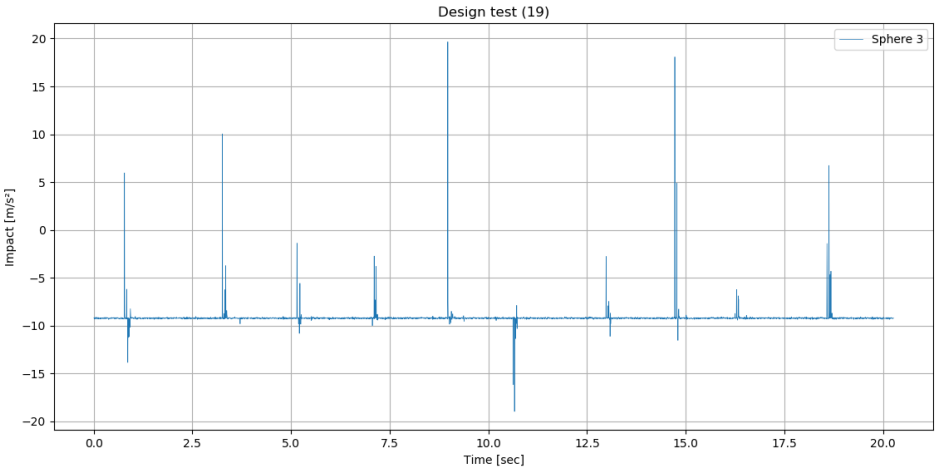
Design test (19)
Sphere 3
Impact [m/s²]
Time [sec]

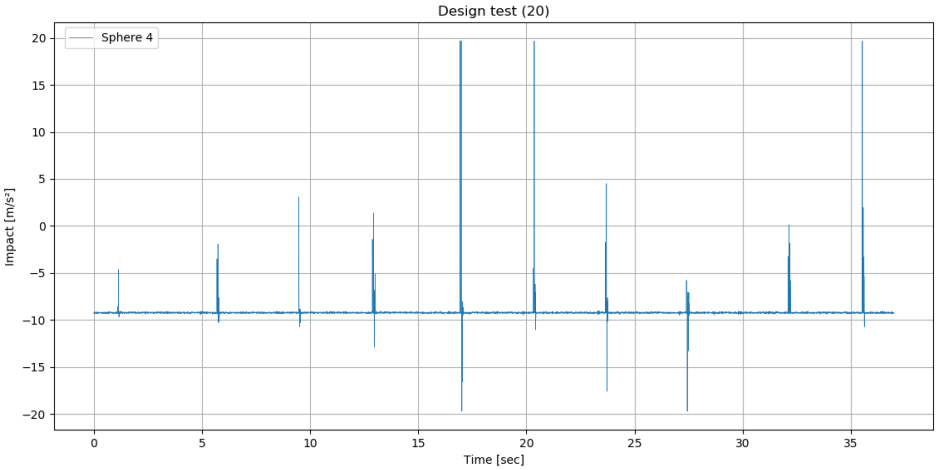
Design test (20)
Sphere 4
Impact [m/s²]
Time [sec]

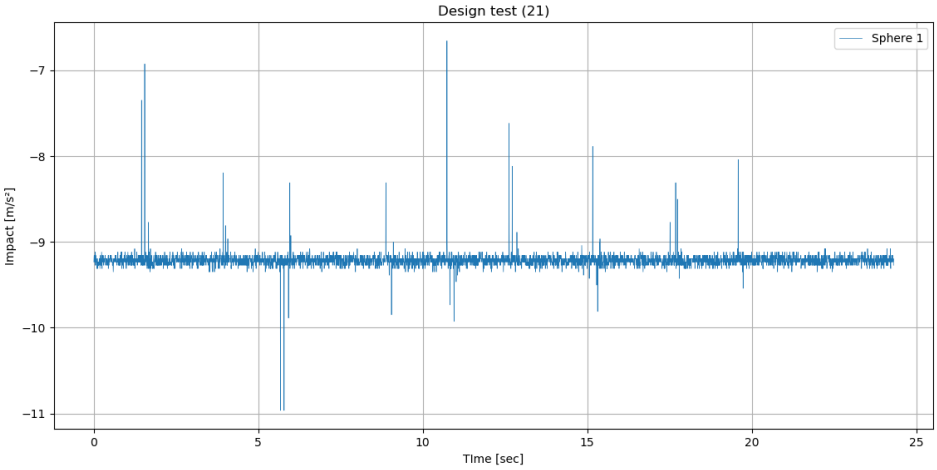
Design test (21)
Sphere 1
Impact [m/s²]
TIme [sec]

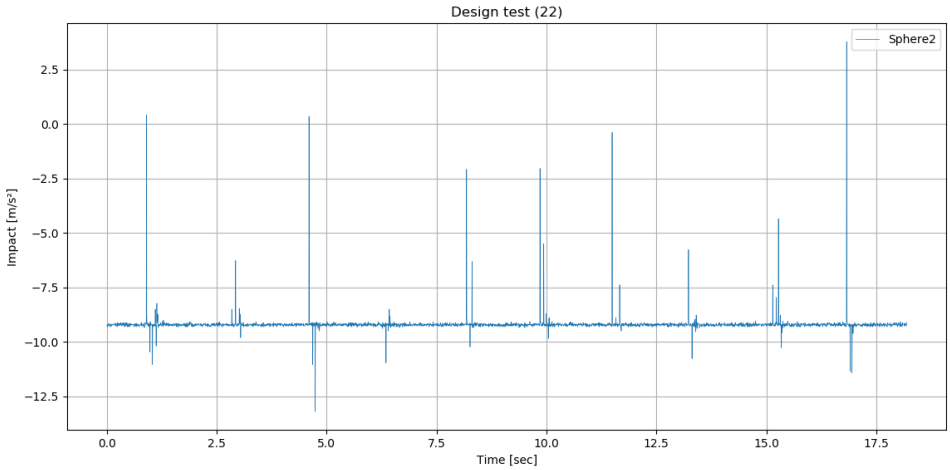
Design test (22)
Sphere2
Impact [m/s²]
Time [sec]

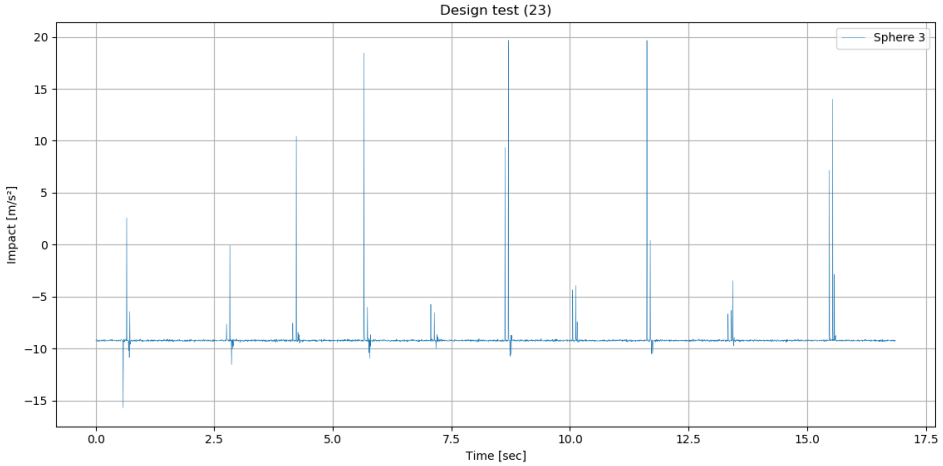
Design test (23)
Sphere 3
Impact [m/s²]
Time [sec]

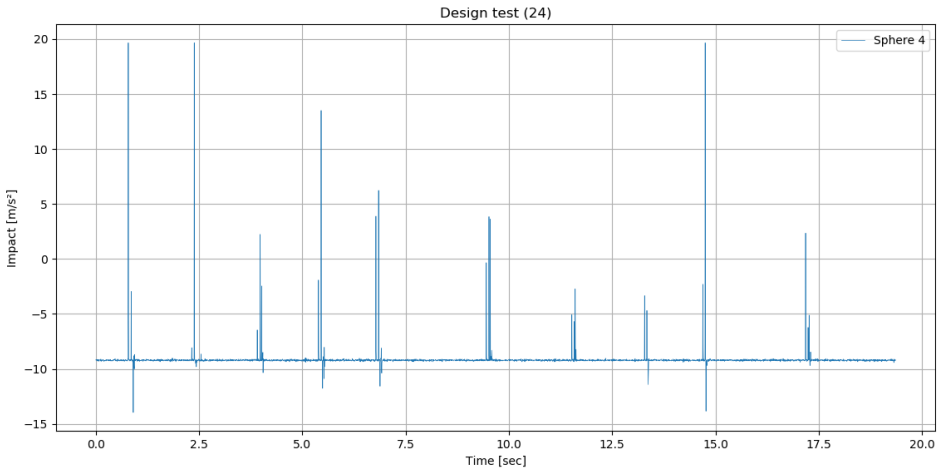
Design test (24)
Sphere 4
Impact [m/s²]
Time [sec]

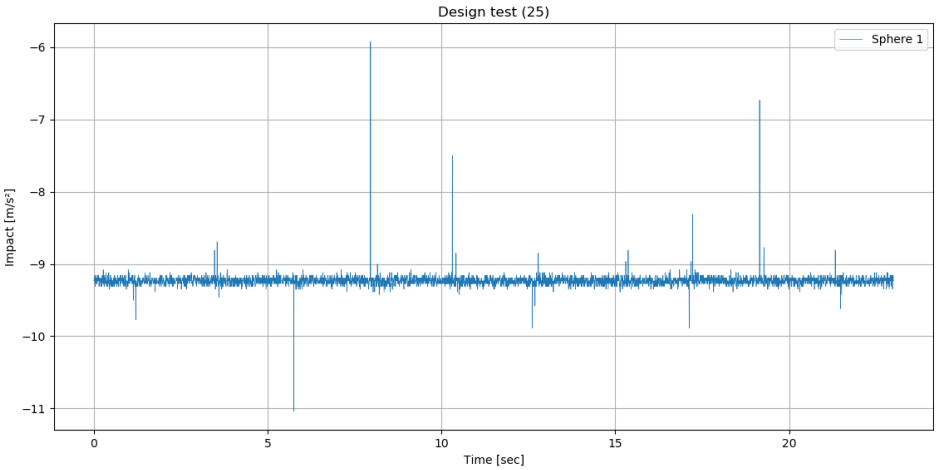
Design test (25)
Sphere 1
Impact [m/s²]
Time [sec]

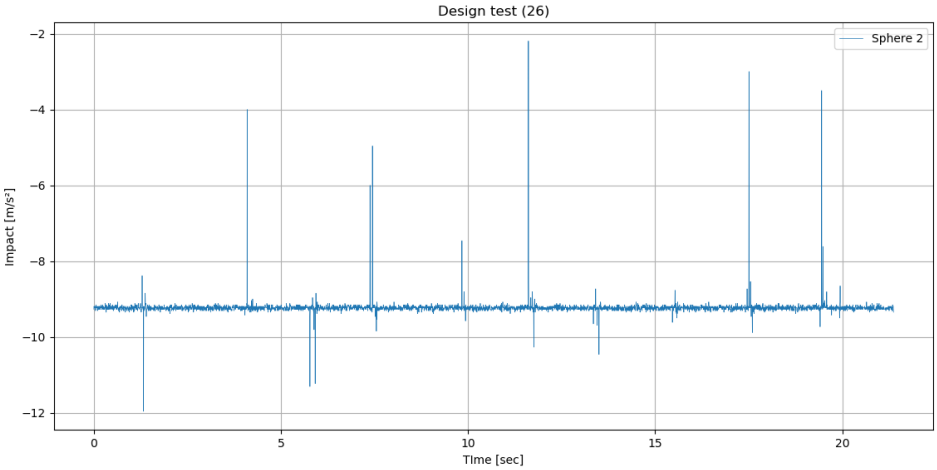
Design test (26)
Sphere 2
Impact [m/s²]
TIme [sec]

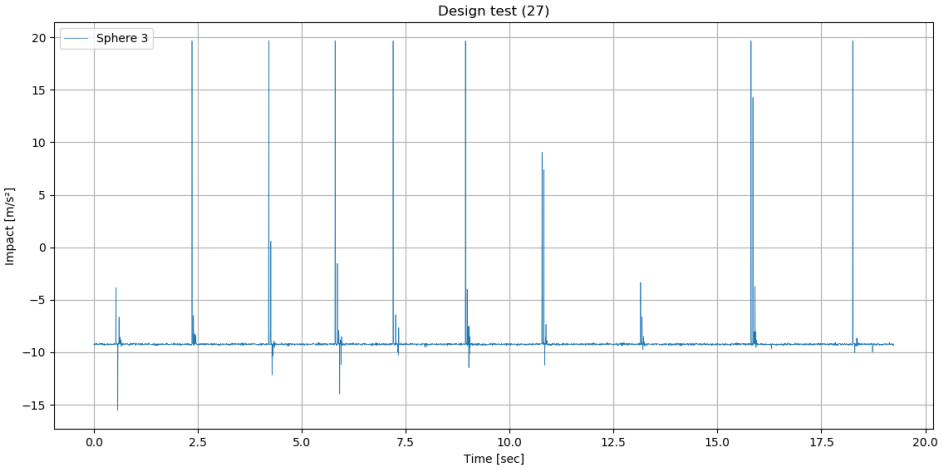
Design test (27)
Sphere 3
Impact [m/s²]
Time [sec]

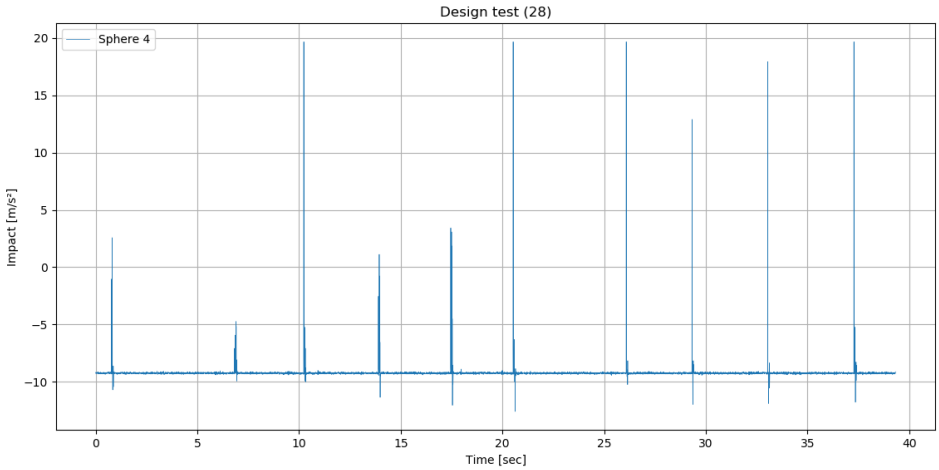
Design test (28)
Sphere 4
Impact [m/s²]
Time [sec]

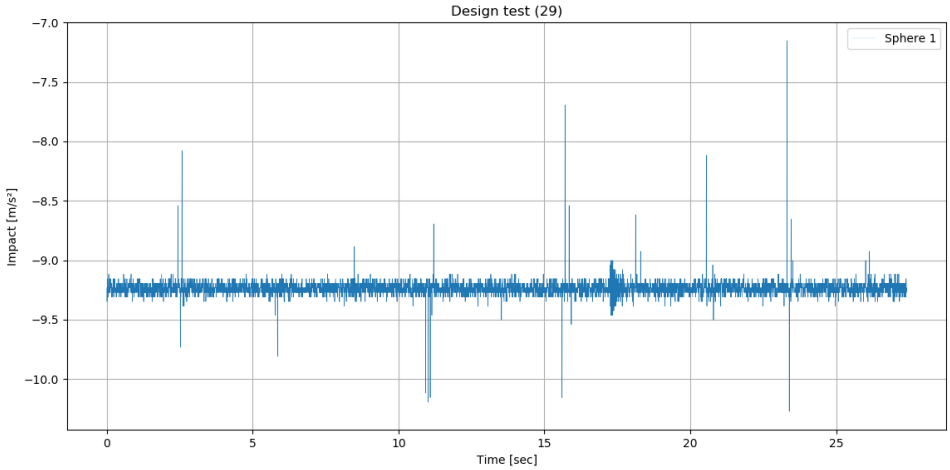
Design test (29)
Sphere 1
Impact [m/s²]
Time [sec]

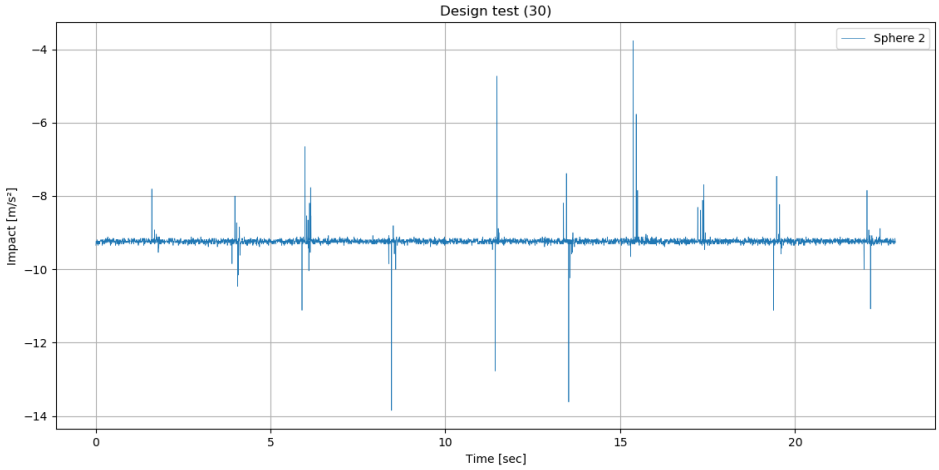
Design test (30)
Sphere 2
Impact [m/s²]
Time [sec]

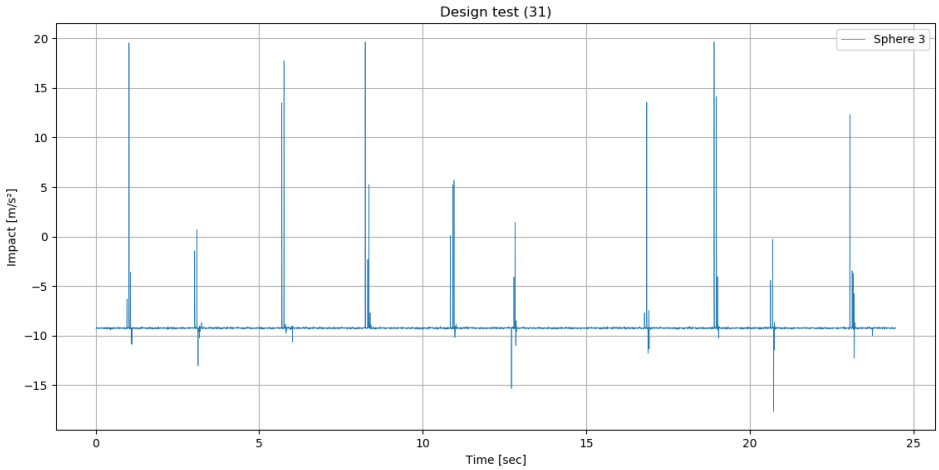
Design test (31)
Sphere 3
Impact [m/s²]
Time [sec]
20
15
10
5
0
−5
−10
−15
0
5
10
15
20
25

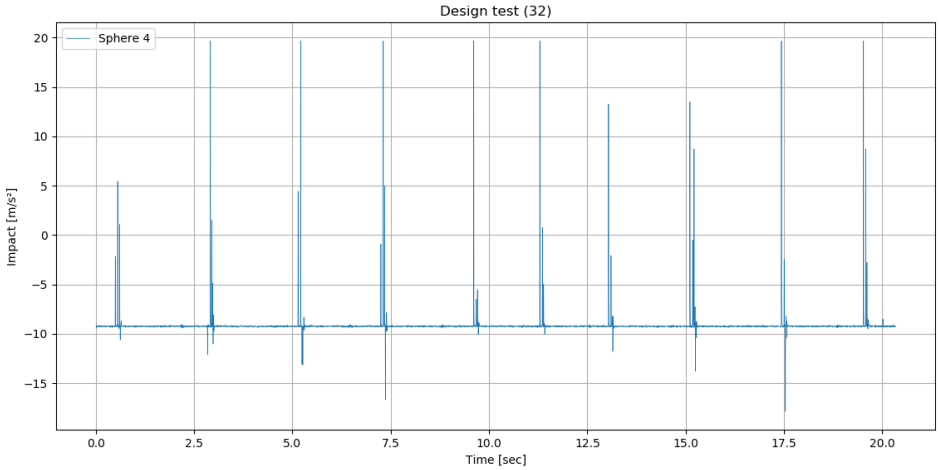
Design test (32)
Sphere 4
Impact [m/s²]
Time [sec]
20
15
10
5
0
−5
−10
−15
0.0
2.5
5.0
7.5
10.0
12.5
15.0
17.5
20.0

Frequency test graphs (spheres)

No.	Padding	Screw torque [Nm]	Height [mm]	Frequency [Hz]	Sphere	Range
1	Hard	20	100	3200	2	16
2	Hard	20	100	3200	2	2
3	Hard	20	50	3200	2	16
4	Hard	20	100	3200	2	16
5	Hard	20	100	3200	2	16
6	Hard	20	100	1600	2	16
7	Hard	20	100	1600	2	16
8	Hard	20	100	1600	2	16
9	Hard	20	100	800	2	16
10	Hard	20	100	400	2	16
11	Hard	20	100	200	2	16
12	Hard	20	100	100	2	16
13	Hard	20	100	50	2	16
14	Hard	20	100	25	2	16
15	Hard	20	100	3200	4	16
16	Hard	20	100	3200	4	2
17	Hard	20	100	3200	4	16
18	Hard	20	50	3200	4	16

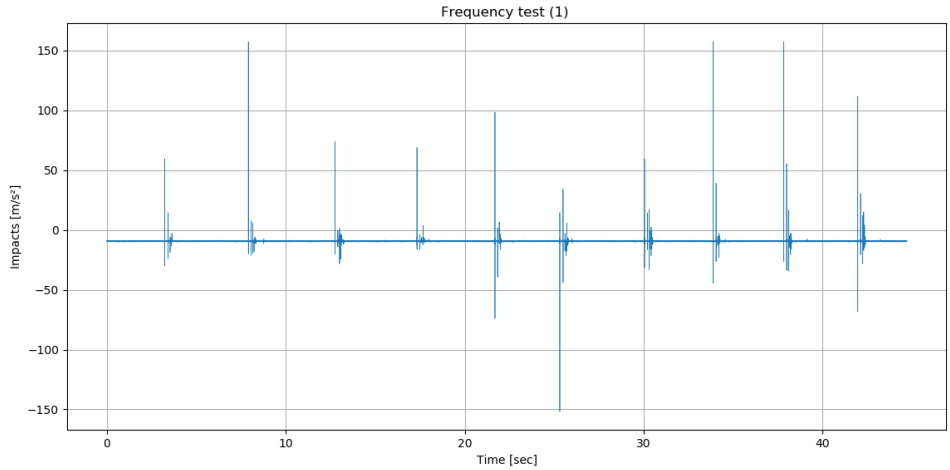

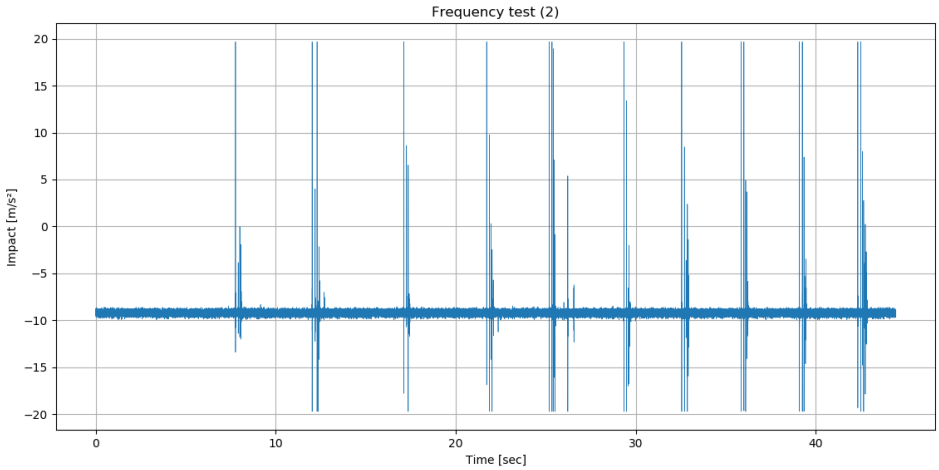
Frequency test (2)
Impact [m/s²]
Time [sec]

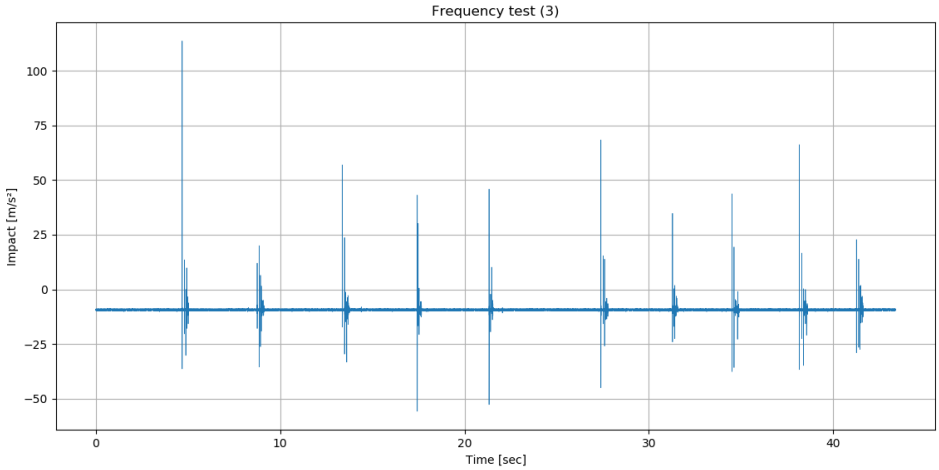
Frequency test (3)
Impact [m/s²]
Time [sec]

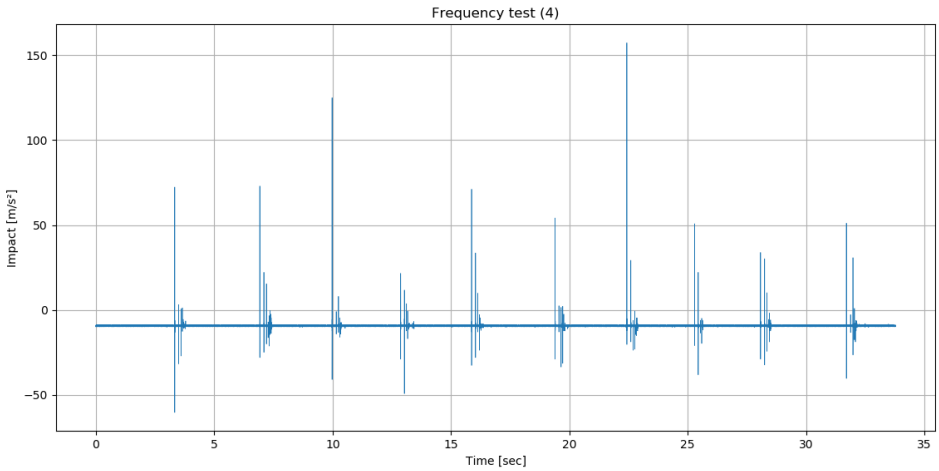
Frequency test (4)
Impact [m/s²]
Time [sec]

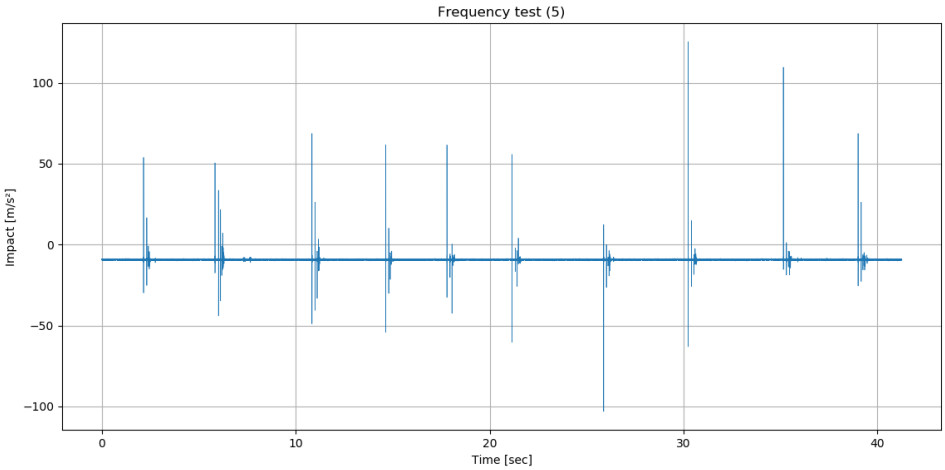
Frequency test (5)
Impact [m/s²]
Time [sec]

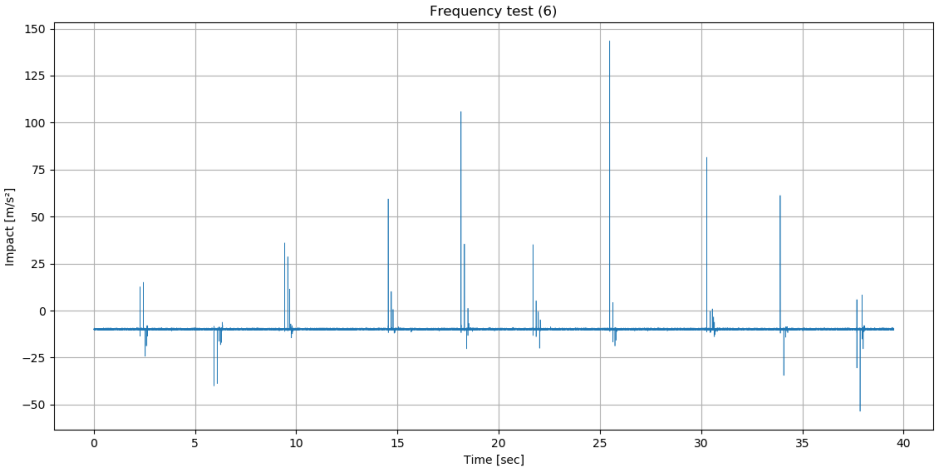
Frequency test (6)
Impact [m/s²]
Time [sec]

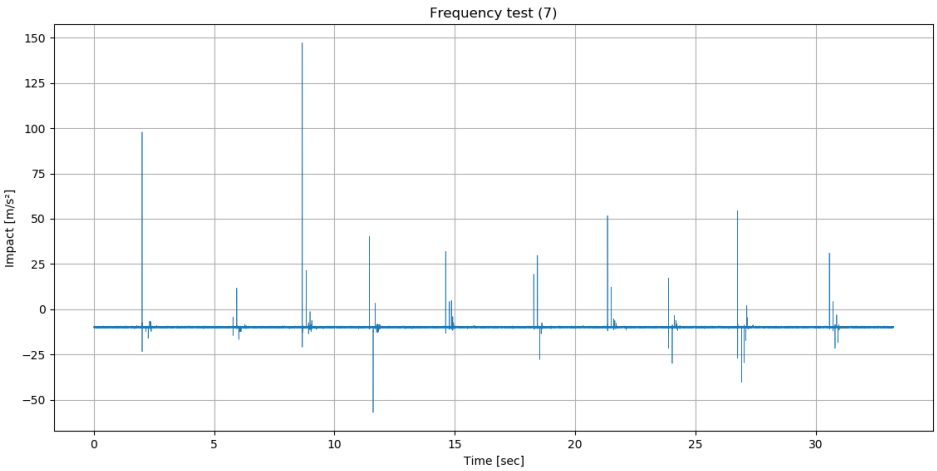
Frequency test (7)
Impact [m/s²]
Time [sec]

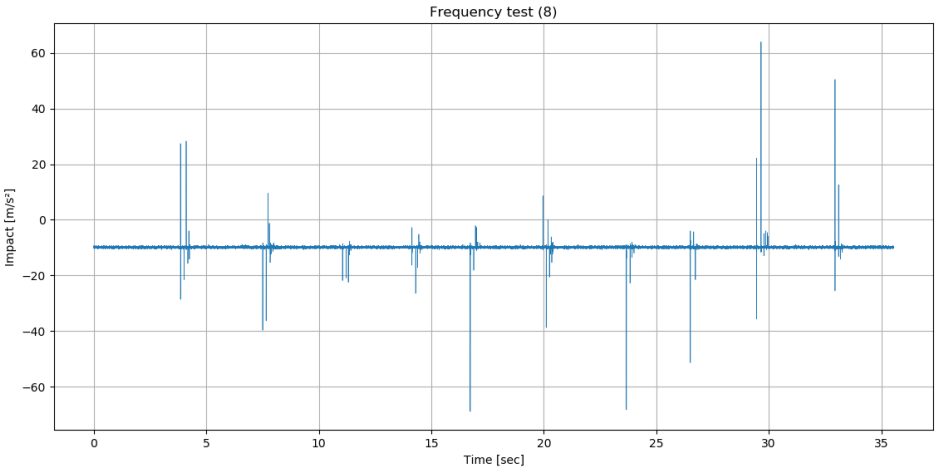
Frequency test (8)
Impact [m/s²]
Time [sec]

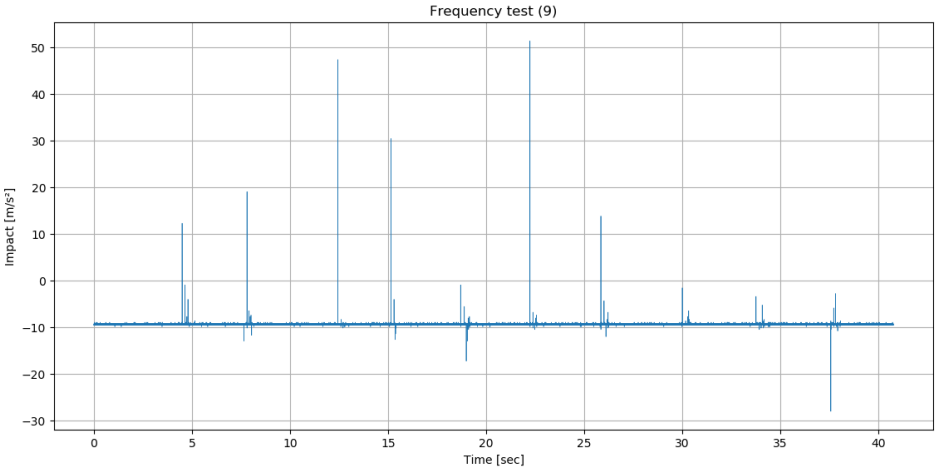
Frequency test (9)
Impact [m/s²]
Time [sec]

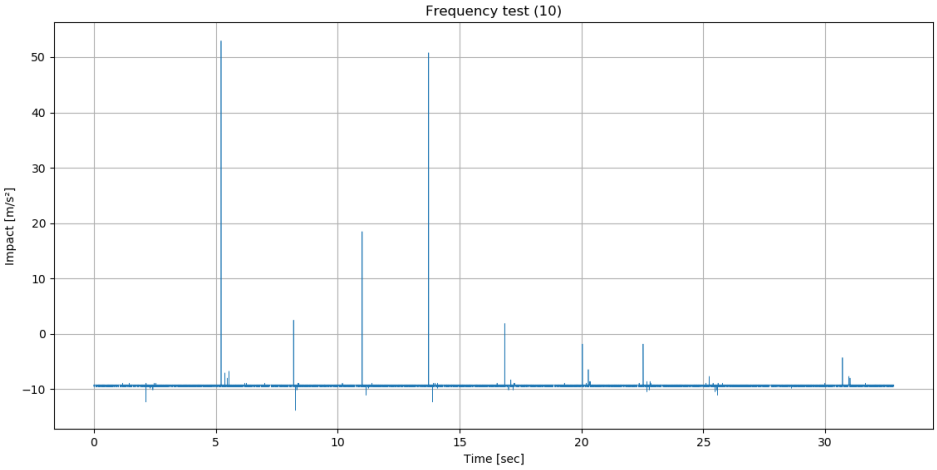
Frequency test (10)
Impact [m/s²]
Time [sec]

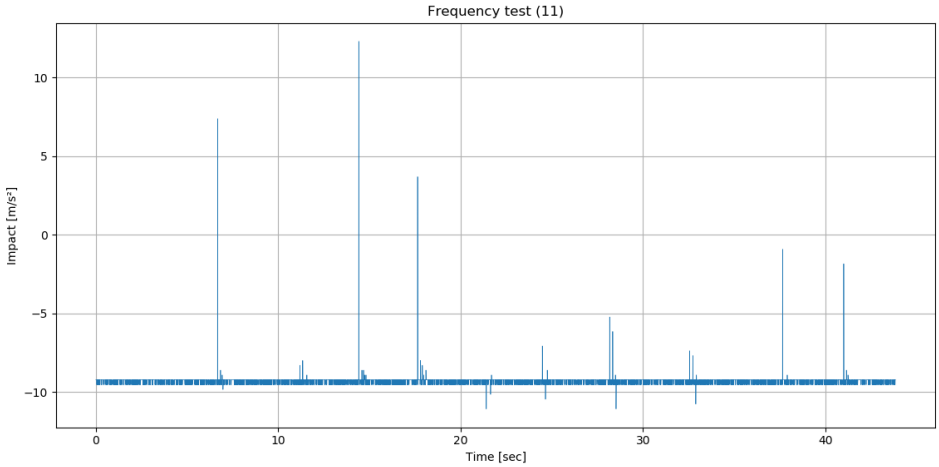
Frequency test (11)
Impact [m/s²]
Time [sec]

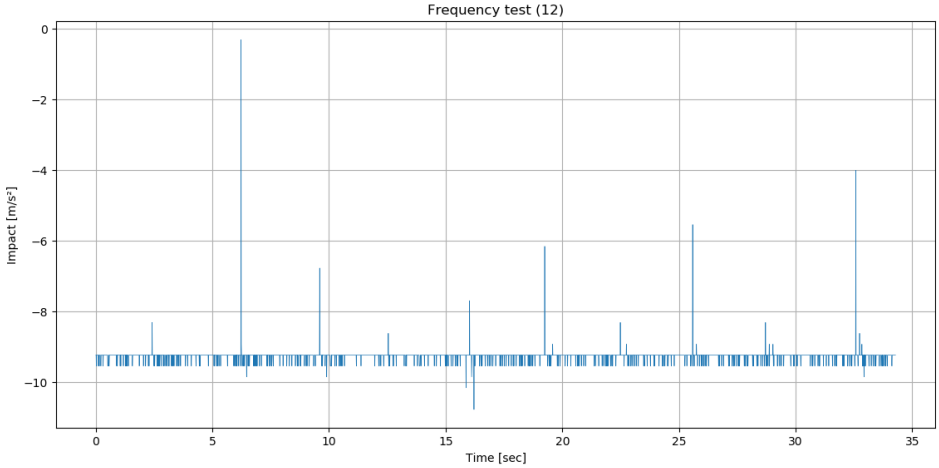
Frequency test (12)
Impact [m/s²]
Time [sec]

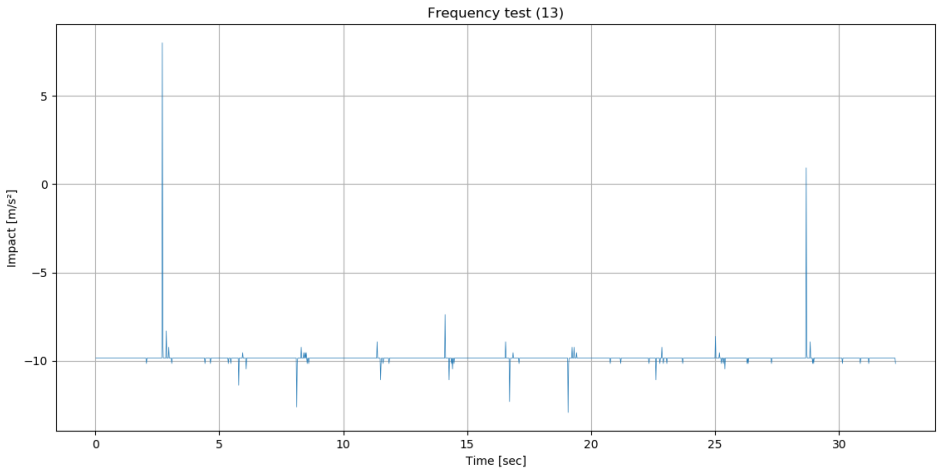
Frequency test (13)
Impact [m/s²]
Time [sec]

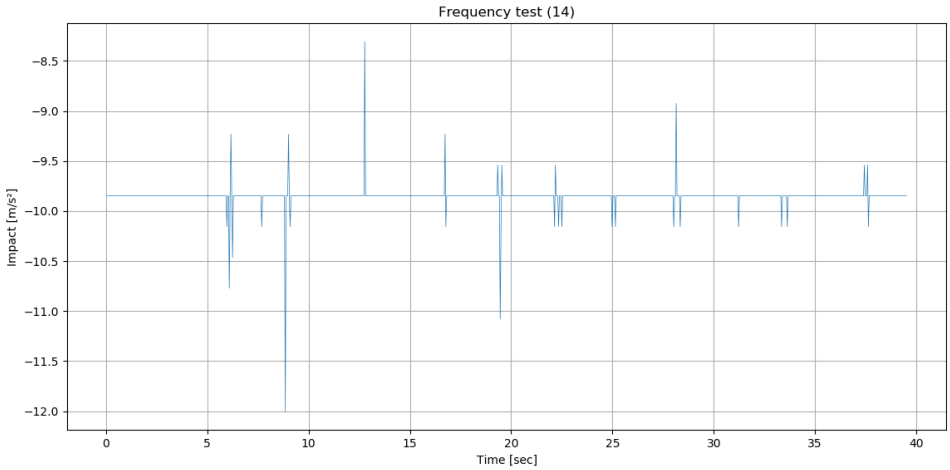
Frequency test (14)
Impact [m/s²]
−8.5
−9.0
−9.5
−10.0
−10.5
−11.0
−11.5
−12.0
0
5
10
15
20
25
30
35
40
Time [sec]

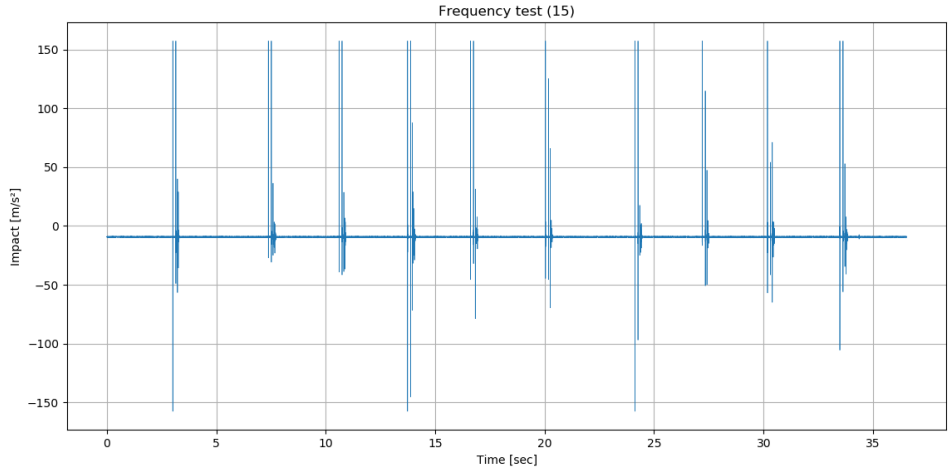
Frequency test (15)
Impact [m/s²]
150
100
50
0
−50
−100
−150
0
5
10
15
20
25
30
35
Time [sec]

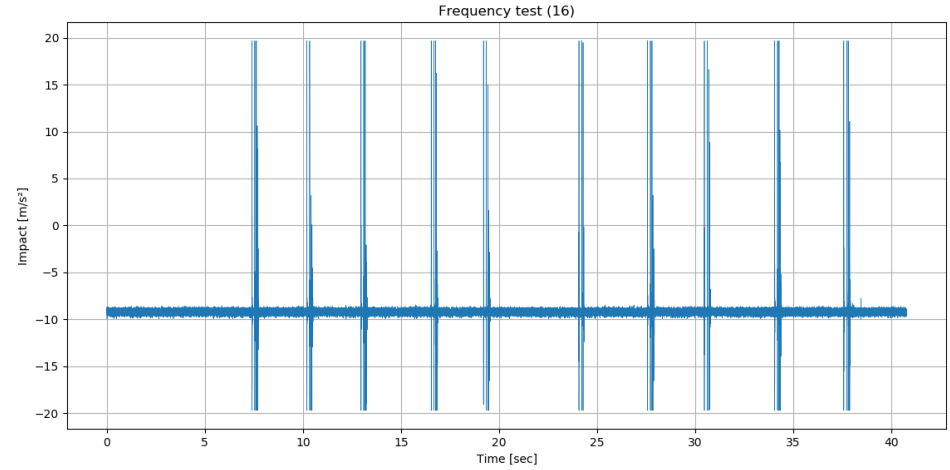
Frequency test (16)
Impact [m/s²]
20
15
10
5
0
−5
−10
−15
−20
0
5
10
15
20
25
30
35
40
Time [sec]

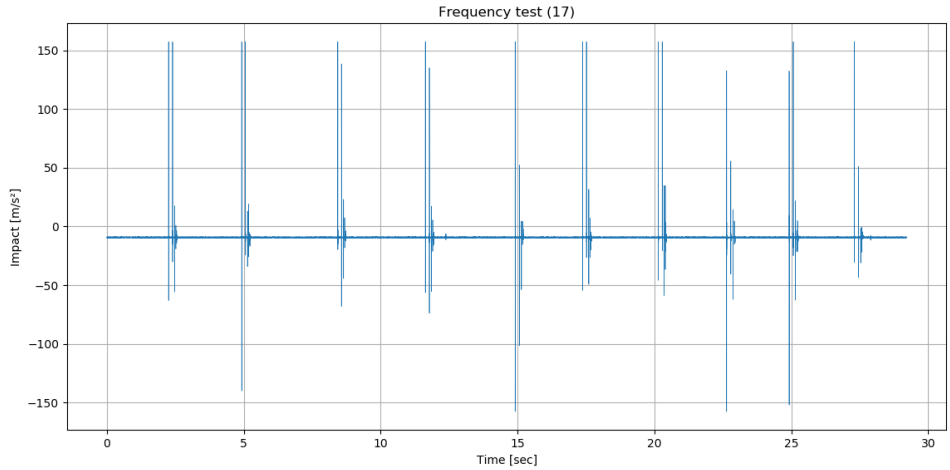
Frequency test (17)
Impact [m/s²]
Time [sec]
150
100
50
0
−50
−100
−150
0
5
10
15
20
25
30

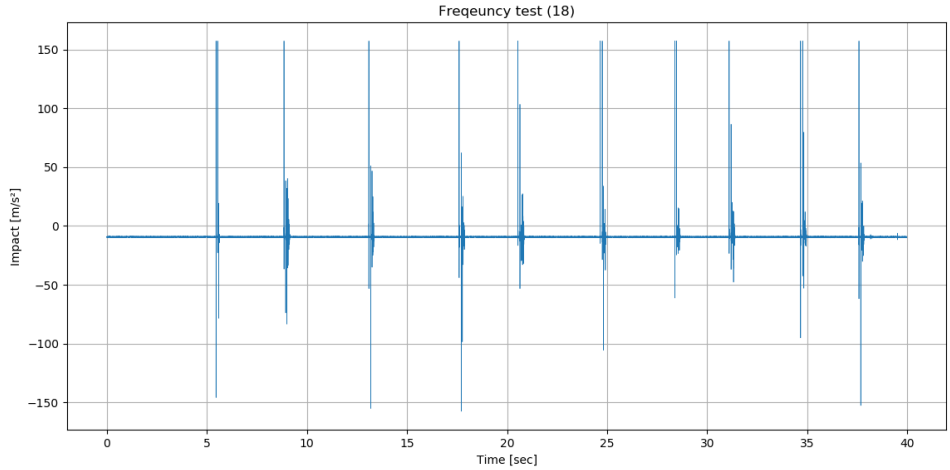
Freqeuncy test (18)
Impact [m/s²]
Time [sec]
150
100
50
0
−50
−100
−150
0
5
10
15
20
25
30
35
40

Water test graphs (spheres and pebbles)

No.	Screw torque [Nm]	Height [mm]	Frequency [Hz]	Range	Water flow	Testing material	repetitions
1	20	100	3200	16	Yes	Sphere 4	10
2	20	100	3200	16	Yes	Sphere 4	10
3	20	Rolling	3200	16	Yes	10 stones (ca. 10cm)	
4	20	Rolling	3200	16	Yes	10 stones (ca. 10cm)	
5	20	100	3200	16	Yes	2 stones (ca. 10cm)	
6	20	100	3200	16	Yes	2stones (ca. 10cm)	
7	20	100	3200	16	Yes	10 stones (ca. 10cm)	
8	20	100	3200	16	Yes	5 stones (ca. 10cm)	
9	20	100	3200	16	Yes	Stones (ca.10cm)	
10	20	100	3200	16	Yes	Stones (ca.10cm)	
11	20	100	3200	16	Yes	different discharge	
12	20	Rolling	3200	16	Yes	Sphere 4	10
13	20	Rolling	3200	16	Yes	Sphere 4	1
14	ERROR	ERROR	ERROR	ERROR	ERROR	ERROR	ERROR
15	20	100	3200	16	Yes	Sphere 4	50
16	20	100	3200	16	Yes	Sphere 4	50
17	20	100	3200	16	Yes	Sphere 4	50
18	20	100	3200	16	Yes	Sphere 4	50
19	20	100	3200	16	Yes	Sphere 4	50
20	20	100	3200	16	Yes	Sphere 2	50
21	20	100	3200	16	Yes	Sphere 2	50
22	20	100	3200	16	Yes	Sphere 2	50
23	20	Rolling	3200	16	Yes	concrete sphere	50
24	20	Rolling	3200	16	Yes	concrete sphere	50
25	20	Rolling	3200	16	Yes	Sphere 2	50
26	20	Rolling	3200	16	Yes	Sphere 2	50
27	20	Rolling	3200	16	Yes	concrete sphere	50

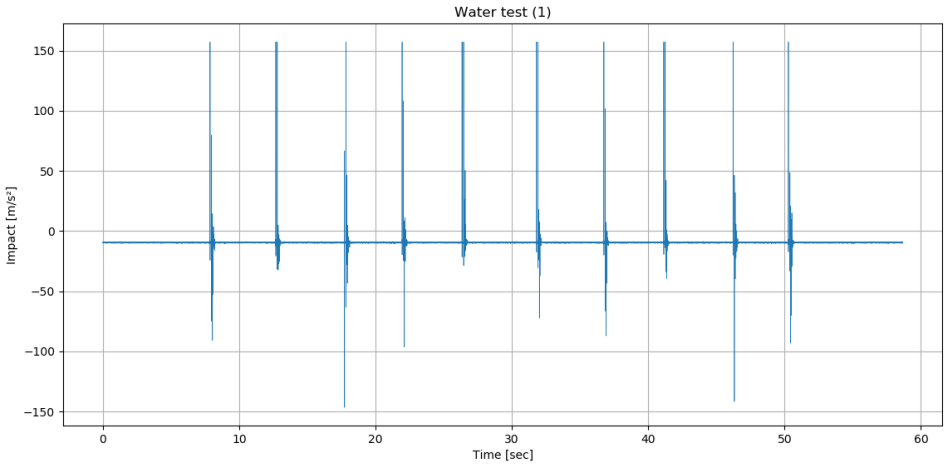

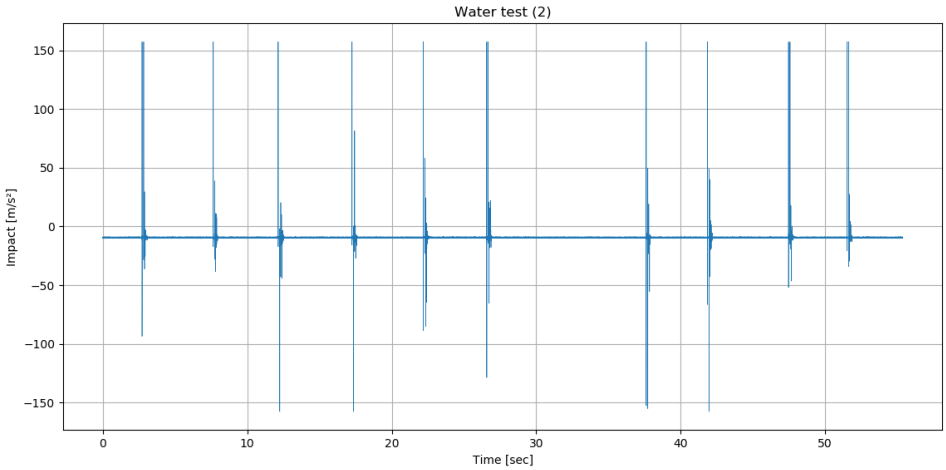
Water test (2)
Impact [m/s²]
Time [sec]

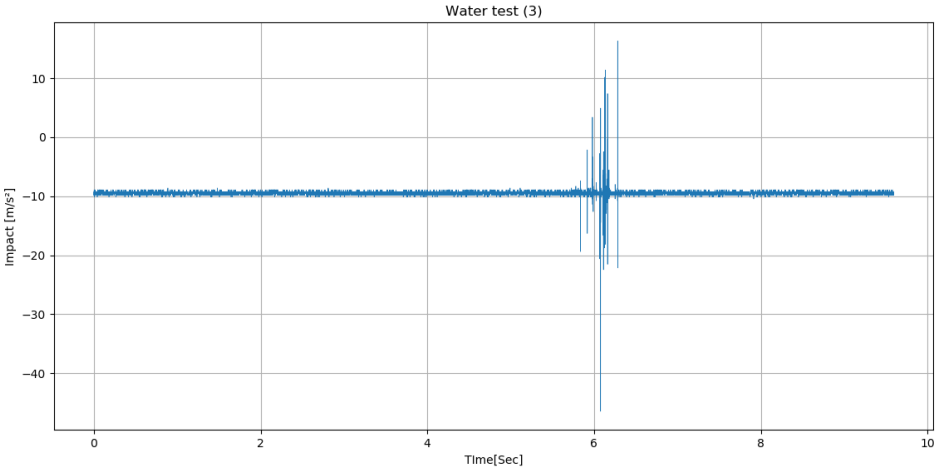
Water test (3)
Impact [m/s²]
TIme[Sec]

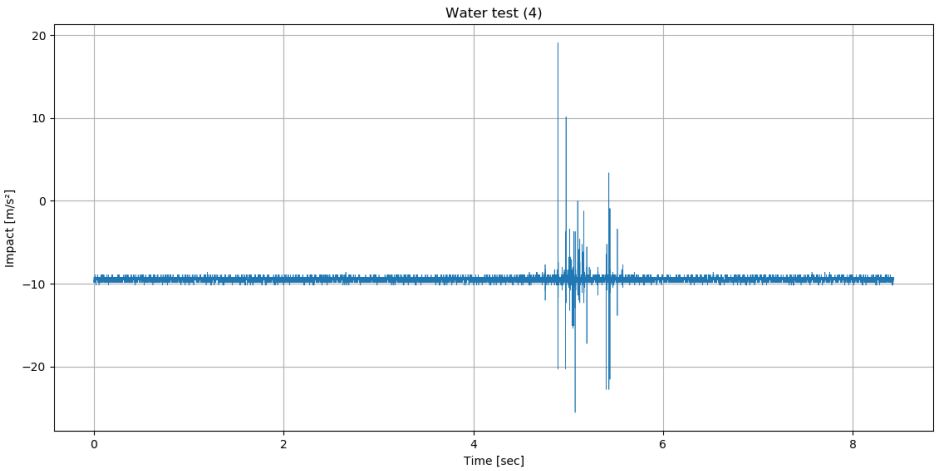
Water test (4)
Impact [m/s²]
Time [sec]

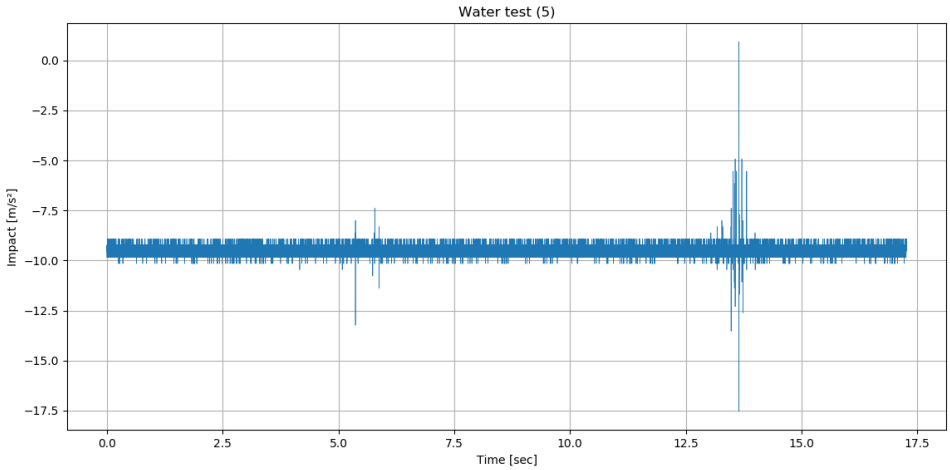
Water test (5)
Impact [m/s²]
Time [sec]
0.0
−2.5
−5.0
−7.5
−10.0
−12.5
−15.0
−17.5
0.0
2.5
5.0
7.5
10.0
12.5
15.0
17.5

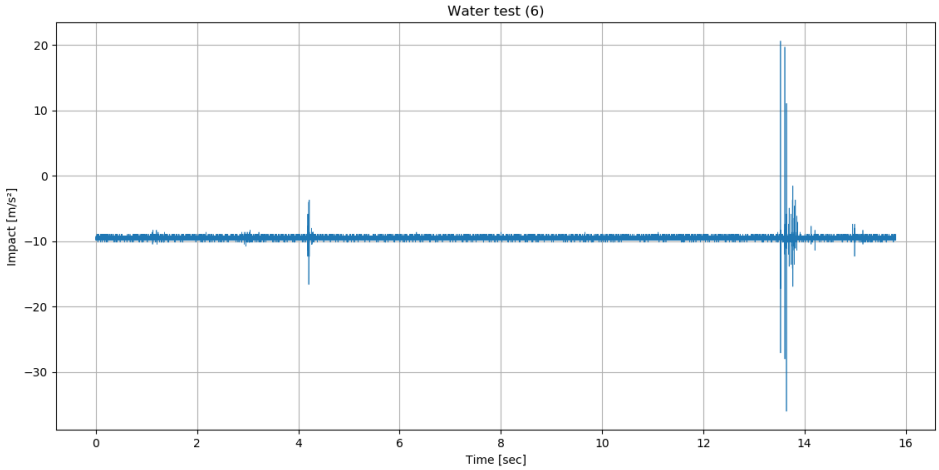
Water test (6)
Impact [m/s²]
Time [sec]
20
10
0
−10
−20
−30
0
2
4
6
8
10
12
14
16

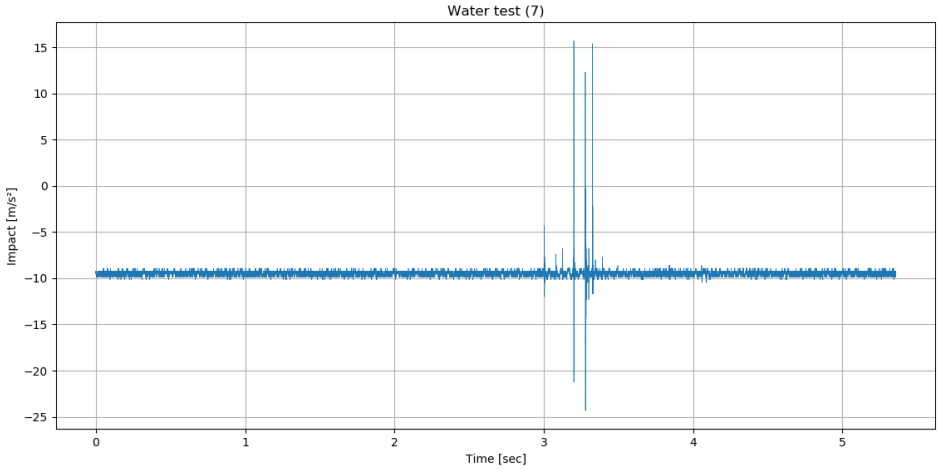
Water test (7)
Impact [m/s²]
Time [sec]
15
10
5
0
−5
−10
−15
−20
−25
0
1
2
3
4
5

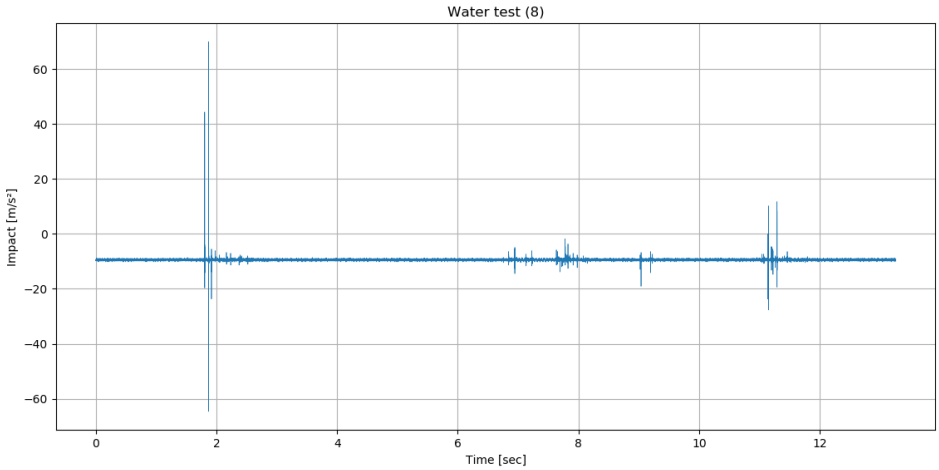
Water test (8)
Impact [m/s²]
Time [sec]

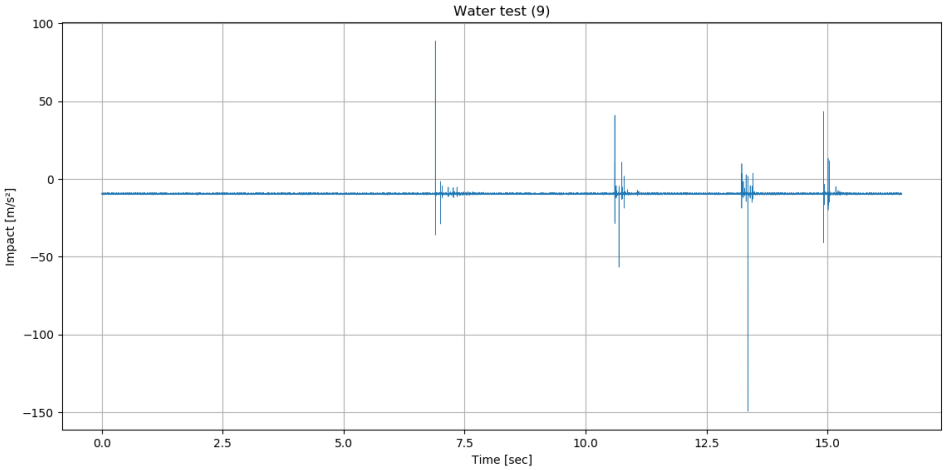
Water test (9)
Impact [m/s²]
Time [sec]

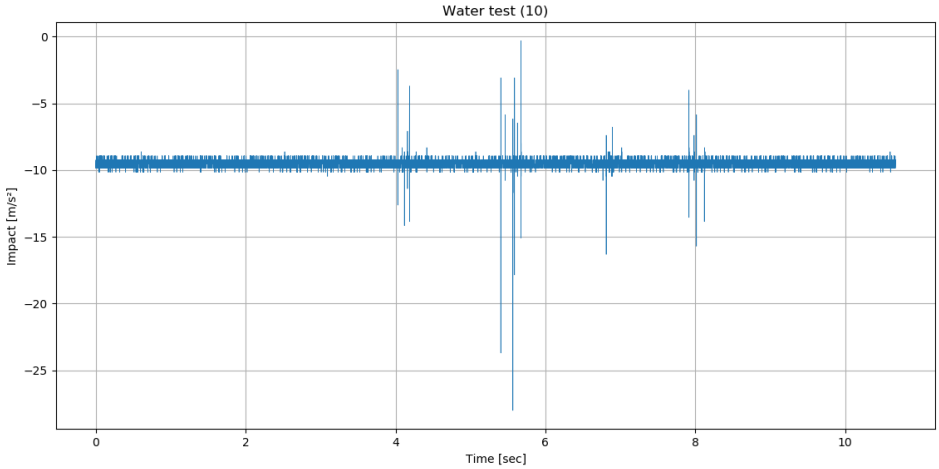
Water test (10)
Impact [m/s²]
Time [sec]

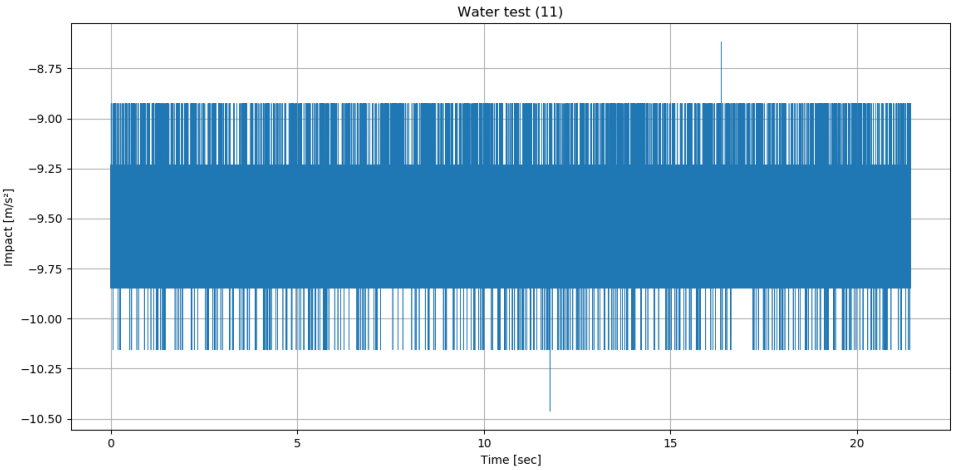
Water test (11)
Impact [m/s²]
−8.75
−9.00
−9.25
−9.50
−9.75
−10.00
−10.25
−10.50
0
5
10
15
20
Time [sec]

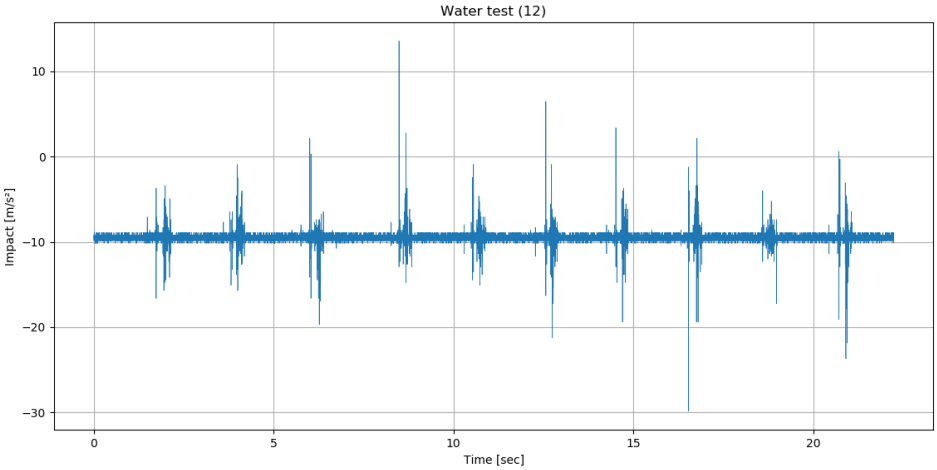
Water test (12)
Impact [m/s²]
10
0
−10
−20
−30
0
5
10
15
20
Time [sec]

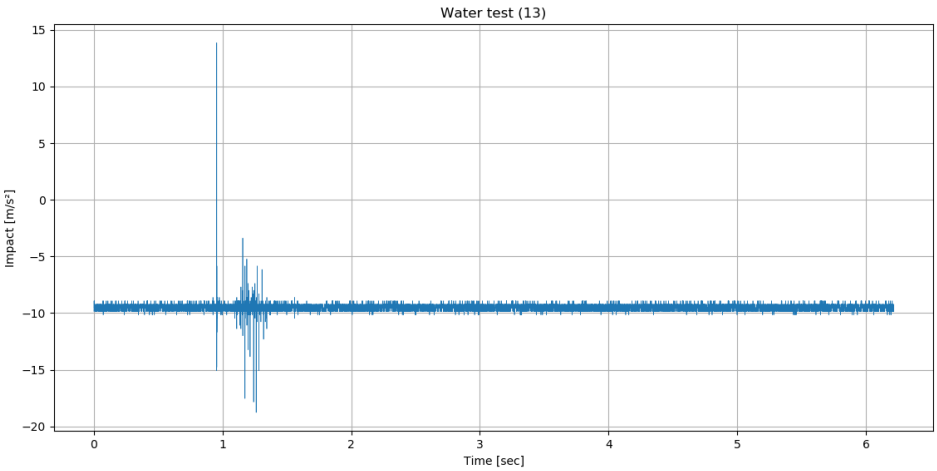
Water test (13)
Impact [m/s²]
15
10
5
0
−5
−10
−15
−20
0
1
2
3
4
5
6
Time [sec]

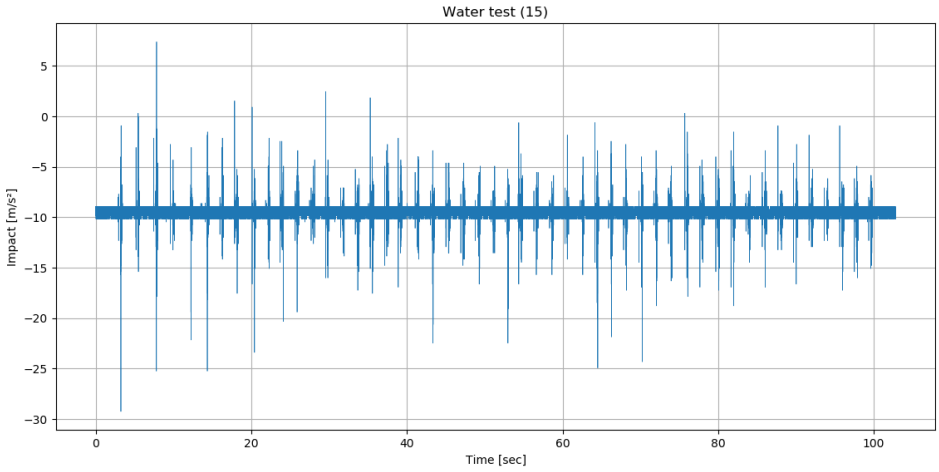
Water test (15)
Impact [m/s²]
Time [sec]

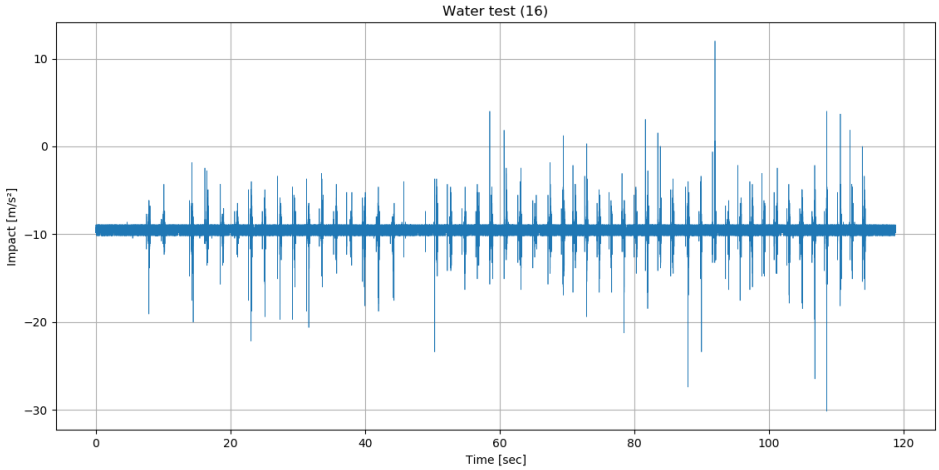
Water test (16)
Impact [m/s²]
Time [sec]

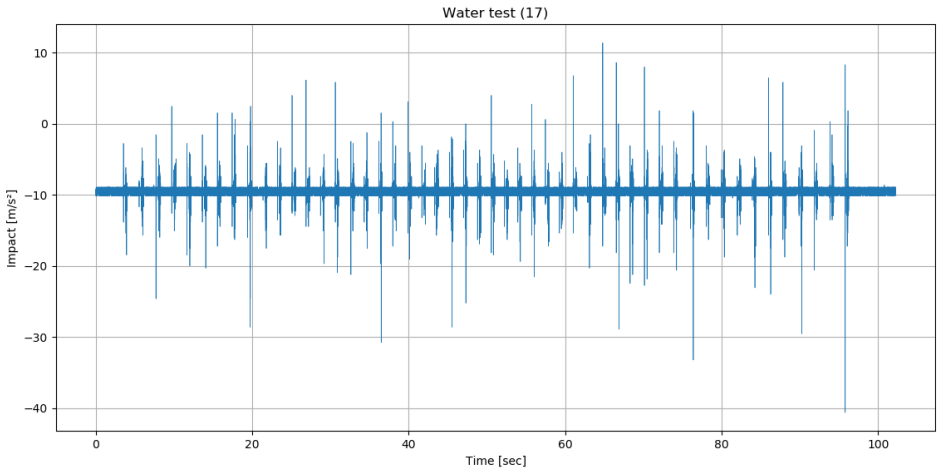
Water test (17)
Impact [m/s²]
Time [sec]

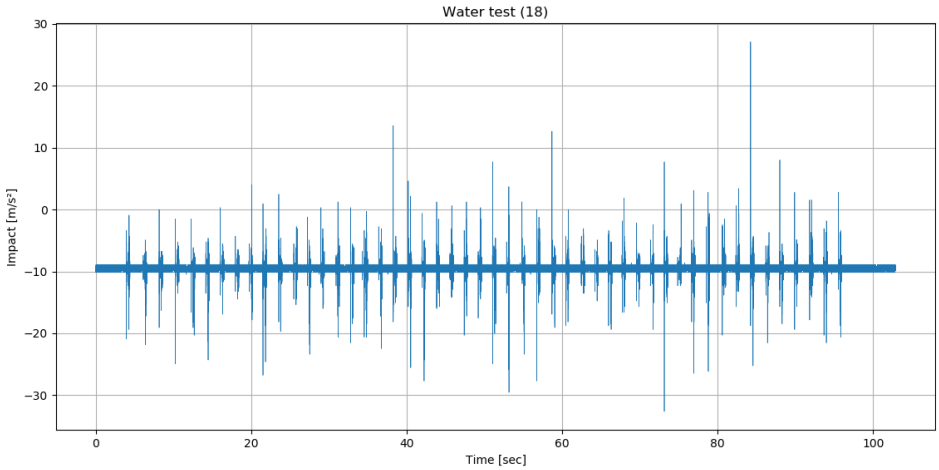
Water test (18)
Impact [m/s²]
Time [sec]

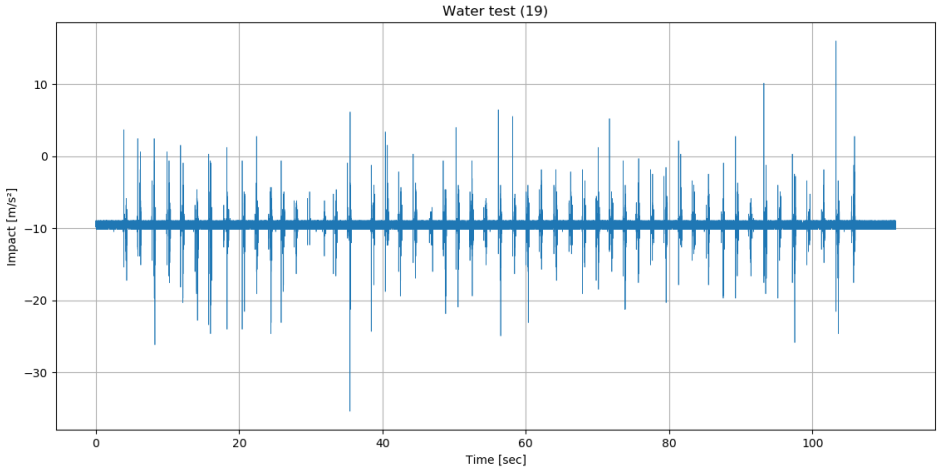
Water test (19)
Impact [m/s²]
Time [sec]

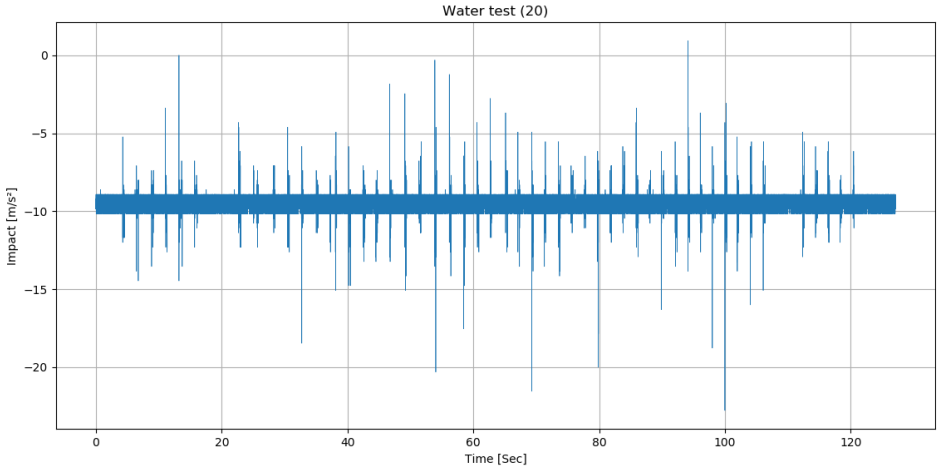
Water test (20)
Impact [m/s²]
Time [Sec]

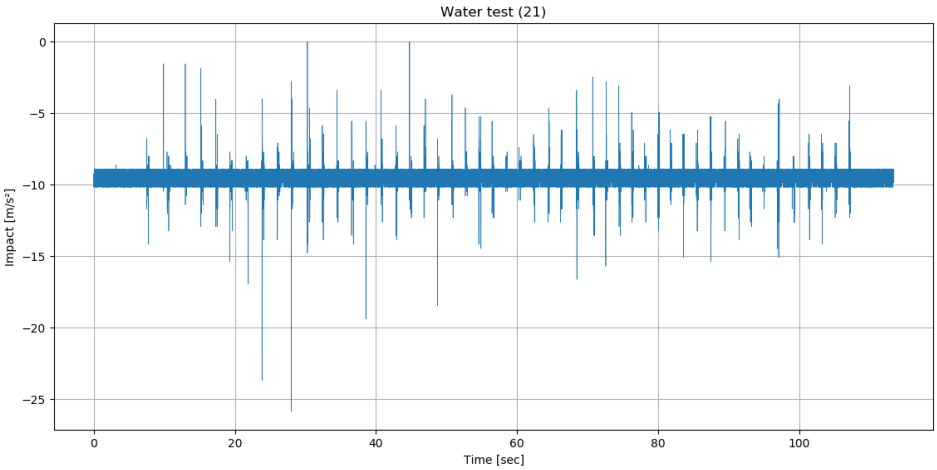
Water test (21)
Impact [m/s²]
Time [sec]

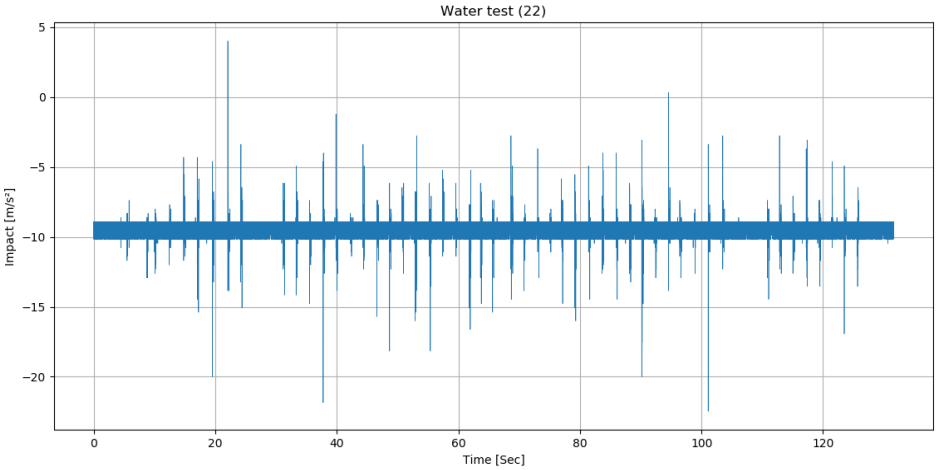
Water test (22)
Impact [m/s²]
Time [Sec]

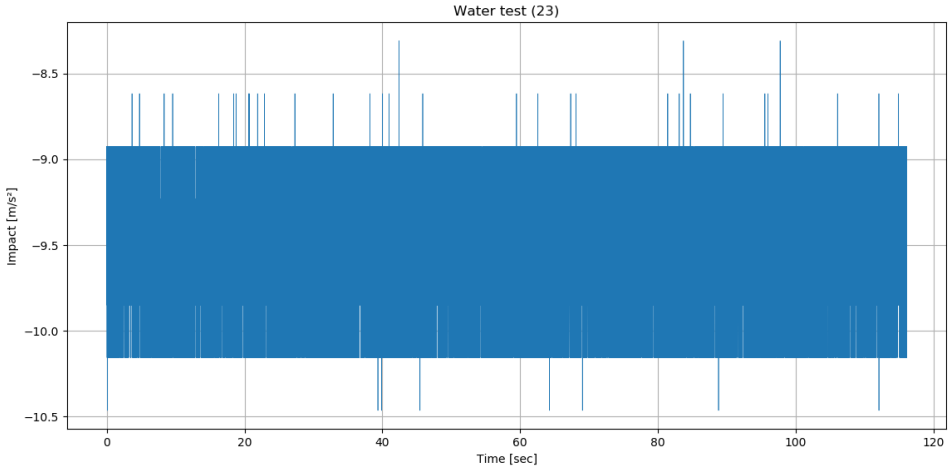
Water test (23)
Impact [m/s²]
Time [sec]

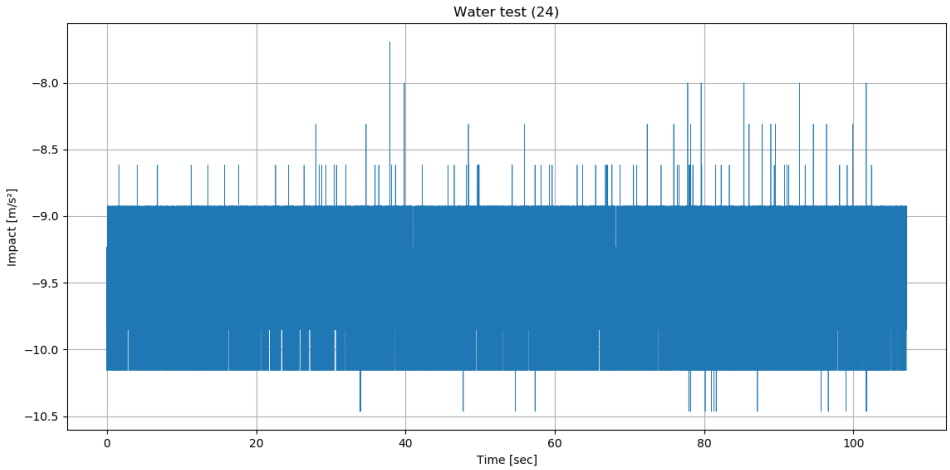
Water test (24)
Impact [m/s²]
−8.0
−8.5
−9.0
−9.5
−10.0
−10.5
0
20
40
60
80
100
Time [sec]

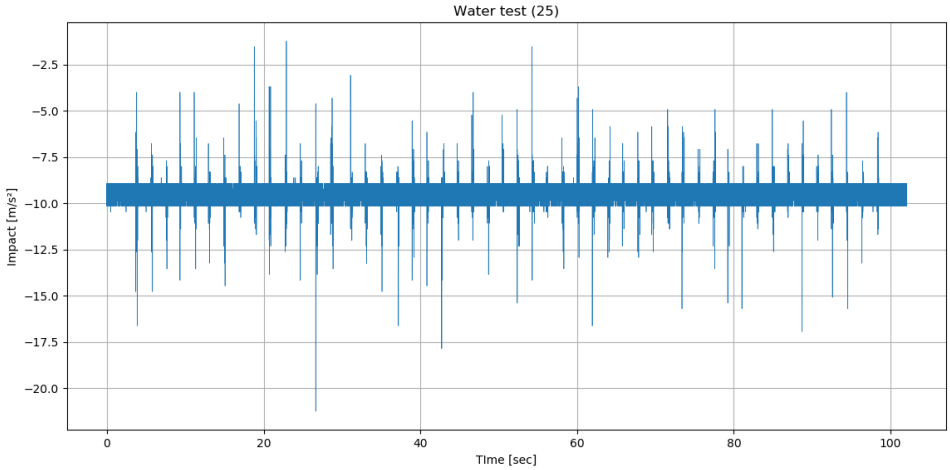
Water test (25)
Impact [m/s²]
−2.5
−5.0
−7.5
−10.0
−12.5
−15.0
−17.5
−20.0
0
20
40
60
80
100
TIme [sec]

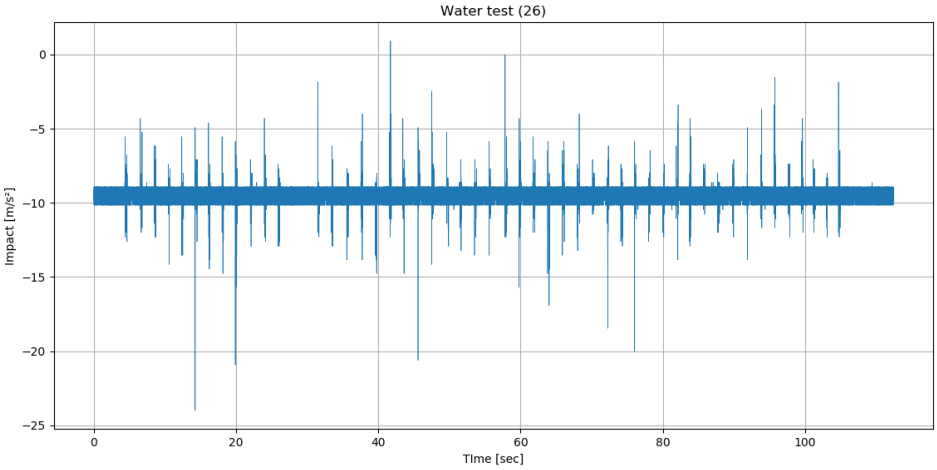
Water test (26)
Impact [m/s²]
0
−5
−10
−15
−20
−25
0
20
40
60
80
100
TIme [sec]

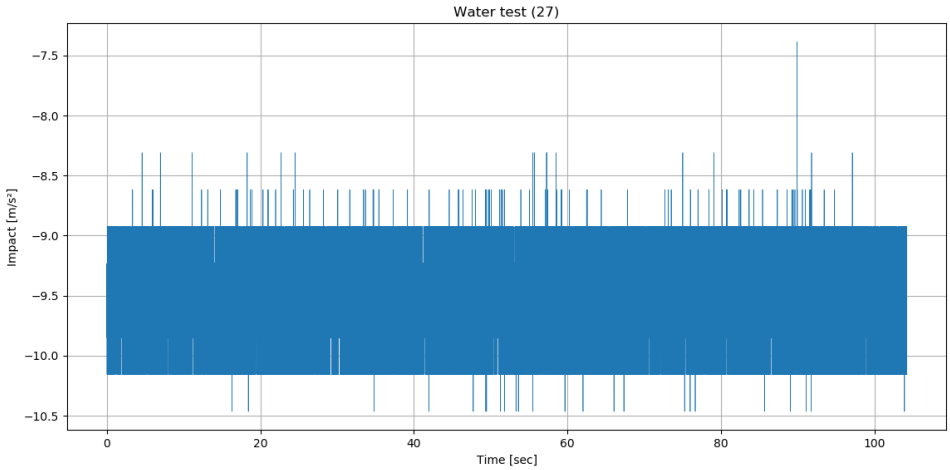
Water test (27)
Impact [m/s²]
−7.5
−8.0
−8.5
−9.0
−9.5
−10.0
−10.5
0
20
40
60
80
100
Time [sec]

Frequency test graphs (buckets)

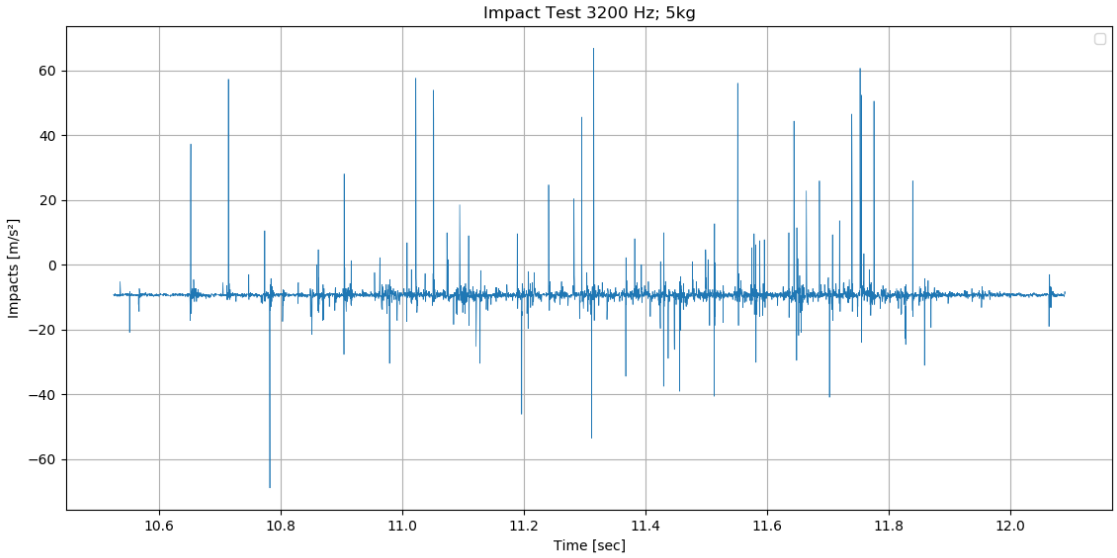

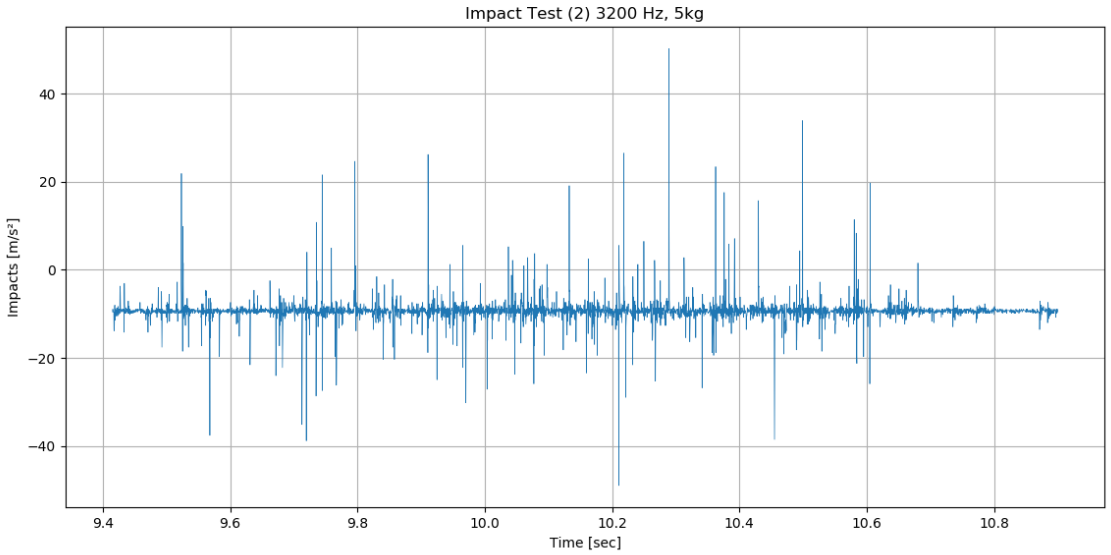

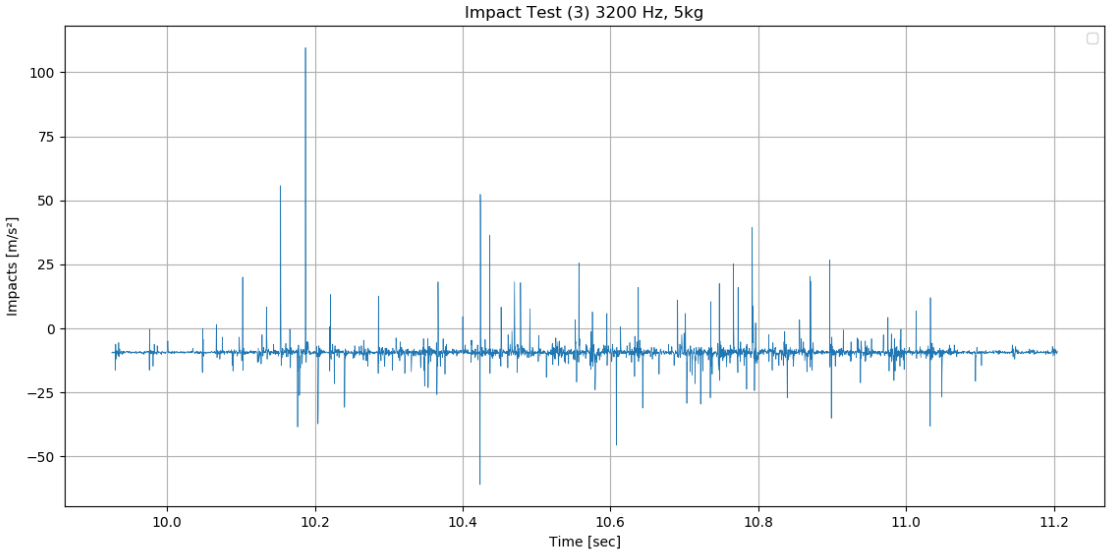
Impact Test (3) 3200 Hz, 5kg
Impacts [m/s²]
Time [sec]
100
75
50
25
0
−25
−50
10.0
10.2
10.4
10.6
10.8
11.0
11.2

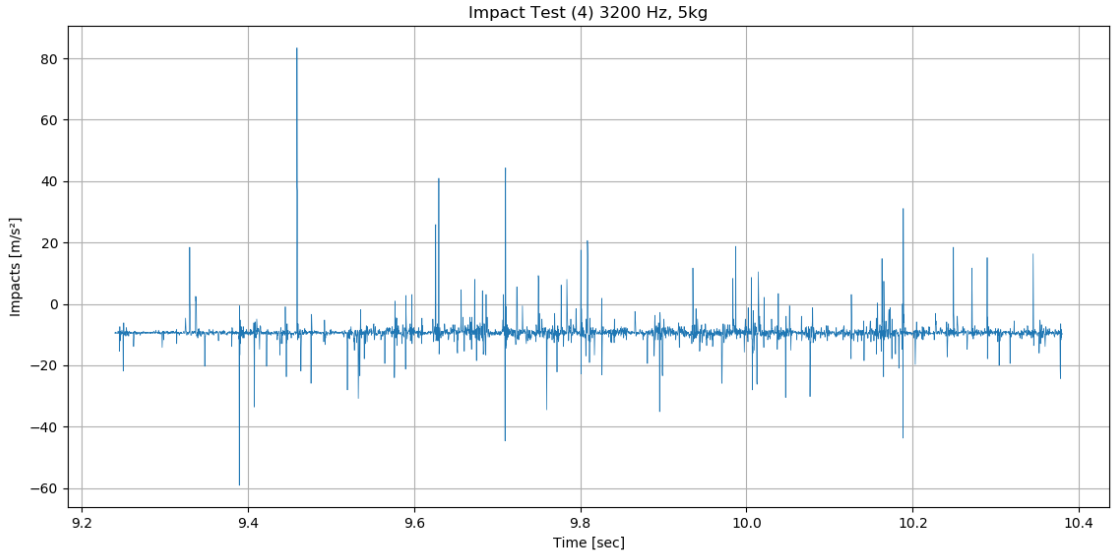
Impact Test (4) 3200 Hz, 5kg
Impacts [m/s²]
Time [sec]
80
60
40
20
0
−20
−40
−60
9.2
9.4
9.6
9.8
10.0
10.2
10.4

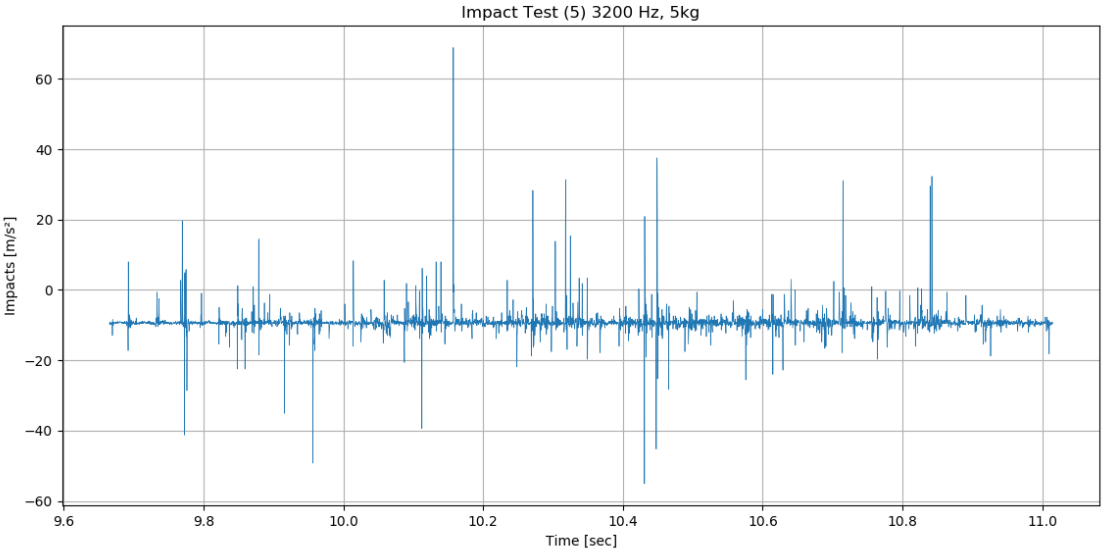
Impact Test (5) 3200 Hz, 5kg
Impacts [m/s²]
Time [sec]
60
40
20
0
−20
−40
−60
9.6
9.8
10.0
10.2
10.4
10.6
10.8
11.0

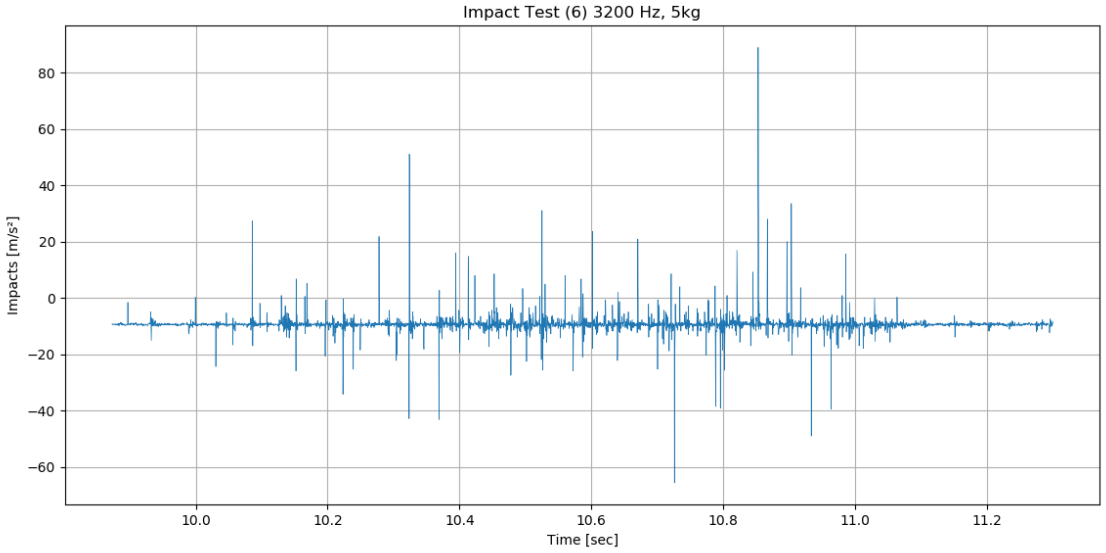
Impact Test (6) 3200 Hz, 5kg
Impacts [m/s²]
Time [sec]
80
60
40
20
0
−20
−40
−60
10.0
10.2
10.4
10.6
10.8
11.0
11.2

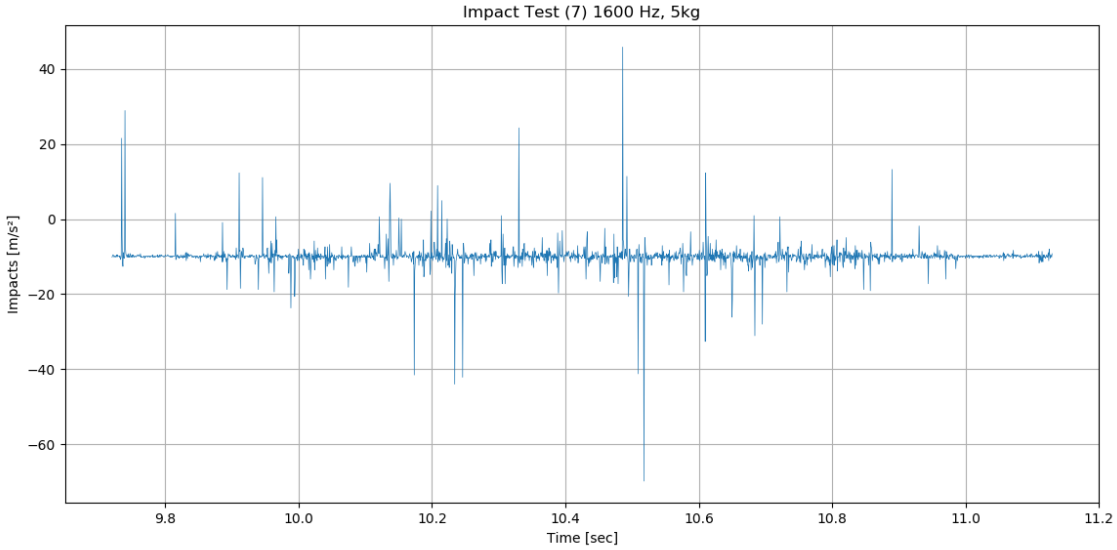
Impact Test (7) 1600 Hz, 5kg
Impacts [m/s²]
Time [sec]
40
20
0
−20
−40
−60
9.8
10.0
10.2
10.4
10.6
10.8
11.0
11.2

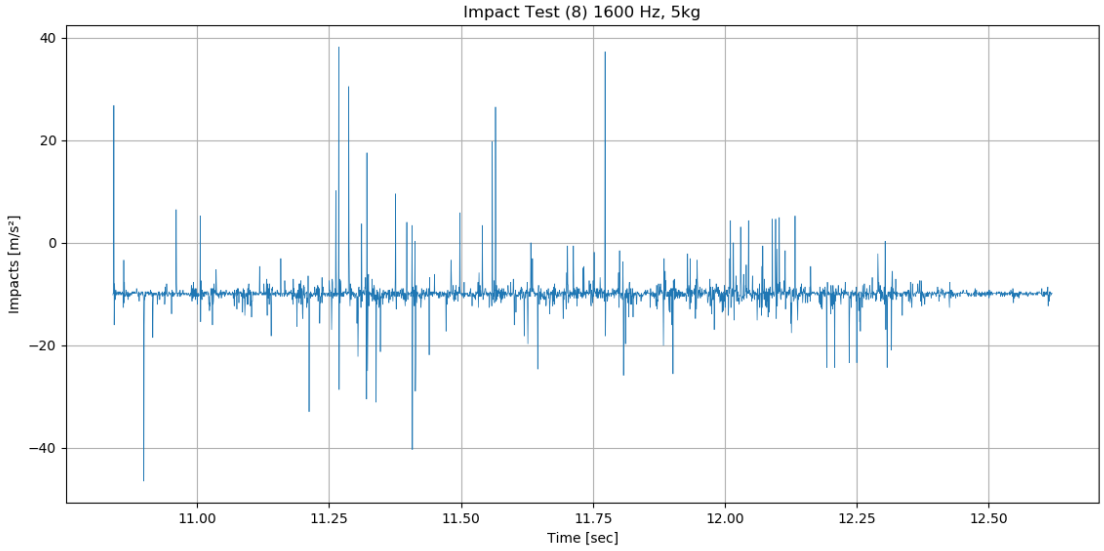
Impact Test (8) 1600 Hz, 5kg
Impacts [m/s²]
Time [sec]
40
20
0
−20
−40
11.00
11.25
11.50
11.75
12.00
12.25
12.50

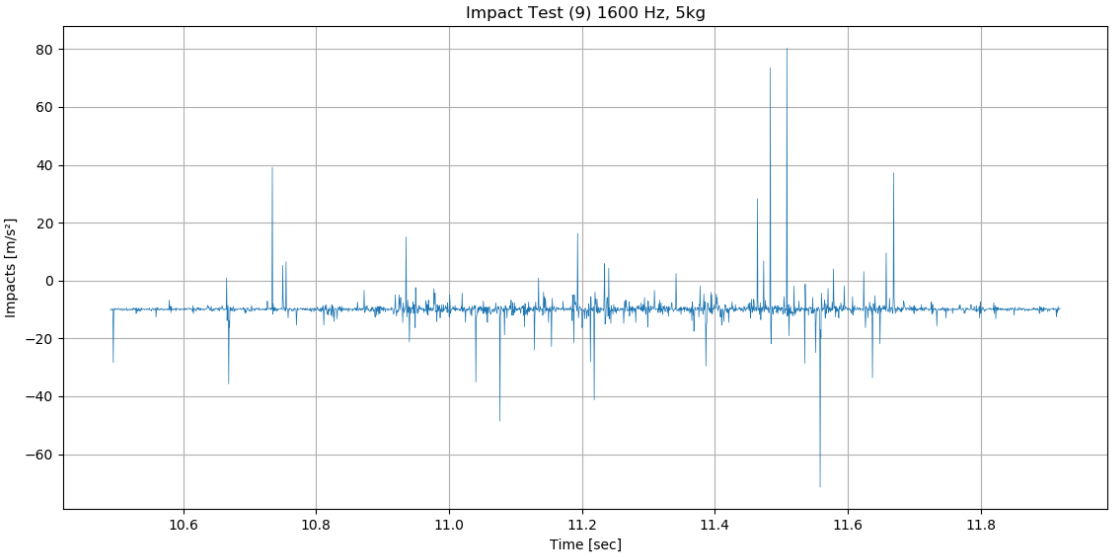
Impact Test (9) 1600 Hz, 5kg
Impacts [m/s²]
Time [sec]
80
60
40
20
0
−20
−40
−60
10.6
10.8
11.0
11.2
11.4
11.6
11.8

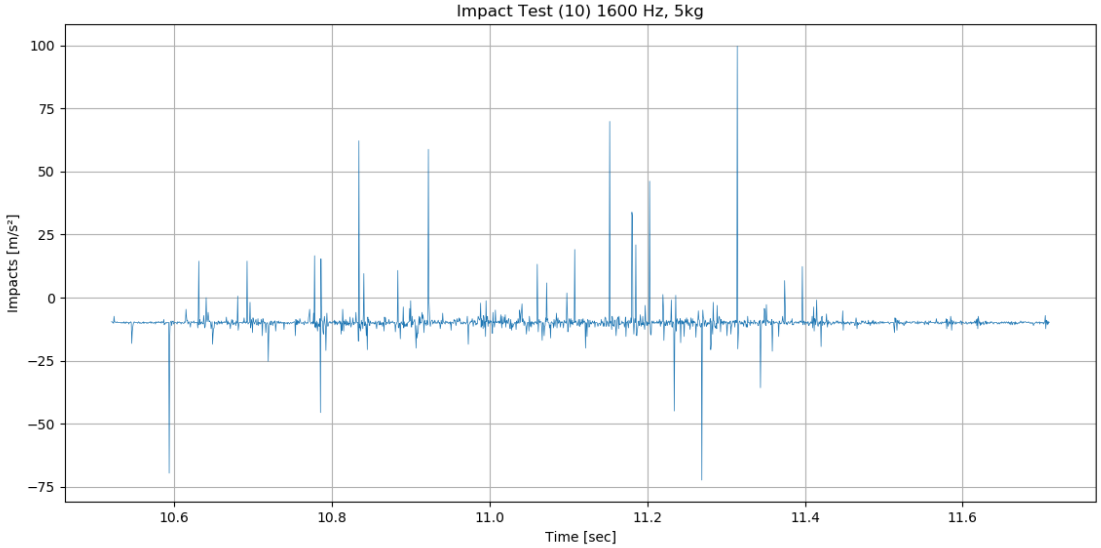
Impact Test (10) 1600 Hz, 5kg
Impacts [m/s²]
Time [sec]
100
75
50
25
0
−25
−50
−75
10.6
10.8
11.0
11.2
11.4
11.6

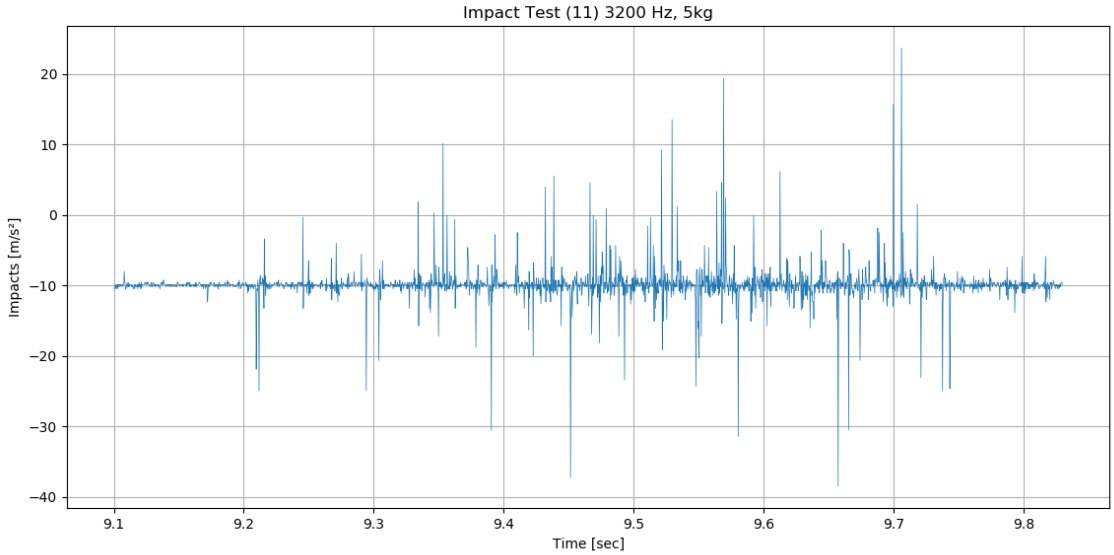
Impact Test (11) 3200 Hz, 5kg
Impacts [m/s²]
Time [sec]
20
10
0
−10
−20
−30
−40
9.1
9.2
9.3
9.4
9.5
9.6
9.7
9.8

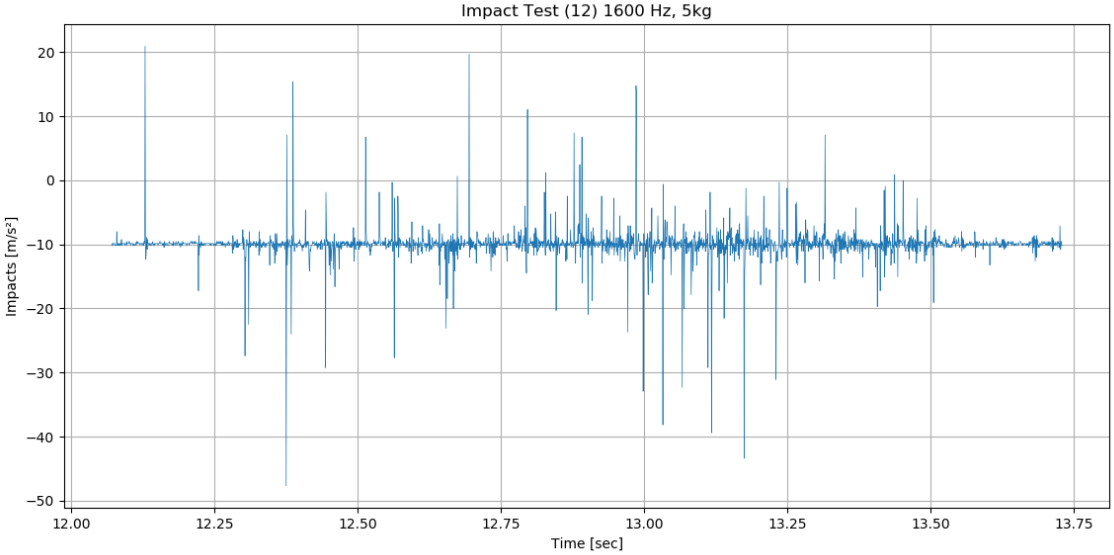
Impact Test (12) 1600 Hz, 5kg
Impacts [m/s²]
Time [sec]
20
10
0
−10
−20
−30
−40
−50
12.00
12.25
12.50
12.75
13.00
13.25
13.50
13.75